HUMAN EMBRYONIC STEM CELLS FOR BONE ENGINEERING APPLICATIONS

Giuseppe Maria de Peppo

UNIVERSITY OF GOTHENBURG

Department of Biomaterials, Institute of Clinical Sciences,
Sahlgrenska Academy at University of Gothenburg,
Göteborg, Sweden

2011

Department of Biomaterials
Institute of Clinical Sciences
Sahlgrenska Academy
University of Gothenburg

Correspondence:
Giuseppe Maria de Peppo
Department of Biomaterials
Institute of Clinical Sciences
Sahlgrenska Academy at University of Gothenburg
Box 412
SE 405 30 Göteborg
Sweden

E-mail: giuseppe.de.peppo@gu.se; depeppo@hotmail.com

ISBN: 978-91-633-8767-8

Printed in Sweden
Geson Hylte Tryck

Printed in 250 copies

To Marcello

with esteem

What I cannot create, I do not understand.

(Richard Feynman)

TABLE OF CONTENTS

1. ABSTRACT 9

2. LIST OF ORIGINAL ARTICLES AND MANUSCRIPTS 11

3. ABBREVIATIONS AND SYMBOLS 13

3.1 Abbreviations 13

3.2 Gene and Protein Symbols 15

4. INTRODUCTION 19

4.1 Tissue Engineering 19

4.1.1 The Tissue Engineering Quadriad 19

4.1.2 Stem Cells 20

4.1.3 Scaffolds 22

4.1.4 Inductive Cues 23

4.1.5 Bioreactors 23

4.1.6 Social Impact and Experimental Trends 24

4.2 The Skeletal System 25

4.2.1The Human Skeleton 25

4.2.2 Bone Cellular Components 25

4.2.3 Bone Extracellular Matrix 25

4.2.4 Woven and Lamellar Bone 27

4.2.5 Structural Types of Bone 28

4.2.6 Bone as a Composite Material 29

4.2.7 Bone Histogenesis 29

4.2.8 Bone Remodeling and Repair 30

4.2.9 Molecular Regulation of Bone Histogenesis 32

4.3 Bone Deficiency, Clinical Needs and Current Treatments 35

4.4 Bone Engineering 37

4.4.1 Scaffolds for Bone Engineering Applications 37

4.4.2 Stem Cells in Bone Engineering 38

4.4.3 Cultivation Requirements and Strategies 40

5. AIMS OF THE THESIS 43

6. MATERIAL AND METHODS 45
6.1 Scaffolds 45
6.1.1 Ceramic Scaffolds 45
6.1.2 Fibrin Gel 45
6.1.3 Metallic Scaffolds 45
6.2 Free-form Fabrication of cp-Ti and Ti6Al4V Scaffolds 46
6.3 Surface Characterization of cp-Ti and Ti6Al4V Scaffolds 46
6.4 Scaffold Cleaning and Sterilization 47
6.5 Cells 48
6.5.1 Undifferentiated Human Embryonic Stem Cells 48
6.5.2 Matrix-free Growth Human Embryonic Stem Cells 48
6.5.3 Human Embryonic Stem Cell-derived Mesodermal Progenitors 48
6.5.4 Human Mesenchymal Stem Cells 48
6.6 Cell Derivation and Isolation 49
6.7 Cell Expansion 51
6.8 Osteogenic Stimulation 52
6.9 Cell Transduction 52
6.10 Cell Seeding Techniques and Preparation of Cell/scaffold Constructs 53
6.11 Culture in Bioreactor 54
6.12 Cell Staining with Fluorescein Diacetate 55
6.13 Microscopic Investigation 56
6.13.1 Scanning Electron Microscopy 56
6.14 Cell Disruption and Extraction of Biological Materials 57
6.14.1 DNA Extraction 57
6.14.2 RNA Extraction 58
6.14.3 Protein Extraction 58
6.15 Total DNA Content 59
6.16 Techniques for Gene Expression Studies 60

6.16.1 Gene Microarray 60
6.16.2 Real-time Polymerase Chain Reaction 61
6.17 Bioinformatic Tools 63
6.17.1 Comparative and Statistical Analysis of Microarray Data 63
6.17.2 Scatter Plots 64
6.17.3 Hierarchical Clustering 64
6.17.4 Protein-Protein Interaction Networks 65
6.18 Flow Cytometry 65
6.19 ELISA 67
6.20 Telomerase Activity and Telomere Length 68
6.21 Colorimetric Assays 69
6.21.1 Calcium Content 69
6.21.2 Phosphate Content 70
6.21.3 Alkaline Phosphatase Activity 70
6.21.4 Total Protein Content 71
6.22 TOF-SIMS Analysis of Mineralized Matrix 72
6.23 Lactate Dehydrogenase Assay 73
6.24 Animal Testing 73
6.25 *In vitro* and *in vivo* Bioluminescence Imaging 74
6.26 White Blood Count 75
6.27 Serum Preparation 76
6.28 Histological Techniques 76
6.29 Histochemical Staining 77
6.29.1 Von Kossa 77
6.29.2 Oil-red O 78
6.29.3 Haematoxylin-eosin-safranin 78
6.29.4 Sirius Red 79
6.29.5 Toluidine Blue 79
6.30 Immunohistochemistry 79
6.31 Statistical Analyses 80
6.32 Ethical approval 81

7. SUMMARY OF RESULTS 83
7.1 Study 83
7.2 Study II 84
7.3 Study III 85
7.4 Study IV 86
7.5 Study V 86
7.6 Study VI 87

8. GENERAL DISCUSSION 89
8.1 Clinical need for bone-engineered substitutes 89
8.2 The Stem Cell Dilemma 89
8.3 Ossification genes display different profile of expression in MFG-hESCs and hMSCs 91
8.4 MFG-hESCs display higher mineralization properties than hMSCs 92
8.5 MFG-hESCs differentiation is associated with downregulation of hESC-specific genes 93
8.6 hES-MPs and hMSCs display comparable gene expression profiles 94
8.7 hES-MPs display higher proliferation potential than hMSCs 95
8.8 hES-MPs do not exhibit tumorigenic potential 96
8.9 hES-MPs display optimal osteogenic potential and higher mineralization properties than hMSCs 98
8.10 hES-MPs are hypoimmunogenic and do not elicit immune response *in vivo* 101
8.11 hES-MPs are not affected by the chemical composition of cp-Ti and Ti6Al4V scaffolds 103

9. SUMMARY AND CONCLUSIONS 105

10. FUTURE DIRECTIONS 107

11. ACKNOWLEDGEMENTS 109

12. REFERENCES 111

1. ABSTRACT

The human skeleton represents the supporting structure of the organism and accounts for about 20 percent of the total body mass. Despite its intrinsic capacity to regenerate and self-repair, this ability is limited and repair therapies are needed in a large number of clinical cases. Bone engineering holds the potential to alleviate the increasing burden of bone deficiencies by constructing viable substitutes for replacement therapies. However, before bone engineering can realize its full potential, it is critical to assess the suitability of stem cells derived from different sources for the large-scale construction of bone-engineered substitutes.

The aim of the present thesis was to evaluate the potential of stem cells of embryonic origin for bone engineering applications. In particular, we investigated the potential of two cell lines, denoted matrix free-growth human embryonic stem cells (MFG-hESCs) and embryonic stem cell-derived mesodermal progenitors (hES-MPs). Cells were cultured *in vitro* under static and dynamic conditions, with and without ceramic and metal scaffolds as well as implanted *in vivo* as cell/scaffold constructs.

The results demonstrate that, under similar *in vitro* conditions, both MFG-hESCs and hES-MPs undergo osteogenic differentiation and display higher mineralization properties compared to human mesenchymal stem cells (hMSCs). Differentiation was associated with alteration in the expression of genes involved in ossification, and resulted in the synthesis of a matrix with high content of calcium phosphate deposits. Interestingly, following osteogenic differentiation, MFG-hESCs displayed decreased expression of genes involved in pluripotency and self-renewal, which are also responsible for teratoma formation. In particular, hES-MPs displayed morphological and molecular characteristics typical of hMSCs, but exhibited longer telomeric sequences and significantly higher proliferation ability both in monolayer and three-dimensional cultures. In addition, after flow perfusion stimulation, hES-MPs displayed increased tissue formation, denser collagen network and higher calcium content compared to hMSCs. Not least, hES-MPs displayed an immune profile similar to hMSCs, but did not express HLA-DR molecules. Noteworthy, the expression of HLA-DR was not stimulated following expansion, osteogenic differentiation and treatment with INF-γ. In line with this, hES-MPs did not elicit an immune response after subcutaneous implantation in immunocompetent mice. Finally, it was demonstrated that titanium scaffolds supported the attachment and growth of hES-MPs *in vitro*, and did not seem to affect the expression of genes involved in osteogenesis.

In conclusion, this thesis demonstrates that cells of embryonic origin, under experimental *in vitro* conditions, display some comparative advantages over stem cells derived from adult tissues, which are essential prerequisites for the large-scale production of bone substitutes for replacement therapies. Not least, MFG-hESCs and hES-MPs represent optimal cell technology platforms for the generation of experimental models to study bone histogenesis and explore tissue functionality in different conditions.

2. LIST OF ORIGINAL ARTICLES AND MANUSCRIPTS

This thesis is based on the following original articles and manuscripts:

I. Superior Osteogenic Capacity of Human Embryonic Stem Cells Adapted to Matrix-free Growth Compared to Human Mesenchymal Stem Cells.

Narmin Bidgeli, **Giuseppe Maria de Peppo**, Maria Lennerås, Peter Sjövall, Anders Lindahl, Johan Hyllner, Camilla Karlsson; *Tissue Eng Part A. 2010 Nov;16(11) 3427-40.*

II. Human Embryonic Mesodermal Progenitors Highly Resemble Human Mesenchymal Stem Cells and Display High Potential for Tissue Engineering Applications.

Giuseppe Maria de Peppo, Sara Svensson, Maria Lennerås, Jane Synnergren, Johan Stenberg, Raimund Strehl, Johan Hyllner, Peter Thomsen, Camilla Karlsson; *Tissue Eng Part A. 2010 Jul;16(7):2161-82.*

III. Osteogenic Potential of Human Mesenchymal Stem Cells and Human Embryonic Stem Cell-derived Mesodermal Progenitors: a Tissue Engineering Perspective.

Giuseppe Maria de Peppo, Peter Sjovall, Maria Lennerås, Raimund Strehl, Johan Hyllner, Peter Thomsen, Camilla Karlsson; *Tissue Eng Part A. 2010 Nov;16(11):3413-26.*

IV. Human Embryonic Stem Cell-derived Mesodermal Progenitors Display Substantially Increased Bone-like Tissue Formation Compared to Human Mesenchymal Stem Cells after Flow Perfusion.

Giuseppe Maria de Peppo, Martina Sladkova, Peter Sjovall, Anders Palmquist, Peter Thomsen, Herve Petite, Camilla Karlsson; *Submitted.*

V. Human Embryonic Stem Cell-derived Mesodermal Progenitors do not Elicit Immune Response *in vivo*.

Giuseppe Maria de Peppo, Christophe Vidal, Camilla Karlsson, Morad Bensidhoum, Johan Hyllner, Peter Thomsen, Herve Petite, Delphine Logeart-Avramoglou; *In Manuscript.*

VI. Free-form Fabricated Commercially-pure Ti and Ti6Al4V Porous Scaffolds Support the Growth of Human Embryonic Stem Cell-derived Mesodermal Progenitors.

Giuseppe Maria de Peppo, Anders Palmquist, Peter Borchardt, Maria Lennerås, Johan Hyllner, Anders Snis, Jukkaa Lausmaa, Peter Thomsen, Camilla Karlsson; *Submitted.*

3. ABBREVIATIONS AND SYMBOLS

3.1 Abbreviations

3D	Three-dimensional
BCA	Bicinchoninic acid
BMT	Methylthymol blue
BSA	Bovine serum albumin
CAD	Computer-aided design
cDNA	Complementary deoxyribonucleic acid
cp-Ti	Commercially-pure titanium
CPC	O-cresolphthalein complexone
cRNA	Complementary ribonucleic acid
Ct	Cycle threshold
DAPI	4′,6-diamidino-2-phenyldole
DAS ELISA	Dual-antibody sandwich enzyme-linked immunosorbent assay
DIG	Digoxigenin
DMEM	Dulbecco's modified eagle medium
DMEM-HG	High-glucose Dulbecco's modified eagle medium
DMEM-LG	Low-glucose Dulbecco's modified eagle medium
DNA	Deoxyribonucleic acid
dNTP	Deoxynucleotide triphosphate
dsDNA	Double-stranded deoxyribonucleic acid
EBM	Electron-beam melting
ECM	Extracellular matrix
EDTA	Ethylenediaminetetraacetic acid
eGFP	Enhanced green fluorecent protein
ELI	Extra low interstitial
ELISA	Enzyme-linked immunosorbent assay
ESCs	Embryonic stem cells
FBC	Full blood count
FBS	Fetal bovine serum
FC	Fold change
FDA	Fluorescein diacetate
FFF	Free-form fabrication
FITC	Fluorescein isothiocyanate
Fluc	Firefly luciferase
GCOS	GeneChip® operating software
GOA	Gene ontology annotation
HA	Hydroxyapatite
HBBS	Hanks' balanced salt solution
hEL	Human embryonic lung fibroblast
HEPES	4-(2-hydroxyethyl)-1-piperazineethanesulfonic acid

hES-MPs	Human embryonic stem cell-derived mesodermal progenitors
hESCs	Human embryonic stem cells
HLA	Human leucocyte antigen
HLA-ABC	Human leucocyte antigen ABC
HLA-DR	Human leucocyte antigen DR
hMSCs	Human mesenchymal stem cells
hrbFGF	Human recombinant basic fibroblast growth factor
HRP	Horse radish peroxidase
ICM	Inner cell mass
IHC	Immunohistochemistry
iPSCs	Induced-pluripotent stem cells
IVF	*In vitro* fertilization
MEF	Mouse embryonic fibroblast
MFG-hESCs	Matrix-free growth human embryonic stem cells
MOI	Multiplicity of infection
MSCs	Mesenchymal stem cells
NADH	Nicotinamide adenine dinucleotide
NC	Neonatal condrocytes
NCP	Non-collagenous protein
NEAA	Non essential aminoacids
NK	Natural killer
OD	Optical density
PBS	Phosphate buffer saline
PD	Population doubling
PE	R-phycoerythrin
PerCP	Peridinin chlorophyll protein complex
PerCP-Cy5	Peridinin chlorophyll protein complex-cyanine5
PEST	Penicillin-Streptomycin
PI	Propidium Iodide
pNPP	P-nitrophenylphosphate
PPI	Protein-protein interaction
RNA	Ribonucleic acid
ROI	Regions of interest
RT-PCR	Real-time polymerase chain reaction
SAPE	Streptavidin phycoerythrin
SCID	Severe combined immunodeficiency disease
SEM	Scanning electron microscopy
Tc	Lymphocyte T cytotoxic
Th	Lymphocyte T helper
Ti6Al4V	Titanium-aluminum-vanadium alloy
TMB	3,3′,5,5′-tetramethylbenzidine
TOF-SIMS	Time-of-flight secondary ion mass spectroscopy
UV	Ultraviolet

3.2 Gene and Protein Symbols

ALP	Alkaline phosphatase
AP1	Activator protein 1
ATF4	Activating transcription factor 4
AURKB	Aurora kinase B
BGN	Biglycan
BMI1	BMI1 polycomb ring finger oncogene
BMP	Bone morphogenetic protein
BMP1	Bone morphogenetic protein 1
BMP2	Bone morphogenetic protein 2
BMP4	Bone morphogenetic protein 4
BMP7	Bone morphogenetic protein 7
BMPR2	Bone morphogenetic protein receptor, type 2
BSP	Bone salioprotein
BUB1	Budding uninhibited by benzimidazoles 1
BUB1B	Budding uninhibited by benzimidazoles beta
c-FOS	v-fos FBJ murine osteosarcoma viral oncogene homolog
c-JUN	v-jun sarcoma virus 17 oncogene homolog
c-myc	v-myc myelocytomatosis viral oncogene homolog
CAV1	Caveolin 1
CBFB	Core binding factor β
CD34	Cluster of differentiation 34
CD44	Cluster of differentiation 44
CD45	Cluster of differentiation 45
CD47	Cluster of differentiation 47
CD58	Cluster of differentiation 58
CD80	Cluster of differentiation 80
CD86	Cluster of differentiation 86
CD105	Cluster of differentiation 105
CD166	Cluster of differentiation 166
CDC20	Cell division cycle 20 homolog
CDC25A	Cell division cycle 25 homolog A
CDCA8	Cell division cycle associated 8
CDKN2A	Cyclin-dependent kinase inhibitor 2A
CENPA	Centromere protein A
CENPM	Centromere protein M
CLDN3	Claudin 3
CLDN6	Claudin 6
CLDN8	Claudin 8
CLDN10	Claudin 10
COL1	Collagen, type I
COL1A1	Collagen, type I, alpha 1
COL1A2	Collagen, type I, alpha 2
COL3A1	Collagen, type III, alpha 1
COL5A1	Collagen, type V, alpha 1

COL6A1	Collagen, type VI, alpha 1
COL6A2	Collagen, type V, alpha 2
COL11A1	Collagen, type XI, alpha 1
DDR2	Discoidin domain receptor tyrosine kinase 2
DLX3	Distal-less homeobox 3
DLX5	Distal-less homeobox 5
DNMT3B	DNA (cytosine-5-)-methyltransferase 3 beta
DPPA4	Developmental pluripotency associated 4
EGF	Epidermal growth factor
EGFR	Epidermal growth factor receptor
EPHA1	EPH receptor A1
ERCC6L	Excision repair cross-complementing rodent repair deficiency complementation
EREG	Epiregulin
FBN1	Fibrillin 1
FGF	Fibroblast growth factor
FGF5	Fibroblast growth factor 5
FN1	Fibronectin 1
FOXC1	Forkhead box C1
GABRB3	GABA A receptor, beta 3
GAL	Galanin prepropeptide
GDF3	Growth differentiation factor 3
HELLS	Helicase
IGF	Insulin-like growth factor
IL-2	Interleukin 2
IL-4	Interleukin 4
INF-γ	Interferon-gamma
KRT7	Keratin 7
KRT8	Keratin 8
KRT18	Keratin 18
KRT19	Keratin 19
LDH	Lactate dehydrogenase
LHX8	LIM homeobox 8
LIN28	Lin-28 homolog
MAD2	Mitotic arrest deficient-like 1
MCM5	Minichromosome maintenance complex 5
MCM10	Minichromosome maintenance complex 10
MFAP5	Microfibrillar associated protein 5
MLF1IP	Centromere protein of 50 kDa
MSX1	Msh homeobox 1
MSX2	Msh homeobox 2
NANOG	Nanog homeobox
NDC80	NDC80 homolog, kinetochore complex component
NUF2	Cell division cycle-associated protein 1
OC	Osteocalcin
OCT4	Octamer-binding transcription factor 4
ON	Osteonectin
OPN	Osteopontin

ORC1L	Origin recognition complex, subunit 1-like
OSX	Osterix
p53	Tumor suppressor p53
PDGF	Platelet-derived growth factor
POU5F1	POU class 5 homeobox 1
POU5F1P3	POU class 5 homeobox 1 pseudogene 3
POU5F1P4	POU class 5 homeobox 1 pseudogene 4
RUNX2	Runt-related transcription factor 2
SOX2	Sex determining region Y-box 2
SPC24	Spindle pole body component 24 homolog
SPC25	Spindle pole body component 25 homolog
SRGN	Serglycin
TDGF1	Teratocarcinoma-derived growth factor 1
TFAP2A	Transcription factor AP-2 alpha
TFN-α	Tumor necrosis factor alpha
TGF-β	Transforming growth factor beta
TGFβ1	Transforming growth factor beta 1
TGFβ2	Transforming growth factor beta 2
TGFβR2	Transforming growth factor receptor beta 2
TSP	Thrombospondin
TWIST1	Twist homolog 1
TWIST2	Twist homolog 2
VEGF	Vascular endothelial growth factor
ZIC3	Zic family member 3
ZWINT	ZW10 interactor

4. INTRODUCTION

4.1 Tissue Engineering

Tissue and organ failure, originated as a result of congenital malformations, damage or degenerative processes, constitute a major health problem associated with disability and death [1]. Transplantation of tissues and organs from living and deceased donors is today saving the life of several patients worldwide. Despite this, transplantation has never achieved its full potential, especially considering the shortage of tissues and organs [2] and the immunological response to the transplanted material [3, 4]. In fact, even though a patient is able to receive an allotransplant, lifelong immunosuppression is required. The annual global healthcare costs for these patients is enormous and is facing a consistent increase [5], mainly due to the rapid growth of the human population and extension of life expectancy [6, 7]. In this view, the ability to reconstitute biological tissues and manipulate tissue function is going to represent a major scientific revolution (*"paradigm shift"*) with unprecedented social and clinical implications. The emerging field of tissue engineering holds the promise to provide unlimited supply of engineered tissues and organs to reduce the burden of tissue loss and end-stage organ failure, and overcome the limitations encountered with tissue and organ transplantation [1, 8, 9]. Tissue engineering is an interdisciplinary field that applies the principles of engineering and life sciences toward the development of substitutes that restore, replace, maintain, or enhance the function of a particular tissue or organ [1, 10]. In addition to the potential clinical use as an alternative to tissue and organ transplantation, engineered tissues and organs may also be used as three-dimensional (3D) models for the study of complex tissue functions and morphogenesis [11, 12], as well as a tool for *in vitro* drug-screening applications [13].

4.1.1 The Tissue Engineering Quadriad

Tissue engineering aims at promoting the *in vivo* regeneration/restoration of functional 3D tissues through several strategies, such as implantation of acellular matrices, injection of progenitor cells and grafting of cell/scaffold constructs [14-18] (in this view tissue engineering overlaps with the field of regenerative medicine and cell therapy, and the above terms are interchangeably used in this thesis). The implantation of *ex vivo* fabricated cell/scaffold

constructs is currently the major vision in tissue engineering. The *ex vivo* fabrication of tissue-engineered substitutes requires to interface stem cells to biomaterials as suitable scaffolds for the cells to attach, proliferate and differentiate toward the specific lineage [14, 19].

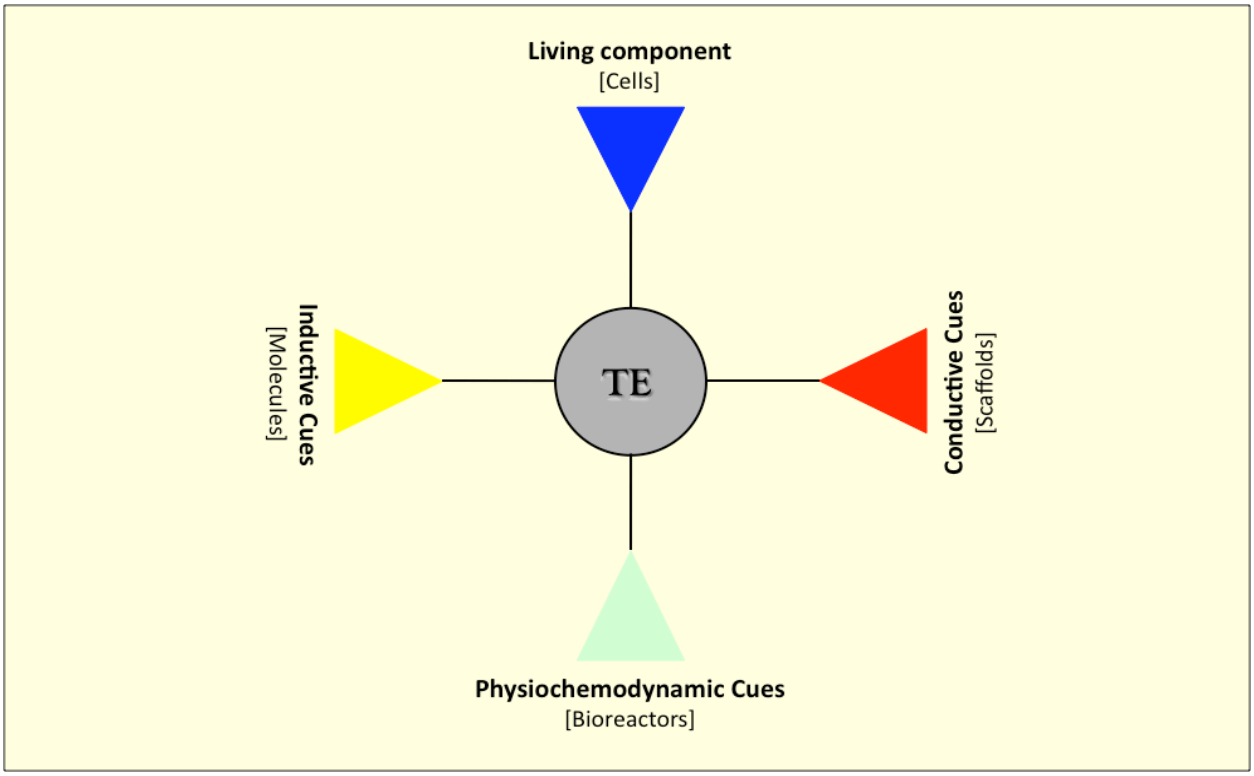

Figure 1: Tissue engineering quadriad.

To induce stem cell differentiation toward the desired lineage, cell/scaffold constructs are eventually treated with appropriate chemicals and cultured within bioreactors to provide the optimal physiochemical conditions for the successful development of functional substitutes [20].
In this view, cells, scaffolds, inductive molecules and bioreactors constitute the key components of tissue engineering as illustrated in Figure 1.

4.1.2 Stem Cells

Stem cells represent the building blocks of our bodies and have been defined as the natural units of embryonic generation and adult regeneration [21]. Stem cells are distinguished from other cell types by two important characteristics. First, they are unspecialized cells capable of renewing

themselves through cell division, sometimes after long periods of inactivity (self-renewal). Second, under certain physiologic or experimental conditions, they can be induced to become tissue- or organ-specific cells with special functions (potency) [22, 23]. These two properties make stem cells unique and ideal for tissue engineering applications [24]. Based on where in the body or what stage in development they are derived from, stem cells are classified as embryonic (derived from the totipotent cells of early embryo), fetal (derived from the developing fetus) and adult stem cells (derived from mature organs in the adult individual) [22]. Recently, induced pluripotent stem cells (iPSCs) were artificially derived from non-pluripotent cells by specifically inducing the expression of genes involved in self-renewal and potency [25-27]. Among the different types of stem cells reported above, embryonic stem cells (ESCs) and iPSCs hold the potential to provide unlimited supply of cells for tissue engineering applications [28-30], especially considering their high proliferative potential and pluripotency (or ability to virtually differentiate toward all cell types constituting the human body). However, the elaborate culture conditions required for their propagation [31] and the tendency to form teratoma after *in vivo* implantation are today hampering their use for clinical applications [30, 32-34].

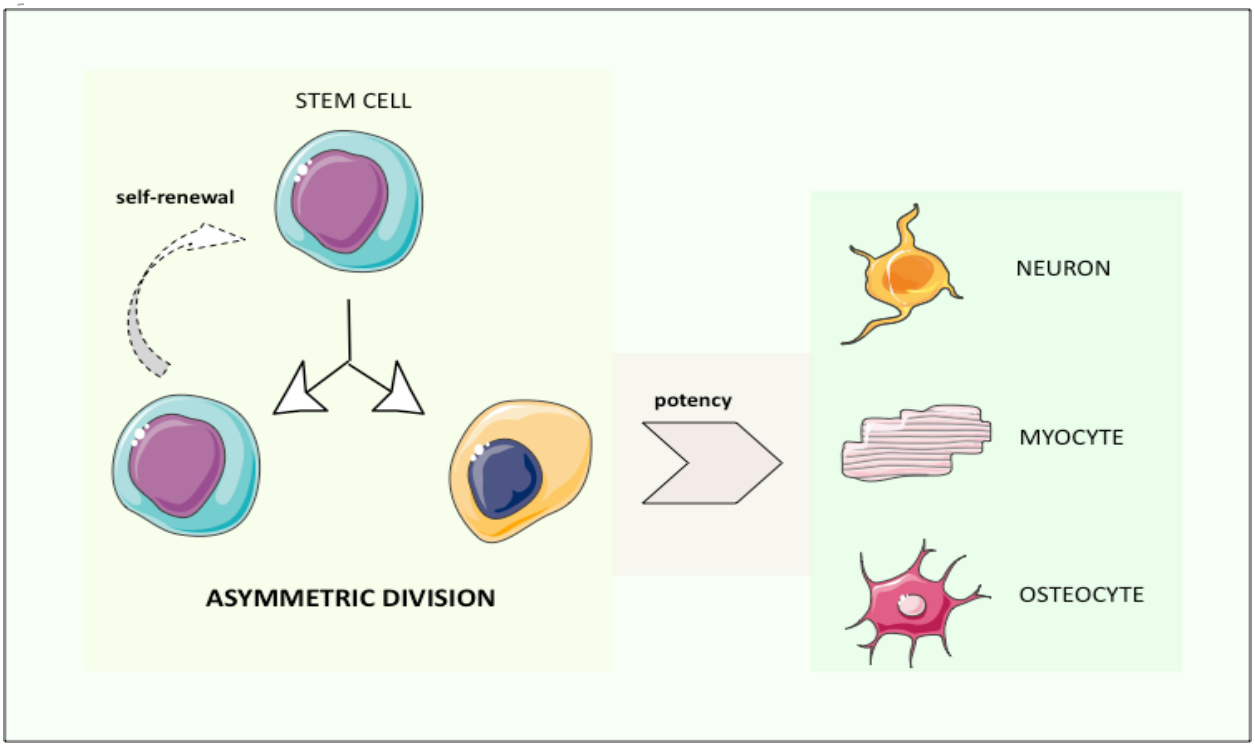

Figure 2: Asymmetric division of a stem cells displaying the properties of self-renewal and potency.

An alternative is to use ESCs as source for the derivation of alternative cell lines, which display relevant properties and comparative advantages over stem cells derived from adult tissues, including availability, homogeneity, higher proliferative ability and good tissue-forming capacity [31, 35-38]. In Figure 2 a schematic illustration representing the stem cell properties of self-renewal and potency is shown.

4.1.3 Scaffolds

In the human body, cells are usually embedded within the extracellular matrix (ECM), which provides structural support and anchorage for the cells, regulate cell function and intercellular communication and plays a central role in developmental and regeneration [39]. Based on this knowledge, tissue engineering requires interfacing stem cells with suitable scaffolds for the cells to attach, proliferate and differentiate toward a specific lineage [14, 19]. Different materials have been used for the synthesis and manufacturing of biomaterials for tissue engineering applications, such as metals and alloys [40], ceramics [41], polymers [42] (both natural and synthetic) and composites [43]. Each class of material exhibits specific characteristics, mainly due to their particular molecular structures, and therefore become suitable for specific applications [44]. In Figure 3 two scaffold materials used in this thesis are shown.

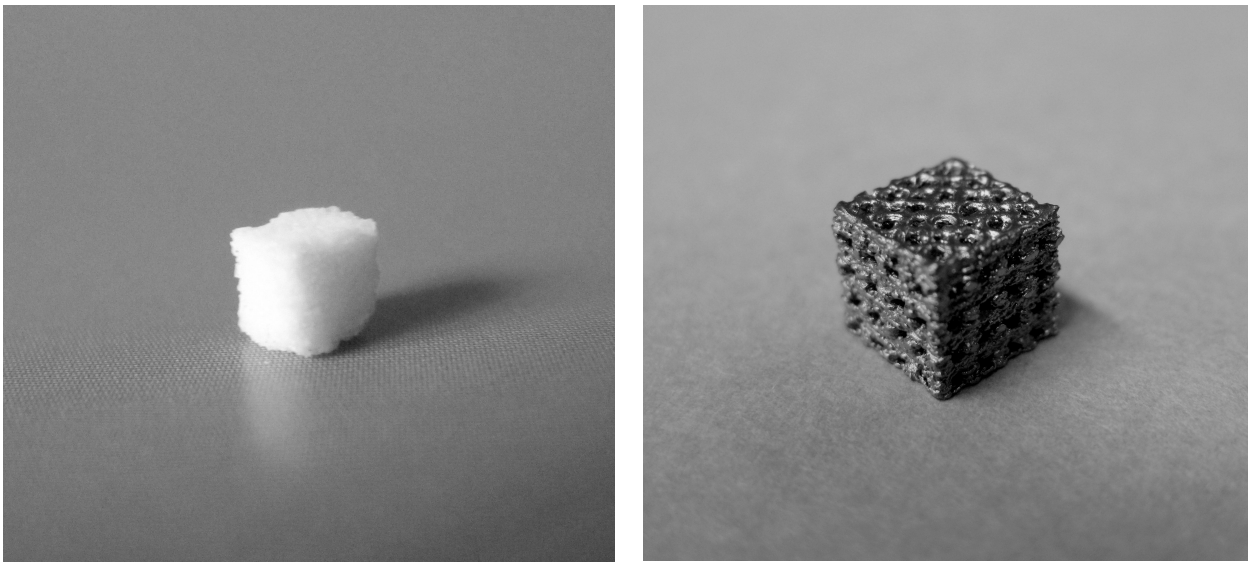

Figure 3: Biocoral (*left*) and commercially-pure titanium (*right*) scaffolds.

4.1.4 Inductive Cues

Cell proliferation, differentiation and function are thoroughly coordinated during development and tissue homeostasis, and are dependent on a specific combination of biophysical and biochemical signals [45]. In this view, engineering functional tissues requires the use of specific signaling molecules to promote stem cell proliferation and eventually prime specification of functional cells [46, 47]. A large spectrum of different stimulatory molecules have been used [14], including synthetic molecules [48], growth factors and hormones [49], cytokines [50], vitamins, and others [51, 52].

4.1.5 Bioreactors

Cells in the human body are constantly subjected to temporal and spatial gradients of chemical and mechanical stimuli (physiochemodynamic cues), which ensure cell functionality and contribute to tissue organization [20, 53]. Based on this knowledge, the development of culture strategies is emerging as an essential factor to improve proliferation and differentiation of the cells in the scaffold by enabling nutrient supply, providing mechanical stimulation and a proper environment for the reproducible and large scale production of tissues.

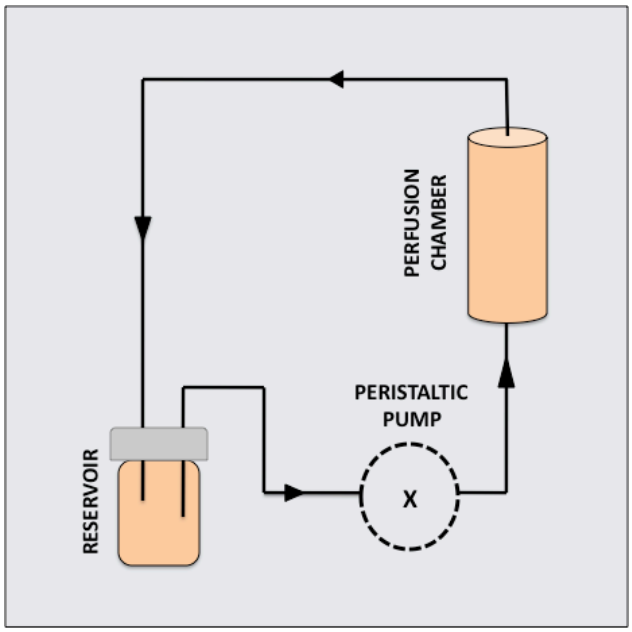

Fig 4: Schematic illustration of a flow perfusion system, showing the medium reservoir, the peristaltic pump, the perfusion chamber and the direction of flow.

Therefore, the use of bioreactors is becoming a fundamental step for the fabrication of functional

3D cell/scaffold constructs for tissue engineering applications. Bioreactors are defined as *"any device which is designed to contain structures, both cellular and molecular, that are capable of taking part in a specific biological process and from which the products of that process can be harvested or extracted"* [54]. Several bioreactors have been designed so far, and successfully used as reaction chambers for the synthesis of tissues and organs, including spinner flasks [55, 56], perfusion systems [57-59], rotating wall vessels [60, 61], pulsatile flow reactors [62, 63], and others [64]. In Figure 4 a schematic illustration of a flow perfusion bioreactor used in this thesis is shown.

4.1.5 Social Impact and Experimental Trends

The possibility to engineer human tissues and organs is generating great enthusiasm throughout the scientific community worldwide, especially in relation to the profound social impact this new technology is going to have by improving the health status and quality of life of patients. So far, despite the technical and regulatory challenges, tissue engineering has shown encouraging results [65], with several tissue substitutes experimentally developed by different investigators around the world, including skin [66], cartilage [67, 68], bone [41], skeletal muscle [69], cardiovascular tissues [70, 71], liver [72], trachea [73], urogenital tissues [74], as well as neural tissues [75]. In particular, especially considering the large volume and functional importance of the skeletal system, as well as the aging of the world population, large efforts have been made over the past years in finding engineering solutions for the construction of bone substitutes. However, despite the ongoing efforts, many challenges remain and no adequate bone substitute has been engineered yet.

4.2 The Skeletal System

In the vertebrates the skeletal system performs the function of providing support and protection, allowing body movements, storing minerals and fat, as well as participating in endocrine regulation of energy metabolism. In addition, in the adult organisms, many bones contain cavities filled with the bone marrow, and represent the anatomical site for blood cells and platelets production (haematopoiesis) [76]. The skeletal system includes all bones of the body, as well as additional tissues involved in bone connection and movement, such as cartilage, ligaments (bone-to-bone connection) and tendons (bone-to-muscle connection) [77].

4.2.1 The Human Skeleton

The human skeleton accounts for about 20 percent of the total body weight in a regular-sized person. The adult human skeleton is composed in average of 206 individual bones (this number does not include human teeth, which are part of the skeleton but display different structure and composition). Individual bones are classified according to their shape in long bones, short bones, flat bones, irregular bones and sesamoid bones [77, 78]. In figure 5 the human skeleton with its individual bones is shown.

4.2.2 Bone Cellular Components

Bones are mainly constituted of three different cell types, categorized as osteoblasts, osteocytes and osteoclasts. Osteoblasts, which derive from mesenchymal stem cells (MSCs) [79, 80], are cuboidal post-proliferative cells with high synthetic activity and responsible for bone extracellular matrix deposition and mineralization [77, 81, 82]. Osteocytes are star-shaped mature osteoblasts, smaller in size, which are embedded in a mineralized matrix and represent 90 percent of all cells in bone [81, 83]. Osteoclasts are instead multinucleated cells of hematopoietic origin with osteolytic properties, and are responsible for bone resorption [84, 85]. The coordinated action of osteoblasts and osteoclasts secure bone homeostasis during development and remodeling throughout lifetime [86].

4.2.3 Bone Extracellular Matrix

The ECM of mature bone tissue is composed of 30-40 percent of organic

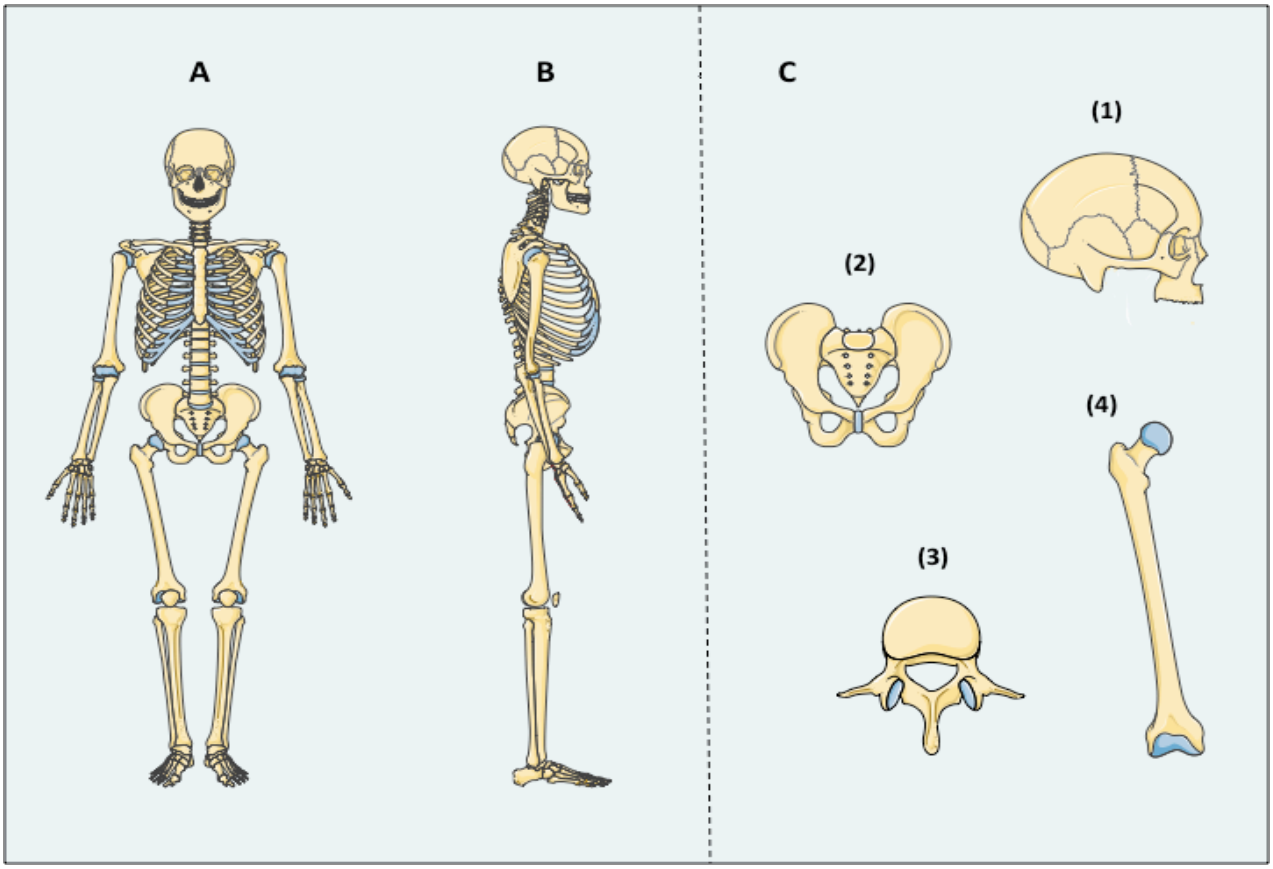

Figure 5: Frontal (A) and lateral (B) view of the complete human skeleton specifically showing details (C) of flat (1), irregular (2, 3) and long (4) bones constituting the human body.

matrix and 60-70 percent (dry weight) of mineral substance. The organic material mainly consists of type I collagen fibrils (85-90 percent) embedded in the ground substance containing proteoglycan aggregates (mainly biglycan and decorin) and glycoproteins. Glycoproteins represent the largest proportion of non-collagenous proteins (NCPs) and include TSP [87], BSP [88], ALP in its extracellular form [89], ON [90], OC [91] and OPN [92, 93]. The sequence of most NCPs includes high density of amino acids with high affinity for calcium, such as aspartic and glutamic acid residues [94]. The inorganic material consists mainly of calcium phosphate crystals in the form of hydroxyapatite (HA) with molecular formula $Ca_{10}(PO_4)_6(OH)_2$ [95], although bicarbonate, citrate, magnesium, potassium and sodium are also found [96]. Both the organic and inorganic components constituting the ECM of bones represent markers of particular interest in order to assess the formation of functional bone substitutes in tissue engineering and regeneration procedures.

Table 1: Major non-collagenous protein properties and functions.

Non-collagenous proteins	Properties	Function
TSP	Glycoprotein	Binds Ca^{++} and collagen Facilitates HA nucleation Modulates development and healing [87, 97]
BSP	Sialoglycoprotein	15% of the total NCPs Binds Ca^{++}, HA and collagen Facilitates HA nucleation Involved in bone mineralization Involved in remodeling [88, 98]
ALP	Glycoprotein	Involved in mineralization [99, 100]
OC	Gla protein	20% of the total NCPs Binds Ca^{++} and HA Regulates mineralization [91, 101, 102]
ON	Glycoprotein	Binds Ca^{++}, HA and collagen Prevents HA crystal growth Involved in cell attachment Modulates MSC osteogenic differentiation [90, 103]
OPN	Sialoglycoprotein	Prevents HA crystal growth Involved in cell attachment Modulates development and healing [92, 104]

4.2.4 Woven and Lamellar Bone

Bone as biological tissue exists in two histological types. Woven bone (or primary bone tissue) is an immature type of bone, characterized by the deposition of randomly orientated coarse collagen fibers, poor mineral content and high osteocyte density [105], and found in early-developed bones and during the initial phases of fracture healing. As opposite, lamellar bone (or secondary bone tissue) is the mature bone and it is characterized by a hierarchical organization of regular structures, in which collagen fibers are orientated in parallel sheets or lamellae (as indicated in Figure 6) [96].

4.2.5 Structural Types of Bone

Microscopically bones exist in two different structural forms: compact and trabecular. Compact or cortical bone forms the cortex, or outer shell, of most bones and contributes to about 80 percent of the weight of a human skeleton. Cortical bone is made of a system of functional units called osteons (or Haversian system), each formed by concentric lamellae of compact bone surrounding the Haversian canal, in which blood vessels and nerves are contained. In between the lamellae osteocytes are laid down, the most abundant cells found in compact bone, which intercommunicate via long cytoplasmic extensions that occupy tiny canals called canaliculi. Each osteon is in direct contact with the periosteum, the bone marrow and other osteons through the Volkmann's canals. Trabecular or cancellous bone instead consists of a series of fine spicules (trabeculae) forming an interconnected network of bone tissue. Each trabecula is made of several concentric lamellae with osteocytes located between the lamellae. The cavities of the cortical bone are filled with bone marrow and occupied by blood vessels. The surface of bones is covered by the periosteum (outer) and endosteum [106], two membranes of connective tissue containing the

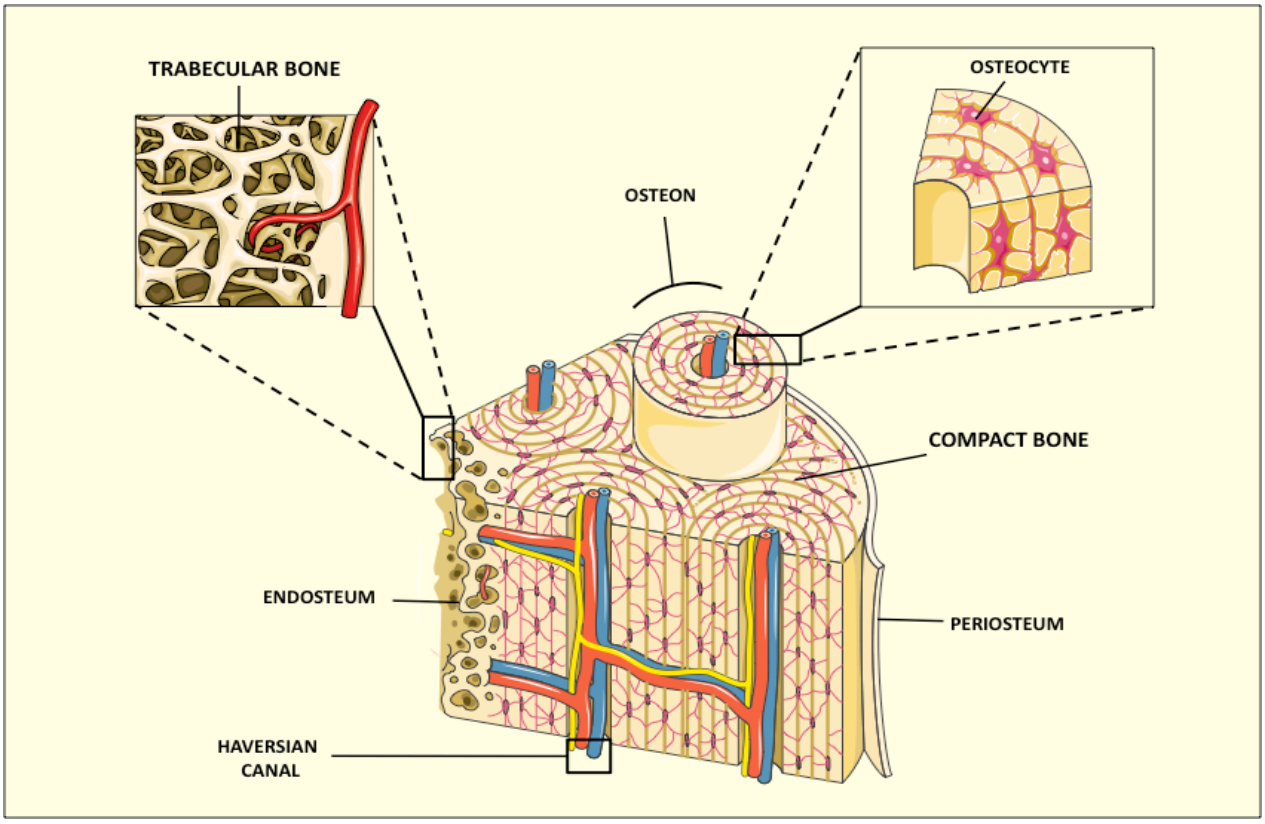

Figure 6: Internal features of a portion of a long bone showing the periosteum, the endosteum, the Haversian systems and structural characteristics of the trabecular bone.

osteoprogenitor cells, which develop into osteoblasts and provide a continuous supply of cells supporting bone growth, remodeling and repair [77, 78]. In figure 6, the structure and organization of compact and trabecular bone are shown.

4.2.6 Bone as a Composite Material

Mature bone is a two-phase porous composite material with a complex hierarchical structure, in which the HA crystals are arranged in parallel layers within the collagen framework [107-109] surrounded by ground substance [96]. The unique composition and organization of the bone matrix is responsible for the exceptional mechanical properties of bone [110]. The collagen fibers within the matrix confer the adequate toughness to the tissue [111], whereas the mineral components provide strength and stiffness [110]. Mineral content and composition, crystal size and orientation, collagen fiber organization, shape and porosity [112] all influence the mechanical properties of bone tissue [113], and alteration in some of these features are recognized to affect bone quality in elderly people and patients with bone-weakening diseases in general [114-116].

Table 2: Mechanical properties of human bone.

CORTICAL BONE	**Strength (MPa)**	**Young's Modulus (MPa)**
Compression test	219 ± 26 Longitudinal 153 ± 20 Transverse	14.1 - 27.6
Tensile test	172 ± 22 Longitudinal 52 ± 8 Transverse	7.1 - 24.5
Torsional test	65 ± 9	-
TRABECULAR BONE	**Strength (MPa)**	**Young's Modulus (MPa)**
Compression test	1.5 ± 9.3	0.1 - 0.4
Tensile test	1.6 – 2.42	10.4 ± 3.5
Torsional test	6.35 ± 2	-

*Compiled from references [117-120].

4.2.7 Bone Histogenesis

Bone histogenesis during fetal development occurs in two different patterns called

intramembranous ossification and endochondral ossification. Intramembranous ossification occurs during development of flat bones and peripheral to the site of the fracture during bone healing. During intramembranous ossification, cells of the mesenchymal lineage, which are embedded into a membrane of connective tissue, directly undergo osteogenic differentiation and synthesize the osteoids (unmineralized matrix), which eventually mineralize. On the other hand, endochondral ossification takes place during the development of short and long bones, the growth of the length of long bones (growth plate), and during the natural healing of bone fractures (callus ossification). Upon endochondral ossification, MSCs aggregate [121] and differentiate toward the chondrogenic lineage, and form a transitory hyaline cartilage tissue (model). Subsequently, the chondrocytes become hyperthrophic and the surrounding matrix calcifies. After calcification the chondrocytes die and a network of blood vessels form, which carry the osteoprogenitor cells responsible for the synthesis and mineralization of the osteoids. During the development of long bones, two ossification centers form, respectively within the diaphyseal (the midsection region of bone) and epiphyseal regions (the round end of bone). In between the primary and secondary ossification centers, areas of proliferating chondrocytes (epiphyseal or growth plate) secure bone formation and growth [77, 122, 123]. In Figure 7 a schematic representation of the endochondral ossification process is shown.

4.2.8 Bone Remodeling and Repair

Bone is a very dynamic tissue, which undergoes constant remodeling throughout lifetime and display regeneration properties after injury. Remodeling is the result of the complex interplay between osteoclasts and osteoblasts, which secure bone resorption and deposition respectively [86], and is regulated by the coordinated action of different biochemical and biophysical stimuli [124]. The process of remodeling mainly occur to repair small bone fractures and is required for the maintenance of a normal healthy bone, as well as for adaptation to external stress and loading [125]. As result of remodeling about 5 percent of cortical bone and 20 percent of trabecular bone are renewed every year [124]. Unbalanced bone formation/resorption activity is associated with bone weakening [126] and is considered to be a major cause leading to osteoporosis [127]. In Figure 8 a schematic illustration of the bone remodeling process is shown. Beside the remodeling ability, bone tissue displays an intrinsic capacity to self-repair structural defects after injury.

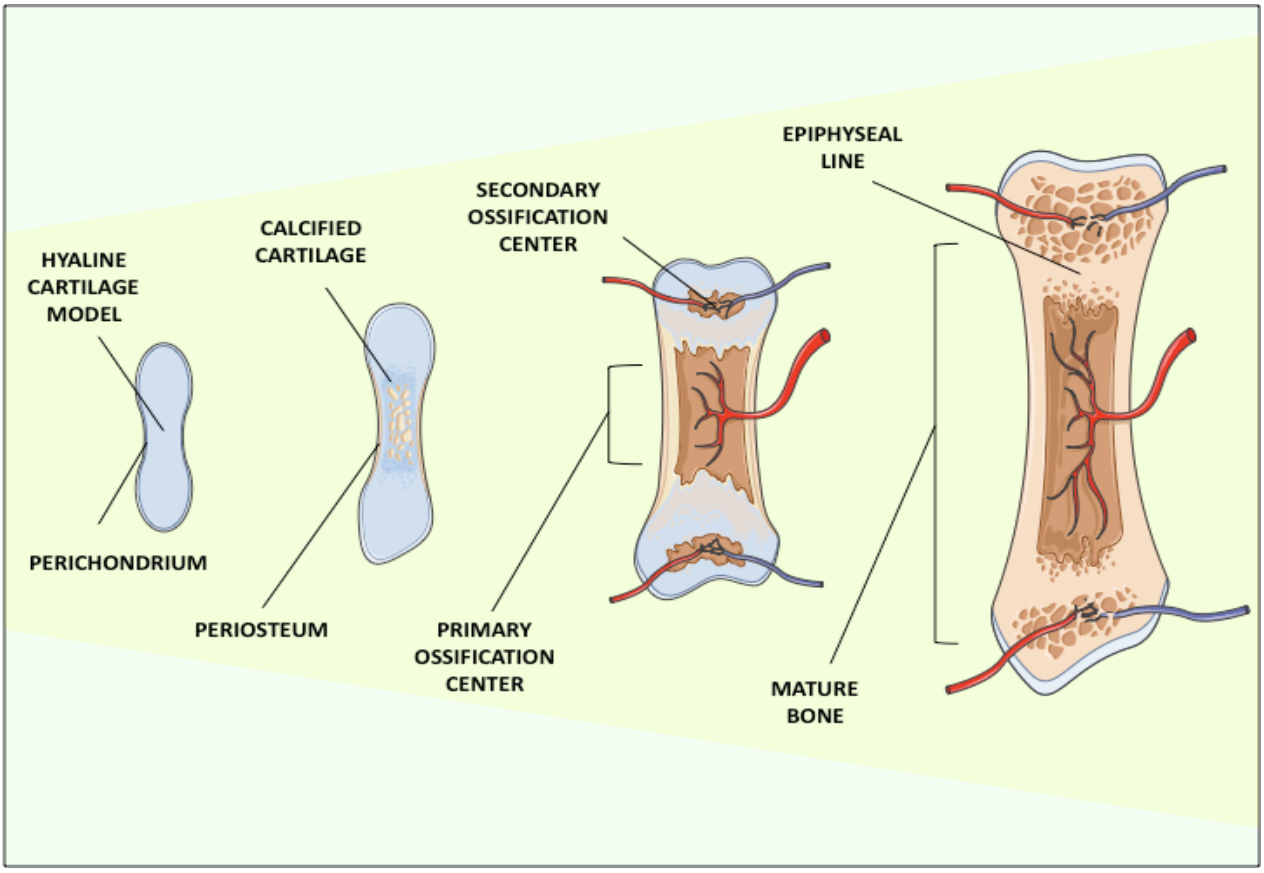

Figure 7: Endochondral ossification process of a long bone showing the formation of the cartilage model, the penetration of blood vessels and the development of the primary and secondary ossification centers.

Soon after damage a blood clot (hematoma) forms and inflammation occurs at the site of injury. This process is associated with the release of several signaling molecules responsible for bone regeneration, such as FGF, BMP, PDGF and VEGF [128]. The lack of blood supply leads to osteocyte death and scar formation. Subsequently, macrophages remove tissue debris, osteoclasts resorb dead bone tissue and fibroblasts deposit a network of collagen fibers holding together the two extremities of the fractured bone. The provisional network of fibrotic tissue is eventually invaded by progenitor cells homing from the bone marrow, endosteum and periosteum, which differentiate toward both the chondrogenic and osteogenic lineage and form an immature tissue of connection (callus), which ossifies toward the formation of woven trabecular bone through a combination of intramembranous and endochondral ossification [77].

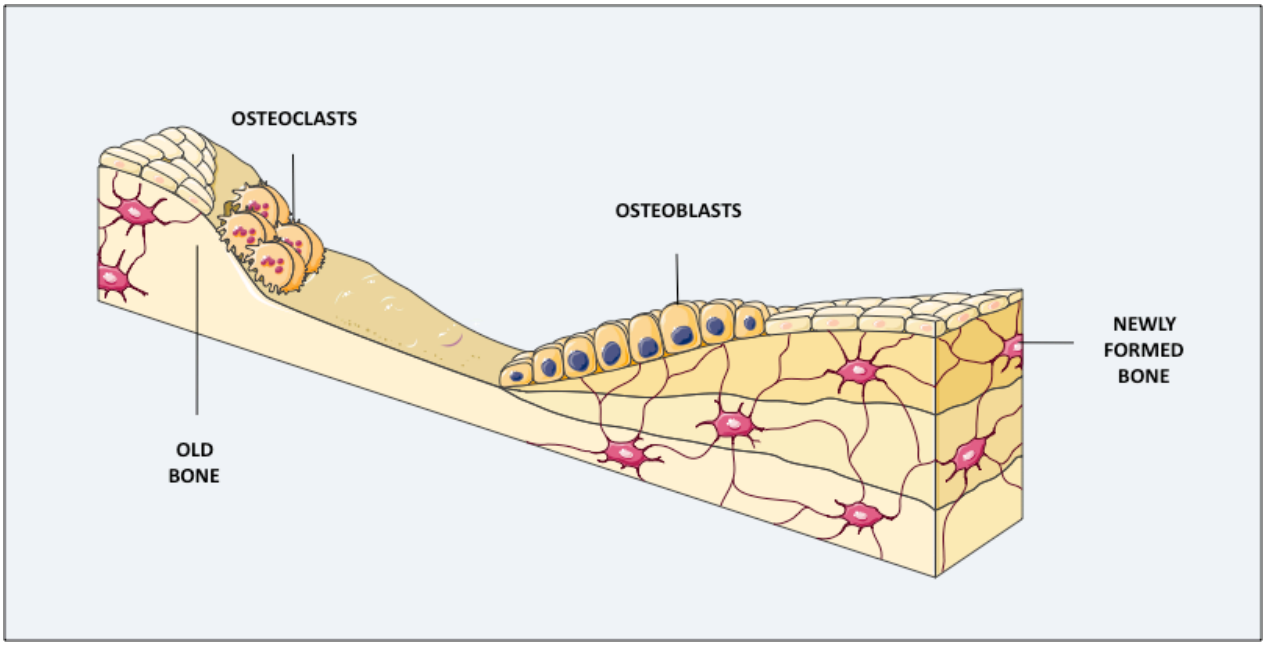

Figure 8: Bone remodeling process showing the coordinated action of osteoclasts and osteoblasts.

The exact contribution of the two ossification mechanisms depends on the site and type of fracture. The repair process is not complete until the transitional woven bone is replaced by mature lamellar bone [130]. In Figure 9 the process of bone repair is shown.

4.2.9 Molecular Regulation of Bone Histogenesis

Bone formation during development, remodeling and repair is regulated by a large number of signaling pathways and transcription regulators. A list of major signaling pathways playing a role in bone histogenesis includes Wnt, TGFβ/BMP, Notch, Hedgehog and FGF pathways [131, 132]. After activation, the different pathways lead to the generation of specific transcription factors and regulators, involved in controlling the expression of genes responsible for proliferation and differentiation. The central role of these signaling pathways in regulating bone formation has been elegantly demonstrated by a large number of loss-of-function studies leading to different types of skeletal abnormalities and *in vitro* studies affecting bone formation [133-153], although a clear and complete elucidation of the regulatory circuits governing bone histogenesis is still far to be achieved. Stem cell specification toward the osteogenic lineage is basically regulated by the combined action of three transcription factors, such as RUNX2, OSX and nuclear β-catenin [154]

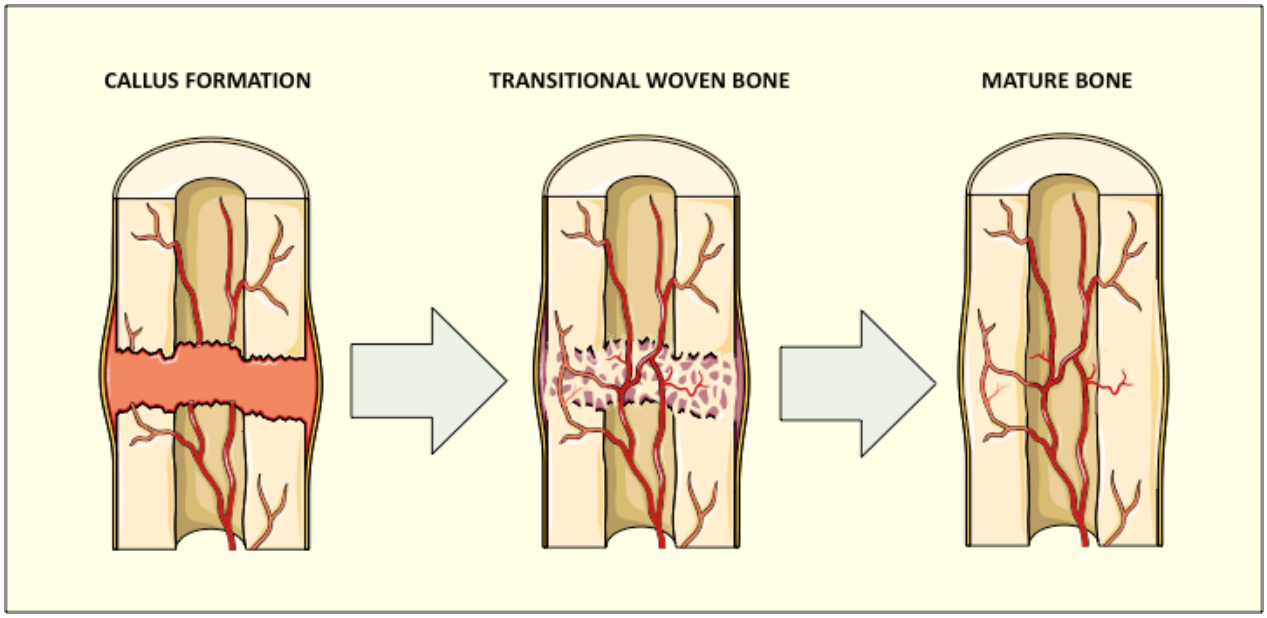

Figure 9: Bone repairing process showing the callus formation, the transitional deposition of woven bone and its final maturation to bone tissue.

(an end-product of the Wnt signaling pathways [155]), and knock-out animal models for these factors display impaired or lack bone formation due to absence of osteoblast differentiation [156-159]. Several experimental studies suggest that RUNX2 directs osteogenesis in the early phases of stem cell differentiation, while OSX and nuclear β-catenin act downstream consolidating the transition toward the osteoblastic phenotype [158, 160-162]. RUNX2, in association with CBFB [163], is recognized to upregulate the expression of several bone matrix genes, including COL1, OP, BSP, and OC [164-167], and therefore largely used as marker for osteogenic differentiation. However, the level of RUNX2 does not always correlate with the expression of the downstream bone matrix genes. In fact, the function of RUNX2 is modulated by a set of several additional transcription factors and co-regulators, which interact with or regulate the expression of RUNX2, hence enhancing or inhibiting its activity, including MSX1 and MSX2 [168], DLX 3 and DLX5 [169, 170], TWIST1 and TWIST2 [171], AP1-related nuclear factors such as c-FOS and c-JUN [172, 173], and ATF4 [174]. In Figure 10 a set of molecular components influencing RUNX2 expression and function are shown.

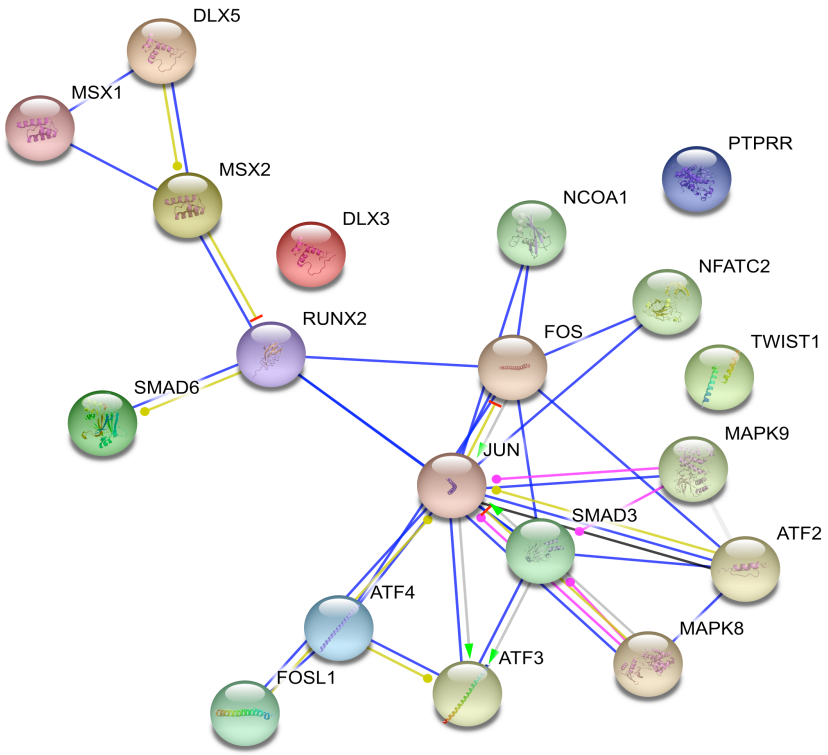

Figure 10: Set of molecular components interacting with RUNX2 and regulating its expression and function. The network shows experimentally-based interactions obtained with STRING web resource 8.3 [175].

4.3 Bone Deficiency, Clinical Needs and Current Treatments

Despite the intrinsic capacity of bone to regenerate and self-repair, this ability is limited to small fractures and therapeutic solutions need to be applied to promote bone healing in case of defects of crucial size (delayed union and nonunion fractures) [176]. Moreover, bone replacement therapies are needed to obviate bone deficiencies associated with reconstruction of congenital [177] and traumatic [178] skeletal defects, cosmetic procedures, degenerative disorders (i.e. osteoporosis) and surgical resection following neoplastic transformation [179] and chronic infection [180]. The worldwide market for bone replacement and repair therapies was estimated to be approximately €300 millions in 2003 [181], with a number of bone grafting procedures reaching 2.2 million in 2006 [182]. Especially considering the burden of nonunion fractures in osteoporotic patients, the need for bone tissue substitutes is constantly increasing due to the rapid growth of human population and extension of life expectancy [7, 183]. Today, the number of elderly reporting age-related fractures is estimated to be nearly 100 million per year worldwide [184-186], and this number is projected to massively increase over the next decades, with the number of elderly people (+65 years) estimated to be about 2 billion by 2050 [187]. In several clinical cases associated with bone deficiency, patient comfort and bone functionality can only be restored by surgical reconstruction. Current treatments for these patients are based on the transplantation of autogeneic and/or allogeneic bone grafts, or implantation of graft materials with osteoconductive and osteoinductive properties [188-190]. Autogeneic bone grafts (autograft) represent the gold standard treatment for bone replacement procedures, due to immune tolerability and provision of essential components supporting bone regeneration and repair, resulting in fast integration and revascularization [191]. However, limited availability and donor site morbidity restrict their use in several clinical cases [192]. On the other hand, allogeneic bone grafts (allograft), which are usually derived from decellularized (and demineralized) living or cadaveric bone tissue, are available in large amounts but integrate slowly [193], carry the risk of infection transmission and may display immune incompatibility leading to transplant rejection [194]. Beside their respective advantages, both autograft and allograft lack the potential to provide large customized bone substitutes for the exact reconstruction of complex bone defects in particular clinical situations. Implantation of synthetic graft materials overcomes some of the restrictions encountered with auto- and allografts, such as disease transmission, complex shape and availability. However, they display poor integration and lack biological functionality and mechanical compliance, which usually lead to implant failure and substitution [195], especially in patients with poor bone quality, associated for

example with degenerative disorders [196] and diabetes [197]. There is therefore an urgent need to find alternative solutions for the design of optimal bone substitutes, which display high osteoinductive and angiogenic potential, biological functionality, large-scale availability, safety and reasonable cost [198]. Bone tissue engineering represents a promising strategy to obviate bone deficiency, allowing the *ex vivo* construction of bone substitutes with unprecedented potential in the clinical practice [198-201].

4.4 Bone Engineering

Bone tissue engineering is a rapidly evolving technology, which aims at generating bone substitutes for the reconstruction of skeletal defects. Beyond the use and implantation of acellular scaffolding biomaterials, bone engineers envision the possibility to interface stem cells to biomaterials for the *ex vivo* construction of bone-engineered constructs that functionally resemble the native tissue and/or promote a stable and enduring integration of the implanted construct. After *in vivo* implantation, the bone-engineered constructs ought to i) establish an appropriate connection with the surrounding tissue, ii) preserve cell viability and promote the regeneration of a functional tissue, iii) be immune tolerated and/or not elicit any adverse reaction [9, 14, 19]. Stem cell-based bone engineering dates back to 1995, when de Bruyn *et al*. reported the ability of bone marrow cells to form bone after ectopic implantation in rabbits [202]. Since then, a large number of experiments have been reported, both *in vitro* [203-209] and *in vivo* in animal models [210-218], assessing the potential of stem cells for bone regeneration and engineering applications, although few examples of clinical applications have been reported so far [219-223], and no approved bone-engineered product exists today [200]. The intramembranous ossification pathway, with stem cells directly primed toward the osteogenic lineage, is adopted as an optimal strategy when engineering bone substitutes, especially due to the inferior time required to achieve bone formation [199]. However, some authors have recently revisited the idea to engineer bone substitutes via the endochondral ossification pathway [224, 225], principally because a cartilaginous template may allow circumventing the limitations associated with low oxygen tension experienced for large engineered constructs. The proper combination of scaffolding materials, cells and pattern of biochemical and biophysical conditions represent today a great challenge for developing clinically relevant bone substitutes for the repair of large skeletal defects.

4.4.1 Scaffolds for Bone Engineering Applications

For bone tissue engineering the scaffold material must create an adequate microenvironment for osteogenesis. Properties such as biocompatibility (or the ability of a material to perform with an appropriate host response in a specific situation [226]), osteoconductivity and osteoinductivity [227], mechanical performance and porosity are crucial factors to be considered in the design of suitable scaffolds for bone engineering applications [40]. Pore distribution, porosity and interconnectivity of the scaffold are especially important parameters considering the structural architecture of bone, and are recognized to play a critical role in promoting bone formation both

in vitro and *in vivo* [228]. In fact, a porous geometry of the scaffold allows cell seeding and migration, bone matrix deposition, mass transport and vascularization [201]. Nonetheless, surface properties such as chemical composition and topography drive interface phenomena and are essential in promoting cell attachment, proliferation and differentiation [229-231], hence playing a significant role in the *ex-vivo* development of a functional substitute and its stable integration with the native bone following implantation. To date, several different biomaterials have been used in the attempt to engineer bone substitutes, such as polymers [42, 232] (including hydrogels [233]), ceramics [41, 234], metals [235] and composites [236], and it is likely that no universal biomaterial exists. In fact, different biomaterials display optimal characteristics for specific applications. For example, metallic biomaterials with mechanical properties matching those of native bone represent optimal choices today when reconstructing bone defects in skeletal locations characterized by load-bearing conditions. Numerous conventional fabrication techniques are nowadays employed for the construction of 3D porous scaffolds for bone engineering applications, each specific for the type of material used and the requirements of the final application [14, 235, 237, 238]. Beyond all, innovative free-form fabrication (FFF) techniques are emerging as excellent strategies for the construction of scaffolds with complex geometrical shapes. Based on computer-aided design (CAD) and computer-aided manufacturing technologies, FFF allows the manufacturing of 3D scaffolds with reproducible architecture and compositional variation across the scaffold, and unprecedented potential for personalized applications in skeletal engineering [239]. Scaffold functionalization with bioactive molecules is largely adopted for the design of advanced scaffolds for bone engineering applications. These molecules, which include for instance growth factors and cytokines, cell-binding and calcium-binding proteins, have the potential to modulate adsorption, direct cell attachment and differentiation, promote tissue formation and mineralization, as well as favor construct vascularization and avoid rejection following implantation [240-247].

4.4.2 Stem Cells in Bone Engineering

Several basic considerations must be taken into account when choosing a cell source for bone engineering applications. Optimal cells should be readily available and highly expandable *in vitro*, display consistent osteogenic properties and be highly biosynthetic, preserve a stable phenotype after specification and not elicit any adverse reaction after implantation (immune acceptance) [14, 200, 248]. Based on the knowledge that bone-forming cells derive from stem cells

residing in the bone marrow [249-251], human MSCs (hMSCs) have historically been the main source of cells for bone engineering applications. hMSCs are multipotent stem cell with the potential to differentiate toward the mesodermal lineages, including the adipogenic, chondrogenic and osteogenic lineages, but can also trans-differentiate toward tissues representative of other embryonic germ layers [79]. To date, stem cells with similar potency have been isolated from different adult tissues, such as cord blood [252], umbilical cord [253], placenta [254] synovial fluid [255], periosteum [256], fat [257] and skeletal muscle [258]. Despite the fact that mesenchymal-like cells derived from different tissues display common attributes such as i) plastic adherence and fibroblast-like morphology, ii) multipotency and iii) a spectrum of characteristic surface markers, differences in gene expression profile and biosynthetic properties have been demonstrated [259, 260]. Over the last years hMSCs have been successfully differentiated toward the osteogenic lineage and largely used for bone engineering applications with promising results [57, 59, 211, 213, 219, 220, 223, 261-265]. Moreover, due to their derivation from adult tissues, hMSCs have the potential to be harvested and reimplanted in the same patient, therefore overcoming the restrictions associated with an immune response against the transplanted cells [266]. Nonetheless, hMSCs are recognized to be hypoimmunogenic and display immunomodulatory capacities [267, 268], which open the possibility to use them in allogeneic applications, although conflicting results exist [269]. However, beside the aforementioned advantages, hMSCs derived from adult tissues manifest important limitations from a tissue engineering perspective. For instance, following harvest, hMSCs must be isolated and enriched, usually resulting in a high degree of heterogeneity [270, 271] that may affect the desired clinical outcome. Moreover, their limited proliferative potential [272, 273] and loss of functionality associated with protracted expansion [274] restrict their use for the construction of functional substitutes for the repair of large skeletal defects. In addition, it is important to note that the majority of patients reporting fractures of the skeletal system are the elderly. These patients are marked by a decline in function of the entire organism that, according to recent theories on aging, is strongly linked to a progressive acquisition of functional defects of the stem cells securing tissue homeostasis [275, 276]. In this view, the isolation of functional hMSCs from these individuals represent a great challenge limiting the possibility to engineer autogeneic bone substitutes with therapeutic outcomes of clinical relevance. Recent findings have in fact demonstrated that the self-renewal and potency of hMSCs become compromised with donor age [277-279]. On the other hand, human ESCs (hESCs) hold the potential to provide a ready-to-use and unlimited supply of functional cells for bone engineering applications, and the possibility to

directly differentiate hESCs toward the osteogenic lineage has been reported [280-284]. However, the elaborate conditions required for their culture and propagation, as well as their intrinsic tumorigenic potential are today hampering their potential use for clinical applications [285]. An alternative is the use of embryonic-derived cells, which may overcome the above disadvantages and display optimal properties for bone engineering applications. Over the last years several attempts have been made to derive such cells, resulting in the production of several progenitor cells with high potential for the construction of functional substitutes for bone replacement therapies [31, 35, 37, 286-288]. However, for a clinical use of these cells an extensive characterization is needed and a comparative advantage over hMSCs for skeletal engineering applications must be shown.

4.4.3 Cultivation Requirements and Strategies

Optimal culture conditions are fundamental to support stem cell proliferation and stimulate osteogenic differentiation, allowing the construction of functional bone substitutes. In addition to provide essential nutrients supporting cell growth and survival, osteogenic differentiation is usually promoted by stimulating the cells with specific additives able to promote matrix deposition and mineralization, as well as stimulate the expression of genes involved in stem cell commitment toward the osteogenic phenotype. Current protocols utilize a cocktail of ascorbic acid [289-291], β-glycerophosphate [292] and dexamethasone [293, 294] in different ratios and concentrations, as well as specific growth factors recognized to play a primary role in bone histogenesis, including BMP molecules [295], TGF-β [296], VEGF [297], FGF [298, 299], IGF and PDGF [300]. Additional molecules have been recently reported to induce osteogenesis *in vitro* [301-304], indicating that a large set of potential inductive molecules may find applications in bone engineering in the near future. In addition, the construction of functional substitutes relies also on the application of physical stimulation [20, 64, 305]. In fact, in the human body cells are constantly subjected to mechanical stimuli, which impart the proper signal securing tissue homeostasis. Considering the supporting function of the skeletal system, bone-forming cells are particularly sensitive to mechanical load [306], which has been extensively demonstrated to foster osteogenesis and increase the biosynthetic activity of bone-forming cells [58, 59, 307-309]. Based on this knowledge, the use of specific bioreactors plays a fundamental role for the cultivation of cell/scaffolds for bone engineering applications [46]. Nonetheless, bioreactors improve cell proliferation and

differentiation by enabling nutrient supply, and are essential for the reproducible and large-scale production of large functional substitutes for use in clinical settings [310].

5. AIMS OF THE THESIS

- To investigate the molecular changes occurring upon derivation of human embryonic stem cell-derived mesodermal progenitors (hES-MPs) and assess any similarity in gene expression profile with hMSCs.

- To study and compare the proliferation potential of hES-MPs and hMSCs.

- To investigate and compare the osteogenic properties of hES-MPs and hMSCs in relation to their degree of expansion.

- To investigate the potential of matrix-free growth human embryonic stem cells (MFG-hESCs) to undergo osteogenic differentiation and assess the molecular changes associated with lineage specification.

- To investigate the effect of flow perfusion stimulation on the osteogenic differentiation of hES-MPs and hMSCs interfaced to 3D ceramic scaffolds.

- To investigate the immunological properties of hES-MPs and hMSCs.

- To investigate the potential of hES-MPs to be interfaced to 3D metallic scaffolds and study the effect of the biomaterial chemical composition on hES-MPs behavior.

6. MATERIALS AND METHODS

6.1 Scaffolds

Three-D scaffolds made of either ceramic or metallic materials were exploited to conduct the studies reported in the present thesis. In study V, a gel of fibrin was used in combination with the ceramic scaffolds to hold the particles together. Scaffolds were interfaced with either hES-MPs (study IV, V and VI) or hMSCs (study IV), and the resulting cell/scaffold constructs investigated both *in vitro* and *in vivo*. All scaffolding materials were biocompatible and had previously been used for bone engineering applications [40, 204, 217, 311, 312].

6.1.1 Ceramic Scaffolds

Porous ceramic scaffolds of natural coral (*Porites* species) were provided by Biocoral Inc. (Levallois-Perret, France; www.biocoral.com). They consisted of calcium carbonate (98% to 99%) in the form of aragonite with trace elements (0.5% to 1%) and amino acids (0.07 ± 0.02%). In study IV, scaffolds were in form of cubes, with a dimension of about 3x3x3 mm, whereas in study V the scaffolds were in form of particles with a size ranging from 600 μm to 1000 μm. The scaffolds had volume porosity and mean pore diameter of 49±2% and 250 μm (range 150-400 μm), respectively. All pores were interconnected.

6.1.2 Fibrin Gel

The fibrin gels were obtained by mixing fibrinogen (Tissucol®; 18 mg/ml) with a solution of thrombin (100UI/mg). Thrombin is a plasma protein which catalyze the hydrolysis of fibrinogen to fibrin during clot formation [313].

6.1.3 Metallic Scaffolds

Metallic scaffolds of commercially-pure titanium (cp-Ti) and titanium-aluminum-vanadium (Ti6Al4V) alloy, with a dimension of about 1x1x1 cm, were manufactured and provided by Arcam (Arcam AB, Mölndal, Sweden; www.arcam.com). Both the cp-Ti and Ti6Al4V had an average pore size of 620 μm in diameter and a volume porosity of about 70-75%. All pores were interconnected [314].

6.2 Free-form Fabrication of cp-Ti and Ti6Al4V Scaffolds

A collection of different rapid prototyping techniques are currently used for the manufacturing of solid 3D objects for biomedical applications [315]. Among these, electron-beam melting (EBM) represents a promising technique for the high-speed and high-volume fabrication of customized metallic implants with excellent properties for personalized applications in skeletal engineering [316]. The EBM technology relies on the layer-by-layer building of metal powder melted by an electron beam with a layer thickness of 0.1 mm. Each layer is melted to the exact geometry defined by the 3D CAD model.

In study VI, FFF scaffolds were produced in an Arcam EBM S12 system from standard Arcam cp-Ti and Ti6Al4V extra low interstitial (ELI) powders with a particle size of between 45-100 μm. The cubic scaffolds were made from a 3D CAD model, with each side measuring approximately 6.8 mm. All the implants were produced in two separate builds, one for cp-Ti and one for Ti6Al4V. The building temperature of the powder bed was 700°C for cp-Ti and 750°C for Ti6Al4V, respectively. The vacuum pressure inside the chamber was $2x10^{-3}$ mbar for both builds. The control settings of the build process were in accordance with standard settings provided by Arcam AB. After building, the scaffolds were cooled in a He environment at a pressure of $2x10^{2}$ mbar until they reached a temperature of about 100°C. Air was then introduced into the chamber. All scaffolds were finally blasted with the same ELI powders used for building the cp-Ti and Ti6Al4V scaffolds.

6.3 Surface Characterization of cp-Ti and Ti6Al4V Scaffolds

Surface composition and oxide thickness were analyzed by time-of-flight secondary ion mass spectroscopy (TOF-SIMS), which allows the detection of secondary atomic or molecular ions generated after bombardment of any solid material with a pulsed ion beam. The secondary ions are then directed to a detector using a high voltage potential and their mass is determined measuring their time-of-flight from the samples to the detector [317]. One important feature of TOF-SIMS is the ability to provide 2-dimensional spatial distribution of the elemental composition of any material surface, including inorganic and organic samples [318], as well as the excellent mass resolution, good sensitivity and high spatial resolution. In addition, depth profile

analyses may also be performed using a complementary sputter ion gun [319]. TOF-SIMS analysis was also used to study matrix mineralization as described in paragraph 7.19.

In study VI, TOF-SIMS analysis was performed using a TOF-SIMS IV instrument equipped with Bi and C_{60} cluster ion sources. Clusters of Bi ions were used in order to increase the yield of secondary ions, especially high-mass ions, while keeping an adequate image resolution. Before analysis, samples were ultrasonicated in ethanol (99%) for 5 min (3 times), followed by ELGA/Milli-Q H_2O for 15 minutes. Then, samples were dried in a flow of N_2 gas before analysis. Mass spectra of positive and negative secondary ions were measured from two areas of 100x100 μm (divided into 128 pixels)^2 on each sample, with a data acquisition time of 50 s. Bi_3^+ (25 keV) were used as primary ions, with a target current of 0.1 pA. Each spectrum was calibrated by assigning theoretical masses to known peaks. For depth profiles, the sample areas were sputtered with a beam of C_{60}^+ ions (10 keV, target current 0.4-0.5 nA, area 250 x 250 μm). The depth profiles (positive mode) were done with cycles of sputtering for 5 s, followed by data acquisition for 10 s (same area and pixels as above) with a pause of 1 s. The depth profile measurements were continued until the TiO_2 related peak (main TiO^+ at m/z 64) intensity had leveled out in the metal (after 250-300 s of total C_{60}^+ sputtering). The thickness of the oxide layer measured in the depth profiles was calculated from the time required to sputter through the oxide layer. Conversion of the sputter time to depth was done by calibration of the sputter rate of TiO_2 on a standard titanium plate with a known oxide thickness.

6.4 Scaffold Cleaning and Sterilization

Cleaning and sterilization of biomedical devices are of fundamental importance to avoid any undesired and/or adverse effect associated with the presence of non-biological and biological contaminants. In the present thesis, contaminants were removed by ultrasonic cleaning, whereas scaffolds sterilization was carried out by autoclaving. Ultrasonic cleaning relies on the treatment of the scaffolds with high frequency sound waves in presence of H_2O and/or detergents. The formation of cavitation bubbles is responsible for the removal of the contaminants adhering to the scaffold surface. On the other hand, autoclaving represents a simple sterilization procedure based on the use of pressurized steam to destroy contaminating microorganisms [320].

In study IV and V, biocoral scaffolds were collected in round-bottom tubes and steam autoclaved at 115°C for 20 min, which was shown not to affect the composition [321].

In study VI instead, after blasting, the scaffolds were ultrasonically cleaned for 5 min each in two successive baths of MIS 024 detergent, then 3 times for 5 min in ELGA/Milli-Q H_2O. Following ultrasonic treatment, the scaffolds were let to dry in air in a sterile environment. The scaffolds were then sealed in sterile bags and steam autoclaved for 15 min at 120°C.

6.5 Cells

Both human embryonic and adult stem cells have been used to conduct the studies presented in this thesis. All cells were isolated, derived and cultured in line with the principles of the Good Cell Culture Practice [322] in order to comply with international standards and ensure quality of the data.

6.5.1 Undifferentiated Human Embryonic Stem Cells

Undifferentiated hESCs were derived from surplus human embryos from clinical *in vitro* fertilization (IVF) treatments. Derivation, establishment, subcloning, characterization and subsequent culture of hESC lines SA167, SA002.5 and SA461 were performed at Cellartis (Cellartis AB, Gothenburg, Sweden; www.cellartis.com) as previously described [323, 324].

6.5.2 Matrix-free Growth Human Embryonic Stem Cells

The MFG-hESCs were derived from the hESC line AS034.1. Derivation, adaptation and subsequent culture of MFG-hESCs were performed at Cellartis as previously described [31].

6.5.3 Human Embryonic Stem Cell-derived Mesodermal Progenitors

The hES-MPs were derived from the three undifferentiated hESC lines described above. Derivation, characterization and expansion were performed at Cellartis as previously described [35].

6.5.4 Human Mesenchymal Stem Cells

The hMSCs were isolated from marrow aspirates from patients undergoing spinal fusion (age range 13-43 years). The isolation, derivation and characterization were performed at the

University of Gothenburg.

6.6 Cell Derivation and Isolation

To derive the hESC lines used in this study, donated embryos were cultured to blastocysts until the age of 6-7 days as previously described [325]. Briefly, after grading the blastocysts according to Dokras *et al.* [326], the inner cell masses (ICM) were plated on a layer of mitotically inactivated early passage mouse embryonic fibroblasts (MEFs). The mitotic activity of the MEFs was abolished by an incubation with 10 μg/ml mitomycin C for 3 hours at 37°C, after which the cells were seeded at a density of $13x10^4$ cells/ml in IVF cell culture dishes in Dulbecco's-modified Eagle's medium (DMEM) supplemented with 10% fetal bovine serum (FBS), 100 U/ml penicillin G, and 1X Glutamax. ICM outgrowths were passaged to plates with fresh medium and MEF cells by mechanical dissection using Stem Cell Tool™, and established hESC lines were routinely passaged every 4-5 days as previously described [323].

For subcloning, hESC colonies were mechanically dissociated and treated with 0.5 mM ethylenediaminetetraacetic acid (EDTA) for 20 min at 37°C. The cells were triturated carefully with a pipette and diluted in knockout KnockOut™ DMEM medium supplemented with 15% concentrated conditioned medium, 3.5 mM glucose, 1 mM Glutamax, 1% nonessential amino acids (NEAA), and 4 ng/ml human recombinant basic fibroblast growth factor (hrbFGF). Single cells were then transferred into individual wells with MEF-coated plates. To analyze the long-term pluripotency and replicative immortality of the established hESC lines, cells were characterized by examining the morphology, marker expression, telomerase activity, karyotype, and pluripotency *in vitro* and *in vivo* as previously described [324].

Feeder-free Matrigel™-propagated hESC line AS034.1 was used for the adaptation process to matrix-free growth culture conditions. Adaptation to plastic cultures represents a fundamental step for the generation of homogenous and highly expandable undifferentiated hESCs with potential in stem cell-based applications. To initiate the adaptation process, the human embryonic lung fibroblast (hEL)-conditioned hESC [consisting of 80% KnockOut™ DMEM and 20% KnockOut™ serum replacement, supplemented with 1% Penicillin-Streptomycin (PEST), L-Glutamine (2 mM), 1% NEAA, 1% L-glutamin, β-mercaptoethanol (0.1 mM) and 4 ng/ml

hrbFGF] medium was replaced by neonatal condrocyte (NC)-conditioned hESC medium 1 day before passage. The procedure was used to passage the hESCs, which in the end was resuspended in NC-conditioned hESC medium and transferred to a rehydrated Matrigel™ coated dish and subsequently cultured in a humidified atmosphere at 37°C in 5% CO_2. The hESCs were cultured for 20 days without passaging, while culture medium was renewed every second or third day. After 20 days in culture with NC conditioned hESC medium, cells were passaged enzymatically as previously [31] described and cultured on regular culture dishes. After 11 days in culture, the MFG-hESCs colonies were passaged to Primaria® dishes and the NC-conditioned hESC medium was substituted with hEL-conditioned hESC medium.

hES-MPs were derived from the undifferentiated hESC lines SA167, SA002.5 and SA461. The derivation allows the generation of a population of progenitor cells with high potential for mesodermal tissue engineering studies. Briefly, cells were removed from the supporting feeder layer, enzymatically dissociated with TrypLE™ Select, and plated onto 0.1% porcine gelatin coated cell culture dishes at high density cultures of about $1.5x10^5$ cells per cm^2 in medium consisting of high-glucose DMEM (DMEM-HG; with glutamax, without pyruvate) supplemented with 10% FBS and 10 ng/ml hrbFGF. The plated hESC lines were left to differentiate for 7 days in a humidified atmosphere at 37°C and 5% CO_2 resulting in an outgrowth of heterogeneous cell types. Following this, the hESCs were enzymatically dissociated (passage 1, P1) and passaged as a single cell suspension using TrypLE™ Select to gelatin coated culture dishes. In this and in all following passages or transfer steps, no selection was performed and all cells were transferred. This procedure was repeated every 7 days until the cell population became homogeneous for hES-MPs morphology (at P2-P3).

For the isolation of hMSCs, the bone marrow was aspirated using heparin-coated syringes to prevent coagulation. After aspiration, the bone marrow was mixed with 5 ml of phosphate buffer saline (PBS) containing Heparin and centrifuged at 1800rpm for 5 min. Following the removal of the lipid-containing layer, the cell suspension was fractioned by density gradient centrifugation using cell preparation tubes prefilled with Ficoll. The density gradient allows the separation of mononuclear cells (containing the hMSCs) from platelets, granulocytes and erythrocytes upon centrifugation at 3400rpm for 20 min at a temperature between 18-25°C. The layer at the interface medium-Ficoll containing the mononuclear cell fraction was gently collected, and the

cell suspension diluted in a Turk's solution (1:10) to lyse contaminating red blood cells. After washing, cells were plated and expanded in culture flasks to prompt enrichment of hMSCs.

6.7 Cell Expansion

In all studies presented in this thesis, cells were expanded *in vitro* in order to reach a sufficient number for further investigations or to examine osteogenic differentiation in relation to the degree of expansion. Different cells were expanded using specific culture conditions as described below.

For propagation of hESCs, colonies were mechanically cut into pieces of about 200x200 μm and transferred to new culture dishes coated with fresh MEFs. Cells were cultured using VitroHES™ medium supplemented with hrbFGF (4 ng/ml) and passaged every 4-5 days.

MFG-hESCs were expanded in Primaria® dishes in conditioned hESC medium and passaged every 4 to 6 days. Briefly, cells were treated with collagenase type IV for 5 min at 37°C. The MFG-hESCs suspension was pelleted by centrifugation at 1600rpm for 5 min and subsequently washed twice in KnockOut™ DMEM. The cells were then resuspended in conditioned hESC medium and transferred to Primaria® dishes. The medium was changed every second or third day and cells cultured at 37°C in 5% CO_2

hES-MPs were expanded in culture flasks in presence of DMEM-HG, supplemented with 10,000U/ml PEST, L-glutamine (2 mM), 10% FBS and 10 ng/ml hrbFGF. Briefly, cells were treated with trypsin for 5 min at 37°C and subsequently centrifuged at 2000rpm. The pellet was then resuspended in complete expansion medium and cells plated and expanded in culture flasks. Cells were seeded at a density higher than 10% to avoid apoptotic death of neglect, and passaged when reaching 80% confluence to avoid death by metabolic decay and/or spontaneous differentiation. Media were changed every 3-4 days and cells cultured at 37°C in 5% CO_2

hMSCs were expanded in medium consisting of low-glucose DMEM (DMEM-LG) supplemented with the same additives as described above for the hES-MPs, and passaged using similar protocols as for hES-MPs. Media were changed every 3-4 days and cells cultured at 37°C in 5% CO_2.

6.8 Osteogenic Stimulation

In order to prime cell differentiation toward the osteogenic lineage, cells were plated and cultured in a medium consisting of DMEM-LG, supplemented with 10,000U/ml PEST, L-glutamine (2 mM) and 10% FBS (20% in study I in order to favor attachment of the MGF-hESC), and containing the osteogenic additives ascorbic acid (45 μM), dexamethasone (1 μM) and β-glycerophosphate (20 mM). These additives are recognized to respectively promote the synthesis of collagen, prompt osteogenic differentiation and favor matrix mineralization [290-294]. When investigating codifferentiation toward the osteogenic and adipogenic lineage in study III, the ostegenic medium described above was supplemented with BMP2 (25 ng/ml). In the same study, medium was supplemented with IFN-γ (100 U/ml) to study the expression of immunological markers. Lower concentrations of the above additives were used in study V, where cells were expanded under osteogenic conditions along 2 weeks before *in vivo* implantation, with the objective not to inhibit proliferation significantly. In this study, the concentrations of ascorbic acid and dexamethasone were 0.1 μM of and 15 μM, respectively. All other supplements were used in the same concentrations as described above. All cells were incubated at 37°C in 5% CO_2. In study IV, the osteogenic medium was supplemented with the zwitterionic agent 4-(2-hydroxyethyl)-1-piperazineethanesulfonic acid (HEPES) to maintain the pH at optimal levels. Media were changed every 2-3 days and cells were cultured under osteogenic stimulation up to 5 (study IV) or 6 (study I, III and VI) weeks.

6.9 Cell Transduction

Several strategies for delivering genetic material into host cells have been developed over the last decades, including physical, chemical and viral methods. Among all, methods based on recombinant viral vector represent the most efficient means since they take advantage of the natural ability of viruses to get inside the cells and, in the case of retroviral vectors, integrate their genetic material inside the host genome allowing a stable expression of the transduced genes [327].

In study V, hES-MPs were transduced with the bicistronic lentiviral vector PCHMWS-eGFP-T2A-Fluc, containing a fused gene encoding for firefly luciferase (Fluc) and enhanced green fluorescent protein (eGFP), for monitoring of cell survival after *in vivo* implantation. The T2A sequence ensures efficient coexpression of both reporter genes [328, 329]. The PCHMWS-eGFP-

T2A-Fluc vectors were kindly provided by Dr. Ibrahimi (Katholieke Universiteit Leuven). Briefly, cells were seeded in a 24-well plate at a density of $5x10^4$ cells/well under expansion conditions (see above for descriptions). After 24 h, medium was aspirated and cells rinsed twice with PBS, before adding 250 µl of a solution containing the viral particles at a multiplicity of infection (MOI) of 100. Then, cells were incubated at 37°C in 5% CO_2. After 1 h, 2 ml of medium were added per each well and cells expanded at 37°C in 5% CO_2 as described above.

6.10 Cell Seeding Techniques and Preparation of Cell/scaffold Constructs

Interfacing cells to 3D scaffolds requires seeding them using appropriate seeding methods, which are essential to ensure a homogenous distribution of cells through the scaffolds and may play an important role in affecting cell differentiation and tissue formation [330]. Both static and dynamic methods are generally used to inoculate cells in 3D scaffolds, including the droplet [331], cell suspension [332] and centrifugal seeding techniques [333], as well as dynamic methods using bioreactors [334]. In this thesis both static and dynamic seeding techniques were used.

In study IV, the static cell suspension seeding technique was used. Cells were seeded at a density of about $1x10^5$ cells per coral scaffold placed in 15 ml tubes. Briefly, cells were detached, filtered with 40 µm nylon strainers to remove clusters of cells and counted. After centrifugation at 1200rpm for 5 min, cells were resuspended in expansion medium consisting of DMEM-HG supplemented with the same additives as described above. Aliquot of single cell suspension were then added per each tube containing the scaffolds. In order to favor a homogenous distribution of cells across the scaffolds, tubes were gently shaken and tilted every 30 min for 4 h, then incubated at 37°C in 5% CO_2 for 3 days before being transferred into flow perfusion bioreactors for osteogenic differentiation. Three days after seeding, medium was collected and cells not attached to the corals counted in a haemocytometer in order to evaluate the degree of cell attachment.

In study V, hES-MPs were seeded using a suspension technique followed by centrifugation. After 2 weeks of culture under osteogenic conditions, the medium was removed and cells rinsed with 4 ml of Hanks' balanced salt solution (HBSS, without Ca^{2+} and Mg^{2+}) containing 30 mM of HEPES and 1% PEST. After rinsing, cells were detached with 4 ml of a solution of Clostridium histolyticum type IV collagenase in HBSS (1mg/ml) for about 20 min. Then, cells were collected,

filtered with 40 μm nylon strainers and counted with a haemocytometer. After centrifugation at 1200rpm for 5 min, cells were resuspended in DMEM without Phenol red containing 10% FBS for seeding. Forty mg of biocoral particles were aliquoted in 50 ml Falcon tubes and 1 ml of DMEM without Phenol red containing 10% of FBS was added to each tube to precondition the coral particles. In order to remove air bubble entrapped inside the particles, samples were vacuum treated and centrifuged, before being incubated overnight at 37°C in 5% CO_2. After removing the preconditioning medium, 100 μl of cell suspension (10^7 cells/ml) were added per each aliquot of coral particles and samples incubated for 4 h at 37°C in 5% CO_2 to allow attachment. Afterward, samples were centrifuged for 5 min at 1200 rpm to promote attachment before embedding in a gel of fibrin and medium was collected. Cells not attached to the corals were counted in a haemocytometer in order to evaluate the degree of cell attachment. After adding 100 μl of fibrinogen (18mg/ml), samples were allowed to homogenize for 10 min. Then, 5 μl of a solution of thrombin (100UI/mg) were added per each sample for embedding. After 15 min, 4 ml of DMEM-LG containing HEPES (20 mM) were added, and the embedded constructs incubated overnight at 37°C in 5% CO_2. Embedded coral particles without cells were prepared as control. Before implantation, embedded constructs were transferred into 24-well plates using a sterile scalpel.

For studying the *in vivo* immune response to the implanted cell/coral constructs, hES-MPs were seeded on coral scaffolds and constructs prepared as described above.

In study VI, a centrifugal seeding technique was used in order to increase cell penetration and attachment across the scaffolds. Briefly, scaffolds were placed in round-bottom tubes and 1 ml of cell suspension (10^6 cell/ml) was added per each scaffold. Tubes containing the cell/scaffold constructs were then centrifuged at 1200rpm for 5 min. After centrifugation, unattached cells were resuspended and cell suspension added again to the tubes containing the scaffolds. The centrifugation procedure was repeated 5 times and the unattached cells counted in a haemocytometer to calculate the degree of cell attachment. Cell/scaffold constructs were finally incubated at 37°C in 5% CO_2 for 24 h.

6.11 Culture in Bioreactor

Tissue engineering can be described as a quadriad composed of four key elements, including

cell, scaffolds, inductive molecules and bioreactors. Bioreactors are culturing devices, which provide the optimal conditions for the fabrication of tissue-engineered constructs, including the spatial and temporal application of chemical and physical stimuli. Several bioreactors have been designed and employed so far for bone engineering applications. In this thesis, a flow perfusion bioreactor was used for the culture of cell/coral scaffolds with the objective to promote bone-like tissue formation. Such bioreactor consisted of a peristaltic pump, four perfusion chambers and related medium reservoirs as described earlier [335].

In study IV, cell/coral constructs were transferred into the flow perfusion bioreactor chambers and cultured for 5 weeks both in static (flow perfusion rate: 0 ml/min) and dynamic (flow perfusion rate: 10 ml/min) conditions using osteogenic medium. This resulted in four groups of investigation denoted (i) hES-MPs static, (ii) hES-MPs dynamic, (iii) hMSCs static and (iv) hMSCs dynamic. All cells were incubated at 37°C. Medium was changed every 3-4 days and cell/coral constructs were harvested every week in order to examine cell proliferation and osteogenic differentiation.

6.12 Cell Staining with Fluorescein Diacetate

In this thesis, cells were stained with fluorescein diacetate (FDA) to examine cell distribution across the coral scaffolds. FDA is a non-fluorescent derivative of fluorescein that can passively penetrate the cell membrane and, once inside the cell, is deacetylated by nonspecific esterases to fluorescein. Fluorescein accumulation inside the cells allows detection under excitation with an ultraviolet (UV) lamp using conventional fluorescence microscopes equipped with FITC filters. FDA staining is usually used for investigating enzymatic activity, cell viability and microbial biomass.

In study IV, cell/coral constructs per each condition were collected at day 0 and weekly after incubation in bioreactor, and incubated 10 min at 37°C with osteogenic medium supplemented with FDA at final concentration of 0.1 μg/ml. Constructs were then visualized under the fluorescence microscope Eclipse TE2000-U.

6.13 Microscopic Investigation

Microscopes are optical systems that allow enlarging the image of the object under observation. Three main types of microscopy exist including light, electron and scanning probe microscopy. In this thesis, both light (including fluorescence microscopy) and scanning electron microscopy (SEM) were used. Light microscopy is based on the transmission of light through a sample or reflection of light from a sample, followed by magnification of the object using a single or multiple lenses. Fluorescence microscopy relies on the use of fluorescent dyes that, after excitation using specific wavelengths, emit light of a different wavelength allowing the visualization of specific structures. SEM overcomes the resolution limitations encountered with light microscopy by using high-energy electrons to image the samples. After interaction with the specimen, different signals are generated and collected by specific detectors, such as for example secondary electrons and back-scattered electrons.

Light microscopes were used mainly to investigate cell proliferation, fat and mineral content following differentiation (after staining with oil-red O and von Kossa) and observe histological sections stained with haematoxylin-eosin-safranin, Sirius red and toluidine blue. Fluorescence microscopes instead were used to examine the distribution of cells stained with FDA, analyze immunohistochemically-stained samples and eGFP-positive hES-MPs.

6.13.1 Scanning Electron Microscopy

SEM investigation was performed to image both the native scaffolds and the cell/scaffold constructs, in order to investigate surface topography and estimate the degree of cell attachment and distribution across the materials, respectively.

In study IV, cell/coral constructs were harvested after 3 days and 5 weeks in bioreactors for SEM characterization. Briefly, cell/coral constructs were rinsed twice in PBS before fixation with a solution of modified Karnovsky fixative, consisting of sodium azide (0.02%), paraformaldehyde (2%) and gluteraldehyde (2.5%) in sodium cacodylate buffer (0.05 M). Constructs were later treated with OsO_4 (1%) in sodium-cacodylate buffer, and stored at 4°C for 4 h. OsO_4 is a staining agent for lipids that provide contrast during SEM imaging by creating high secondary electron emission. After rinsing 5 times with distilled H_2O, constructs were treated with hexamethyldisilazane (1%) before adding again a solution of OsO_4 (1%) in sodium cacodylate

buffer (0.1 M). After dehydration with ethanol of increasing concentration (70%, 80%, 95% and 99.5%), samples were treated twice (10 min) with hexamethyldisilazane (1%) and dried overnight. Then, all samples were sputter coated with palladium for 2 min at 25 mA before SEM examination. Native scaffolds were also SEM characterized following similar protocol. The SEM analysis was performed using a LEO Ultra 55 FEG SEM equipped with a secondary electron detector and an in-lens detector. Overview images were acquired using the secondary electron detector at 5 kVs acceleration voltage, whereas the in-lens detector was used for closer examination of the cell-scaffold interaction at 2 kVs acceleration voltage.

In study VI, surface topography of native scaffolds, as well as cell attachment and distribution across the scaffolds after 2 days of culture under osteogenic conditions, were investigated using the Leo Ultra 55 FEG SEM equipped with a secondary electron detector and an in-lens detector as described above.

6.14 Cell Disruption and Extraction of Biological Materials

Extraction of biological material for biochemical investigation requires disrupting the cell membrane while preserving the integrity of the macromolecules of interest, such as DNA, RNA and proteins. When high purity is needed, subsequent enzymatic treatment with specific nucleases and proteases may be applied. In the present thesis, different reagents and methods (both chemical and physical) were used.

6.14.1 DNA Extraction

In study II, in order to study the length of the telomeric sequences, cells were lysed using the ATL buffer and DNA extracted using the Qiagen DNeasy Blood and Tissue Kit according to the manufacturer's protocol, which also includes a protease K treatment for the nonspecific digestion of contaminating proteins and nucleases.

In study IV, to extract the total DNA for quantification, cell/coral constructs were grinded frozen in liquid N_2 for 1 min at 30 Hz, and cells lysed using a solution of Triton X-100 (0,1%) followed by three freeze-thaw cycles from N_2 to 37°C. Triton X-100 is a nonionic surfactant that allows chemical disruption of the cell membrane, while repeated freeze-thaw cycles cause the shrinking

and swelling of the cells, and facilitate the breakdown of the cell membrane due to the formation of ice crystals.

In study VI, to extract the total DNA for quantification, cell/scaffold constructs were rinsed twice with PBS and then treated with a solution of papain for about 5 min. Papain is a cysteine protease able to digest protein and detach cells, and whose prolonged activity lead to cell disruption. Samples were then placed in oven at 60°C for 1 h to allow homogenization.

6.14.2 RNA Extraction

In this thesis, total RNA was extracted for gene expression studies. In study I, II, III and VI, cells were lysed in 350 μL RLT buffer with addition of 1% β-mercaptoethanol and vortexed for 1 min. The RLT buffer contains guanidine thiocyanate, a chaotropic agent causing protein denaturation and nucleases inhibition, while the β-mercaptoethanol causes protein denaturation by reducing disulfide bonds. The lysate was transferred directly into a QIAshredder spin column and centrifuged for 2 min for RNA purification. Total RNA was then extracted using the RNeasy® Minikit according to the manufacturer's instructions. DNAse treatment was performed to eliminate any contamination from genomic DNA.

In study IV, total RNA was extracted by treating the cells with 1 ml of TRIzol® Reagent according to the manufacturer's instructions. TRIzol® is a guanidinium thyocyanate-phenol-chloroform buffer, which allows cell disruption and DNA/RNA extraction. Homogenized samples were then vortexed 3 times for 20 s and 400 μl of chloroform were added to each sample. After this, 500 μl of the aqueous phase containing RNA was collected and RNA was precipitated with isopropyl alcohol, washed in ethanol, and dissolved in RNase-free water.

6.14.3 Protein Extraction

In study I, III and VI, proteins were extracted to study the ALP activity using the M-PER® reagent, a detergent that dissolves the cell membrane and allows total protein extraction.

In study IV, the total protein content was extracted for quantification using similar protocol as described earlier for the extraction of DNA.

6.15 Total DNA Content

Cell proliferation can be estimated using different methods, including spectrophotometric quantification by determining absorbance at 260 nm and fluorometric assay following DNA staining with specific fluorescent dyes. In this thesis the total DNA content was measured by fluorometry using PicoGreen® and the blue fluorescent Hoechst dye. Fluorometry is more sensitive than spectrophotometric quantification and less susceptible to protein and RNA contamination. PicoGreen® is a fluorochrome that selectively binds double-stranded DNA (dsDNA), which displays an excitation maximum at 480 nm and an emission peak at 520 nm. As free molecule, PicoGreen® has virtually no fluorescence but display a 20-fold increase in fluorescence after binding the dsDNA, therefore resulting in little background signal. Hoechst dyes are bisbenzimidazole derivatives with high affinity for the minor groove of dsDNA molecules [336]. After binding the dsDNA, its fluorescence increases about 2 times. Hoechst dyes are excited by UV light at around 360 nm and emit blue fluorescence at 460-490 nm. The Hoechst-based assay allows the detection and quantification of DNA concentrations as low as 10 ng/ml DNA [337].

In study IV, cell proliferation was estimated using the Quant-iT^{TM} PicoGreen® dsDNA reagent kits according to the manufacturer's instructions. Ten μl aliquots of lysed samples were incubated with 90 μl of 1X TE buffer and 100 μl of PicoGreen® Working Reagent, and fluorescence was read using a fluorescence microplate reader μQuant with ex/em of 480/520 nm. A standard curve of known concentrations of lambda (λ) DNA was used to convert fluorescence to total DNA content.

In study VI, cell proliferation was investigated using the Hoechst-based assay. Briefly, cell lysates were dissolved in 200 μl of phosphate buffer containing EDTA (PBE; 5mM, pH 7.5) and stained with a solution of Hoechst 33258 ($3.7x10^{-8}$ M) in PBE buffer. After an incubation period of 10 min in the dark, samples were excited by UV light at 360 nm and emission read at 460 nm in a SPECTRAmax GEMININI microplate reader using the Softmax® Pro software. A standard curve consisting of serially diluted calf thymus DNA was run in the same microplate and used to convert fluorescence to total DNA content.

Negative controls were used in both analyses and the values acquired subtracted for DNA quantification.

6.16 Techniques for Gene Expression Studies

Gene expression represents the initial event leading to the conversion of the information stored in the DNA molecules in functional proteins, which in general determine the actual phenotype of a specific cell. Gene expression is a very dynamic process, which allows cells to promptly respond and adapt to internal and external stimuli. Moreover, the expression profile of a typical cell depicts its molecular state and is used as molecular signature to distinguish different cell types. In this thesis, gene expression was investigated using two main techniques, such as gene microarray and real-time polymerase chain reaction (RT-PCR).

6.16.1 Gene Microarray

Gene array technology allows simultaneous measurements of the expression of thousand of genes by monitoring the combinatorial interaction of target molecules with a library of complimentary DNA probes. The probes are either synthesized *in situ* on a glass substrate or pre-synthesized and then attached to the array platform (usually glass or nylon) [338]. In this thesis, the Affymetrix® GeneChip microarray platform was used, containing probes corresponding to the entire human genome with the potential to bind 47,000 different target transcripts, and consisting of thousands of spots each containing a large number of identical oligonucleotides of 25 bases directly synthesized onto the chip via photolithography. Each spot contains 16 different probes, which are complementary to different regions of the target gene. In addition, each spot contains both perfectly matched probes and single-base mismatched probes, which allow quantitation and subtraction of signals resulting from non-specific cross-hybridization, respectively. The difference between the two signals provides a good estimation of the specific target abundance.

In study I and II, the total RNA was extracted from the cells using the protocol described above, and subjected to gene expression analysis using the Affymetrix oligonucleotide microarray HG-U133plus2.0 according to manufacturer's recommendations. Briefly, 2 μg of the total RNA were used as a template for the synthesis of the first and second strand of complementary DNA (cDNA) using the GeneChip® One-Cycle cDNA synthesis kit according to the manufacturer's

instructions. A cleanup of the complementary dsDNA was performed using GeneChip® IVT Labeling kit. During the *in vitro* transcription, biotinylated nucleotides were used resulting in the synthesis of biotin-labeled complementary RNA (cRNA). Another cleanup using the GeneChip® Sample Cleanup Module was performed before the quality of the cRNA was checked using the Agilent 2100 BioAnalyzer where the average size of the fragmented cRNA was approximately 100 nucleotides. The samples were prepared for hybridization using the GeneChip® Hybridization Control kit. Biotin-labeled cRNA fragments were then hybridized to the U133plus2.0 GeneChip for 16 h at 45°C, according to the Affymetrix Gene Chip Expression Analysis manual. After washing out the unbound cRNA, the chips were stained using streptavidin phycoerythrin (SAPE) and scanned for data acquisition using a Hewlett Packard Genarray Scanner, controlled by the Affimetrix GeneChip® Operating Software 1.4 (GCOS; Affymetrix). Raw expression data were normalized and subsequently analyzed with the GCOS 1.4. Comparative and statistical analyses between different cell types were performed with the BIORETIS web tool.

6.16.2 Real-time Polymerase Chain Reaction

PCR is a central technology in molecular biology, which relies on the *in vitro* amplification of specific sequences of nucleic acids using designed pairs of oligonucleotides complementary to the 3′ and 5′ of the target sequence [339]. A PCR reaction mix usually consists of a reaction buffer including deoxynucleotide triphosphates (dNTPs), the oligonucleotide primers, a thermostable DNA polymerase and the template to be amplified. Quantification of gene expression using the principle of PCR has grown considerably following the development of real-time techniques in 1993 [340]. RT-PCR also denoted quantitative RT-PCR allows both detection and quantification of gene transcripts with high sensitivity. Before amplification via PCR, the transcripts must be reverse transcribed to complementary dsDNA using the enzymatic action of a reverse transcriptase. The reaction mix is sequentially incubated at 3 different temperatures constituting the PCR cycle. The first step involves incubation at 94-96°C for 10 s to 1 min to allow denaturation of newly synthesized DNA (amplicons), followed by incubation at a temperature that allows primers to anneal to the specific target sequences. The third step is at a temperature that allows the polymerase used to extend the primers using the target sequence as template. Two principal methods for real-time quantification are generally used, including non-specific intercalating fluorescent dyes binding the dsDNA and DNA probes complementary to the target

sequence and labeled with fluorescent reporters. At each cycle, the increase in the emission of the reporter molecules is detected and normalized to a passive reference. Relative concentrations of amplicons during amplification are determined by plotting the emitted fluorescence against RT-PCR cycles, and the fluorescence emitted above a defined threshold, which is called the cycle threshold (Ct), is used for calculation. For estimation of gene expression per cell, RT-PCR values are normalized using housekeeping genes whose expression is recognized to be relatively stable throughout the cells. In the present thesis, both nonspecific dyes and labeled probes were used for real-time quantification, and the ribosomal subunit 18S was used for normalization.

In study I, II, III and VI, RT-PCR was used to verify microarray data and investigate the expression of genes involved in osteogenic differentiation. After extracting the total RNA as described above, each sample was normalized to 50 ng/ml before the reverse transcription. Reverse transcription was carried out using iScript cDNA Synthesis Kit in a 10 µl reaction, according to the manufacturer's instructions. Primers for RUNX2, BMP4, OPN, ALP, FOXC1, TGFβ2, COL1A1, OC, SRGN, OCT4, NANOG, SOX2, TDGF1, TGFβR2, LHX8, BMPR2 and the ribosomal subunit 18S were designed using the Primer3 Web-based software [341]. Design parameters were adjusted to minimize formation of artifact products and to be able to use an annealing temperature in PCR at about 60°C. Primers were designed to yield short amplicons (preferably < 200 bp) and to function well with SYBR Green I fluorescent dye for detection of the PCR products in real time. Primer sequences are available at TATAA Biocenter AB (www.tataa.com). RT-PCR was performed in duplicates using the Mastercycler ep realplex in 20 µl reactions. Cycling conditions were 95°C for 10 min followed by 45 cycles of 95°C for 20 s, 60°C for 20 s, and 72°C for 20 s. The fluorescence was read at the end of the 72°C step. Melting curves were recorded after the run by stepwise temperature increase (1°C/5 s) from 65°C to 95°C. Normalized relative quantities were calculated using the delta Ct method and 90% PCR efficiency ($k \times 1.9^{\Delta ct}$).

In study IV, RT-PCR was performed to investigate the effect of flow perfusion on the expression of genes involved in osteogenic differentiation. After extracting the RNA as described above, the purity and concentration of extracted RNA was measured with the spectrophotometer Nanodrop 1000. Reverse transcription was carried out in the iCycler thermal cycler using the SuperScript™ II Reverse Transcriptase Kit in a 20 µl volume reaction, according to the manufacturer's

instructions. RT-PCR was performed in triplicates using the MyiQ™ Single-Color Real Time PCR in a 20 µl volume reaction containing equal volumes of cDNA, TaqMan Universal PCR Master Mix and TaqMan® Gene Expression Assays composed of FAM™ dye-labeled TaqMan® MGB probe and predesigned unlabeled PCR primers for RUNX2, COL1A1, ALP, OC, ON, OPN and 18S ribosomal subunit. Cycling conditions were 95°C for 10 min followed by 40 cycles of 95°C for 15 s (denaturation), 60°C for 60 s (annealing) and again 60°C for 60 s (extension). The fluorescence was read at the end of the extension step and the data were analyzed using MyiQ™ Software.

For estimation of gene expression per cell, RT-PCR values were normalized using the expression of the 18S ribosomal subunit.

6.17 Bioinformatic Tools

Bioinformatics is defined as the application of computational techniques to understand and organize the information associated with biological macromolecules [342]. Several bioinformatic resources have been used in this theis for the management, analysis and interpretation of high-throughput data obtained by genome-wide microarray experiments, including tools for single and genome-wide comparative and statistical analyses, hierarchical clustering and protein-protein interaction networks.

6.17.1 Comparative and Statistical Analysis of Microarray Data

Analysis of gene microarray data was performed using the BIORETIS Web tool. BIORETIS is a database for the analysis and sharing of microarray data, which allows performing comparative and statistical analyses of selected genes between experimental samples (www.bioretis-analysis.de). Functional classifications of genes in specific categories, including genes involved in ossification (study I), as well as transcription factors, ECM components, growth factors, membrane receptors and cell adhesion molecules (study II) were conducted using the Gene Ontology Annotation (GOA) database (www.ebi.ac.uk/GOA) [343].

In study I, genes were selected for further analysis only if i) >80% of the single comparisons per group comparison were detected as significantly changed by the Affymetrix GCOS 1.4 and if ii)

the genes displayed a mean fold change (FC) ≥2. On the other hand, in study II genes were selected for further analysis only if i) the absolute call for the gene was present for at least one of the three cell types, ii) three out of three comparisons were considered increased or decreased according to GCSO 1.4, and iii) the FC was ≥2. In addition, in study II the BIORETIS Web tool was used to retrieve and investigate the expression of 40 genes specifically expressed in hESCs, as well as 48 genes known to be overexpressed in hESCs and 30 genes underexpressed in hESCs compared with differentiated cell types [344].

6.17.2 Scatter Plots

To observe the similarity in global gene expression across the investigated cell samples, scatter plots were generated between average signals of pairs of samples using standard function in "R". R is a language and environment for statistical computing and graphics (www.r-project.org). The percentage of genes with an FC ≤3 between pairs of samples was calculated for all 3 comparisons (hES-MPs vs. hMSCs, hES-MPs vs. hESCs, and hMSCs vs. hESCs). This FC-threshold was defined based on the results from comparisons of the biological replicates. To define the background variation, the FCs between pairwise replicates were calculated, and the results showed that 90% of all the genes had a FC ≤3 between any two replicates of a sample. Spearman was used as correlation coefficient and genes with missing values were excluded from the calculation. The interpretation of this analysis was as follows: 1 indicated perfect correlation, -1 indicated negative correlation, and 0 indicated no correlation.

6.17.3 Hierarchical Clustering

In this thesis, the Genesis software 1.7.2 was used to perform a hierarchical cluster analysis of selected genes from the microarray datasets. Genesis is a platform independent Java suite developed for the analysis and visualization of gene microarray data (available at http://genome.tugraz.at) [345]. Cluster analysis or segmentation allows grouping a collection of observations into clusters, based on their degree of similarities, so that subsets with close relationships cluster together [346]. Hierarchical clustering is a procedure of transforming a matrix containing the distance between set of pairwise points into a hierarchy of nested partitions [347]. In study I, hierarchical cluster analysis was performed on the selected genes involved in ossification. In study II instead, the analysis was performed on 447 differentially expressed genes (retrieved

from two comparative analyses: hESCs vs. hES-MPs and hES-MPs vs. hMSCs) displaying a FC ≥20. In both cases, clustering was performed using log2-transformed signals of all the replicates and Pearson correlation coefficients were used as similarity values in the distance matrix.

6.17.4 Protein-Protein Interaction Networks

Protein-protein interactions (PPI) are fundamental for cell survival and functionality, and the visualization of PPI networks may help to enlighten important biological processes and attributes [348]. To investigate possible interactions among proteins from differentially expressed genes, and identify hub proteins, the search tool STRING was used. STRING is a database of known and predicted protein interaction (http://string-db.org) [175]. The interactions include direct (physical) and indirect (functional) associations; they are derived from four sources, including genomic context, high-throughput experiments, co-expression, and previous knowledge. However, in this thesis the analysis was restricted to include only experimentally based PPIs, with the objective of increasing the validity of the results. In study I, PPI networks were derived from differentially expressed genes involved in ossification and displaying a FC ≥2. On the other hand, in study II PPI networks were derived from differentially expressed genes retrieved from the entire dataset and displaying a FC ≥10. A gene of interest was classified as a hub if it had at least 5 interactions with other genes [349].

6.18 Flow Cytometry

Flow cytometry is a powerful technique for the analysis of multiple parameters of individual cells within a heterogeneous population. The flow cytometer perform this analysis by passing a large number of cells per second through a laser beam, and measuring the amount of light scattered (which is proportional to cell size and complexity), or fluorescence emitted by the cells (which is proportional to the number of fluorochrome molecules attached to the cells) with specific photodetectors. The detected light is then converted in a voltage pulse. In the present thesis, flow cytometry was used to confirm isolation and enrichment of hMSCs, verify microarray data, examine expression of immunological markers, and investigate the rate of cellular death. Five different antibody-conjugated fluorochromes were used, including peridinin chlorophyll protein complex (PerCP), fluorescein isothiocyanate (FITC), R-phycoerythrin (PE), PerCP-cyanine5 (PerCP-Cy5) and propidium iodide (PI), displaying maximum emission at 670 nm, 525 nm, 575 nm, 690 nm and 620 nm, respectively. Samples were excited with a 488 nm

argon ion laser and fluorescence was routed to the relative detectors using appropriate band pass filters.

To confirm isolation and enrichment of hMSCs, cells in P1 were stained with CD34-PerCP, CD45-FITC, CD105-FITC, and CD166-PE antibodies.

In study II, in order to verify the microarray results, hESCs, hES-MPs and hMSCs were stained with CD44-FITC, CD58-PE, CD47-FITC and CD166-PE.

In study II, to study the expression of immunological markers, hMSCs and hES-MPs were cultured under expansion conditions, with or without IFN-γ (100 U/ml) treatment, and then stained with CD80-FITC, CD86-PerCP-Cy5, HLA-ABC-FITC and HLA-DR-FITC.

In study III instead, hMSCs and hES-MPs at P5 were cultured under osteogenic conditions for 7 days, and then treated with IFN-γ (100 U/ml) and cultured for 7 additional days. The cells were then stained with the same antibodies as described above.

In study VI, in order to estimate the rate of cellular death for cells seeded both onto cp-Ti and Ti6Al4V scaffolds, hES-MPs were harvested after 5 days of culture under osteogenic conditions and stained with Annexin V-FITC and PI using the FITC Annexin V Apoptosis Detection Kit I. The analysis relies on the externalization of the plasma membrane phosphatidyl serine occurring during apoptosis [350]. During the early phases of apoptosis the phosphatidyl serine becomes exposed to the outside of the cell membrane as signal for the phagocytes to engulf the dying cell, thus avoiding the release of proinflammatory molecules. In this phase, the cell membrane is intact and does not allow the PI to penetrate the cells. Later, during the apoptotic process *in vitro*, the cell membrane ruptures and the PI binds to the DNA, indicating cell necrosis.

For all analysis, cells were trypsinated for about 10 min, washed twice with PBS and then treated with the proper fluorochrome-labeled antibodies. After incubation for 15 min at room temperature in the dark, samples were analyzed by flow cytometry within 1 h. All samples were analyzed using the FACS Aria flow cytometer using the FACS Diva software. A 488 nm argon ion laser was used to excite samples, with emission being measured using appropriate band pass

filters. A threshold was set on the scattered light to exclude events associated with debris and cell aggregates. As negative control, isotype specific antibodies conjugated to the fluorochromes were used in order to exclude events associated with non-specific fluorescence. Cells displaying fluorescence higher than 99% of the cells stained with isotype antibodies were considered positively stained.

6.19 ELISA

The enzyme-linked immunosorbent assay (ELISA) is a highly sensitive, robust and cost-effective method for the detection and quantification of antigens within biological fluids [351]. Since its development, the assay has found increasing applications in food science, clinics and basic science research. Several different variations of the method exist today, although all rely on the same principle, namely the specific antibody recognition of target antigens. Among all, the dual-antibody sandwich ELISA (DAS ELISA) is largely used due to its high sensitivity and specificity. The assay relies on the antigen capture by an antibody coated on the ELISA plate. The bound antigen is then recognized by an enzyme-conjugated secondary antibody, thus creating a sandwich. The conjugated enzyme is used to begin a colorimetric reaction in presence of a substrate and the color developed is read using a spectrophotometer. The optical density (OD) measured is considered proportional to the antigen concentration.

In study V, the DAS ELISA Quantikine kits were used to measure the serum concentration (for a description of serum preparation see paragraph 6.27) of mouse tumor necrosis factor-alpha (TNF-α), INF-γ, interleukine-2 (IL-2) and interleukine-4 (IL-4), according to the manufacturer's instructions. Briefly, 50 μl of Assay Diluent and 50 μl of sample were added per each well and incubated for 2 h. After washing 5 times with the Wash Buffer, 100 μl of horse radish peroxidase (HRP)-conjugated secondary antibody were added and plates incubated for 2 h. Samples were then washed again, and 100 μl of 3,3′,5,5′-tetramethylbenzidine (TMB) substrate were added per each well. After incubation at room temperature in the dark, 100 μl of the Stop Solution were added and the OD determined at 450 nm using the microplate reader SpectraMax plus384, with a wavelength correction set at 570 nm. Curves of known concentration of a standard were used to calculate the concentration of the samples.

6.20 Telomerase Activity and Telomere Length

The high proliferation ability of stem cells and tumor cells has been associated with the expression and activity of the ribonucleoprotein telomerase, which is involved in securing the lengthening of the telomeres, the repeated DNA sequences at the end of the eukaryotic chromosomes, thus preventing cell senescence and death [352]. In study II, both the telomerase activity and length of telomeres were investigated and compared for hES-MPs and hMSCs.

The telomerase activity was investigated using the *TeloTAGGG* Telomerase PCR ELISA^{PLUS} kit, a photometric enzyme immunoassay for the quantitative determination of telomerase activity. The assay combines the Telomeric Repeat Amplification Protocol (TRAP), during which the telomerase-reaction products are amplified by PCR, with the ELISA principles of immobilization and detection through an HRP-conjugated antibody and the sensitive peroxidase substrate TMB. Briefly, both hES-MPs and hMSCs at 5 and 50 population doublings (PD) were trypsinized and about $2x10^5$ cells were centrifuged and washed in 200 µl of PBS according to the protocol. Cell lysates were centrifuged at 14000rpm for 20 min at 4°C. The supernatants were transferred to an amplification tube and the reaction mixtures were added. Both the telomerase-mediated primer elongation and the PCR reaction for all the samples were performed using a Thermal Cycler 2720. The PCR products were split in 2 aliquots, denatured and hybridized separately to digoxigenin (DIG)-labeled detection probes specific for the amplified telomere repeats. The resulting products were later immobilized via the biotin label to a streptavidin-coated microplate for 2 h at 37°C, under agitation at 300 rpm. After incubation, samples were treated with 100 µl of a solution of an HRP-conjugated antibody against DIG. After washing, 100 µl of a TMB solution were added and the absorbance evaluated at 450 nm. All samples were analyzed in triplicates and heated samples used as negative control.

The length of telomeric sequences was instead investigated using the non-radioactive chemiluminescent *TeloTAGGG* Telomere Length Assay, which consists of three main steps: i) the digestion of the genomic DNA using a mixture of frequently cutting restriction enzymes, ii) the separation of the obtained fragments by gel electrophoresis and subsequent transfer to a nylon membrane via Southern blotting, and iii) their hybridization to a DIG-labeled probe specific for the telomeric repeats and following incubation with a DIG-specific antibody conjugated with ALP. The ALP then metabolizes the chemiluminescent CDP-star substrate and the signal is

detected using an X-ray. hES-MPs and hMSCs at a PD of 5 and 50 respectively were trypsinized and centrifuged at 1500 rpm for 5 min. Pellets were resuspended in 200 μl of sterile PBS and total DNA isolated as described above. After isolation, DNA from all samples was digested with 1 μl master mix solution of *Hin*f I/*Rsa* I for 2h at 37°C. After digestion, DNA fragments were separated by agorose gel (0.8%) electrophoresis following standard protocols at 5 V/cm in 1x TAE buffer. After separation, a Southern blot was performed and fragments transferred to a positively charged nylon membrane. The transferred DNA was cross-linked at 120°C for 20 min and the blotted fragments hybridized to DIG-labeled probes incubated with a DIG-specific antibody covalently coupled to ALP according to the manufacturer's protocol. After adding the chemiluminescent substrate, the membrane was exposed to X-ray film. A molecular weight marker was used for telomeric length meaurements.

6.21 Colorimetric Assays

Colorimetry is a method for determining the concentration of a chemical element or chemical compound in a solution with the aid of a color reagent or reagents that undergo a measurable color change in presence of the analyte of interest. The method tests the concentration of a solution by measuring its light absorbance at a specific wavelength. In this thesis, colorimetric assays were performed to assess the content of calcium and phosphate within the extracellular matrix, the ALP activity and the total protein content.

6.21.1 Calcium Content

Mineralization of the ECM in bone tissues depends on the deposition of calcium/phosphate minerals. Based on this knowledge, the content of calcium within the ECM produced by the cells is a good indication of the degree of mineralization, and it is often used as parameter to investigate osteogenic differentiation.

In study I and III, the calcium content was measured using the colorimetric method described by Connerty and Briggs [353]. Samples were rinsed twice with DMEM-LG without serum and fixed in Histofix™ for 30 min. After rinsing with distilled H_2O, the samples were incubated with 1 ml of HCl (0.6 N), and agitated on an orbital shaker for 24 h at room temperature to allow dissolution of the calcium ions. The calcium content was then measured using the o-cresolphthalein

complexone (CPC) method. In this method the CPC reacts with the calcium ions to form a purple-colored complex in alkaline solution. 8-hydroxyquinoline is added to the reacting solution to bind and prevent interference from magnesium and iron. The quantity of the calcium-CPC complex was then determined measuring the increase in absorbance at 552 nm, and considered directly proportional to the calcium concentration. The analyses were performed at the accredited laboratory of Sahlgrenska University Hospital.

In study V, determination of total calcium was performed using the method of methylthymol blue (BMT) described by Ripoll [354]. In this method the BMT reacts with the calcium ions forming a complex of blue color. Again, the presence of 8-hydroxyquinoline eliminates the interference due to the magnesium ions. Briefly, cells were lysed using a solution of Triton (0,4%) on ice and scraped with a cell-scraper. Then, 50 µl of cell lysates were added to 50 µl of HCl (1.2 M) and the color intensity of the calcium-BMT complex was measured at 612 nm, and considered proportional to the calcium concentration within the samples.

6.21.2 Phosphate Content

As for calcium, the phosphate content within the ECM is often assayed to investigate the degree of mineralization.

In study I and III, the content of phosphate was determined using the method based on the reaction of phosphate with ammonium molybdate to form ammonium phosphomolybdate without reduction and in presence of sulfuric acid as described earlier [355]. Samples were rinsed with DMEM-LG and fixed in Histofix™ for 30 min before HCl treatment as described above for calcium measurements. The formed yellow-colored complex was then determined colorimetrically in the UV region at 340 nm, and was considered proportional to the phosphate concentration within the samples. The analysis was performed at the accredited laboratory of Sahlgrenska University Hospital.

6.21.3 Alkaline Phosphatase Activity

ALP activity is commonly used to assess cell differentiation toward the osteogenic lineage. In this thesis, ALP activity was measured using the p-nitrophenylphosphate (pNPP) method described by Axelrod [356].

In study I and III, cell lysates were collected and the quantity (in alkaline solution with a pH of 10.4) of the p-nitrophenol produced was then determined measuring the increase in absorbance at 409 nm, and was considered directly proportional to the ALP activity. The assay was performed at the accredited laboratory of Sahlgrenska University Hospital.

In study IV, aliquots of cell extracts (50 µl) were incubated with 250 µl of 2-amino-2-methyl-propanol (pH 10.3) and 250 µl of pNPP (15.2 mM) in $MgCl_2$ (2 mM) at 37°C. The reaction was stopped after 30 min by adding 1 ml of NaOH (1 N). The quantity of p-nitrophenol (yellow) produced was measured colorimetrically at 410 nm using the µQuant reader, and was considered directly proportional to the ALP activity. A standard curve was generated to determine the ALP activity of the samples. Blank measurements were used for background correction.

6.21.4 Total Protein Content

The total content of protein was measured to estimate ECM deposition. In this thesis the total protein content was assayed using the Bicinchoninic Acid (BCA) Protein Assay. The method is based on the reduction of the copper ions (Cu^{2+}) by the peptide bond of proteins in alkaline environment (Biuret reaction), and subsequent formation of a purple intense complex of Cu^{+} with BCA. The purple color results from the chelation of two molecules of BCA with one Cu^{+}. The complex produced from the reaction is highly stable and the intensity of the color proportionally increases over a broad range of protein concentrations [357].

In study IV, in order to quantify the deposited extracellular matrix, cell/coral constructs were grinded frozen in liquid N_2 for 1 min at 30 Hz. Following the addition of 150 µl of Triton (0,1%), three freeze-thaw cycles were performed. A 10 µl aliquot of lysed samples was incubated for 30 min at 37°C with 200 µl of working reagent (mix of Cu and BCA in alkaline pH). Absorbance was read at 562 nm using the µQuant microplate reader. Protein concentration was determined using a standard curve of known concentrations of bovine serum albumin (BSA). A blank standard was used as negative control and its average absorbance measurements subtracted from all the other measurements for calculation.

6.22 TOF-SIMS Analysis of Mineralized Matrix

TOF-SIMS was used in this thesis to investigate the mineralization of the matrix following osteogenic stimulation of the cells.

In study I and III, after 6 weeks of culture under osteogenic conditions, the samples were rinsed twice with DMEM-LG and subsequently treated with ethanol (95%) to dissolve membranes and fix the samples. TOF-SIMS analyses were carried out using a TOF-SIMS IV instrument equipped with a Bi cluster ion source and a C_{60}^+ ion source. Analysis was done with the instrument optimized for high mass resolution (m/Δm ~5000, beam diameter 3.5 μm) using 25 keV Bi_3^+ primary ions at a pulsed current of 0.1 pA or with the instrument optimized for high lateral resolution using 50 keV Bi_3^{++} primary ions at 0.04 pA. Depth profiles and 3D maps were recorded by repeated sputtering of the surface using 10 keV C_{60}^+ ions (300x300 μm, 0.6-2.6 nA) and analysis (Bi_3^+ primary ions, high mass resolution, 200x200 μm, 128x128 pixels) in an alternating mode. The data file acquired during the analysis contains an entire mass spectrum in each of the 128x128 pixels within the analysis area, and at the different sputtering times, allowing for retrospective reconstruction of the data in different forms, such as (i) depth profiles showing the signal intensity of selected ion peaks added over the entire analysis area as a function of sputtering time or sputter dose (number of applied sputter ions per surface area), (ii) two-dimensional images showing the signal intensity of selected ion peaks in selected horizontal or vertical cuts through the sample (in vertical cuts the depth coordinate is represented by the sputtering time) or (iii) mass spectra from a selected 3D region of the sample obtained by selecting a region of interest on the sample surface and a selected range of sputtering times. Several peaks in the mass spectra could be assigned to HA, based on comparison with a reference spectrum recorded on a pure HA sample. A number of peaks were assigned to proteins, originating from the cell material or protein deposits, based on the 3D colocalisation with small nitrogen-containing organic fragment ions.

In study IV, after 5 weeks of culture in bioreactors, cell/coral constructs were harvested for TOF-SIMS analyses. Briefly, samples were mounted on a sample holder allowing for imaging mass spectrometry analysis of cross sections of the cell/coral construct. Two samples each of the four different groups were analyzed by TOF-SIMS using the same equipment and ion sources as described above. Prior to each analysis, the sample surface was sputter cleaned using 10 keV

C_{60}^+ ions over an area of 600x600 μm for 200 seconds at a C_{60}^+ current of 0.3 nA. Acquisition of TOF-SIMS data was done using 25 keV Bi_3^+ primary ions with the instrument optimized either for high mass resolution (bunched mode, mass resolution m/Δm ~7000, lateral resolution Δl ~3-5 μm) or for high image resolution (BA mode, m/Δm ~300, Δl ~200 nm). Spectra and ion images were recorded in the bunched mode over an analysis area of 500x500 μm (256x256 pixels) for 200 s at a pulsed primary ion current of 0.1 pA and over an analysis area of 150x150 μm (256x256 pixels) at a pulsed primary ion current of 0.04 pA for 300 s in the burst alignment mode. For each sample, three areas were analyzed in the bunched mode, and among those a smaller area was selected for high image resolution analysis (BA mode). Ion images showing the localization of the three different components of the sample (calcium carbonate, calcium phosphate and resin) were obtained by adding the signal from several characteristic ions for each component. The reason for using slightly different peaks in the bunched and BA modes is the higher mass resolution in the bunched mode, which allows for better selection of characteristic ions without interference with other ions.

6.23 Lactate Dehydrogenase Assay

Cell death can be quantified using different methods, among which the determination of the activity of cytoplasmatic enzymes released by damaged cells. In this thesis, the proportion of cell death was investigated by measuring the LDH activity. LDH is present in all cells and rapidly released into the cell culture supernatant following rupture of the cell membrane.

In study VI, medium was collected weekly and the LDH activity was determined in an enzymatic test, during which NAD^+ is reduced to NADH by the LDH-catalyzed conversion of lactate to pyruvate. The formation rate of NADH was then determined measuring the increase in absorbance at 340 nm and considered proportional to the catalytic activity of LDH. The analysis was performed at the accredited laboratory of Sahlgrenska University Hospital.

6.24 *In vivo* Experiments

The reasons to perform *in vivo* studies are to investigate biological processes inside living organisms, and to determine the safety of therapeutic products before applications in humans. In

this thesis, mice were used as animal models due to their similarity with humans, low cost and ease of handling.

In study V, *in vivo* experimentation was carried out in order to assess the survival rate of hES-MPs and any possible immune response mounted against the transplanted cells. To study the survival rate, 18 cell/scaffold constructs were placed subcutaneously in three groups of mice, of which two groups of immunocompromised strains, specifically $Lyst^{bg}$ $Foxn1^{nu}$ $BtK^{xid\ 358}$ and Nude mice, and one group of immunocompetent Balb/c mice (all 8-week-old female), with each mouse receiving 2 implants. Before implantation, mice were anesthetized by intraperitoneal injection of Ketalar® (1mg per 10 g of body weight) and Rompun® (0.1 mg per 10 g of body weight), and the implantation site (mouse back) was disinfected with Betadine®. Then, small incisions at both sides of the vertebral axis of each animal were made, pockets were created and implants carefully placed. The soft tissues at the implantation sites were closed with non-absorbable sutures. Eight weeks after implantation, animals were anesthetized by intraperitoneal injection of Ketalar® (1 mg per 10 g of body weight) and sacrificed by intraperitoneal injection of a Dolethal® overdose, and implants retrieved following surgical incision. Following anesthesia, a sterile physiological saline solution was injected subcutaneously when needed.

In order to study the *in vivo* immune response, 32 implants, of which 16 constructs of hES-MPs and 16 coral scaffolds, were placed subcutaneously in 8 male adult Balb/c mice (all 8-week old). Each mouse received 4 implants. Four additional mice received a sham surgery (sham mice). Animals were sacrificed after 10 days and implants retrieved after surgical incision. All surgical procedures were performed as described above.

6.25 *In vitro* and *in vivo* Bioluminescence Imaging

Bioluminescence is the chemical production and emission of light by a living organism, and is the result of an enzyme-catalyzed reaction of O_2 with a substrate. To date, bioluminescence is largely utilized in biomedicine as noninvasive technology that allows the extraction of relevant biological information and enables the *in vivo* monitoring of molecular and cellular events.

In study V, bioluminescence imaging was used to estimate the efficiency of cell transduction and monitor cell survival *in vivo* following subcutaneous implantation of cell/coral scaffolds in Fox,

Nude and Balb/c mice. Two days after transduction, cells were rinsed twice with PBS and 50 µl of a solution of D-Luciferine (1mg/ml) were added per each well to reach a final volume of 250 µl. A standard curve using increasing number of cells was generated to assess signal linearity. Samples were analyzed with the IVIS Lumina Bioluminescent imaging system using the Living Image® 3.1 Xenogen software. Survival of the implanted cells was instead investigated along the entire duration of the experiments, with bioluminescence signal acquisitions taken twice a week during the initial 3 weeks and once a week for the remaining 5 weeks as previously described [359]. Briefly, mice were placed in an induction chamber and anesthetized using a mixture of 4% isofluorane in O_2 and air, each at a flow rate of approximately 2 L/min. After gentle subcutaneous injection of 50 µl of D-Luciferin (20 mg/ml) in proximity of each implant, animals were placed in the acquisition chamber of the IVIS Lumina II Bioluminescent imaging system under constant isofluorane inhalation (1% in O_2 and air) at a flow rate of 1 L/min, and signals (photon/s) acquired for a time period which did not give saturation. The light emission kinetics was previously determined using an acquisition time of 5 min, at 5-min intervals for a total of 40 min**.** The optimal bioluminescence signal occurred at the interval 20-40 min post-administration of D-luciferin (20 mg/ml). Standard regions of interest (ROI) surrounding each implant were manually delineated on bioluminescence images in order to quantify the photons flux emitted by the constructs using the Living Image® software 3.1.

6.26 White Blood Count

Blood is composed of plasma and different types of cells, including erythrocytes, leucocytes and thrombocytes. Leucocytes are cells of the immune system involved in inflammatory and immune response to pathogens and foreign materials. Leucocytes are also involved in the immune rejection of non-syngeneic tissues and organs.

In order to investigate the ability of hES-MPs to elicit an immune response *in vivo*, we evaluated the proportion of white cells in the systemic circulation of Balb/c mice before implantation, as well as after 3 and 10 days following implantation. Blood samples were collected from the retro-orbital region using blood collection capillary tubes as described earlier [360]. To avoid coagulation, blood samples were mixed to a solution of sodium citrate (104 mM) at a ratio of 6 to 1. Then, to investigate the proportion of leucocytes, a full blood count (FBC) analysis was performed using the hematology blood analyzer COULTER® ACT 10.

6.27 Serum Preparation

In the blood, serum is the fraction of liquid without cells, fibrinogen and other clotting factors. It contains all the protein not involved in coagulation, including antibodies, hormones, enzymes and cytokines.

In study V, following sacrifice of the animals 10 days after implantation, blood was collected for serum cytokine profile investigation. Animals were positioned on their back, the abdomen was opened to cut the heart and blood was collected through a syringe. Blood was transferred to Eppendorf tubes and allowed to clot before centrifugation at 8000rpm for 20 min at 4°C. Centrifugation allowed separation of the clot from the serum fraction. The serum was then aspirated and stored at -80°C until examination.

6.28 Histological Techniques

Histology is the study of the structure and composition of cells and tissues. Histological examination is performed by microscopic investigation of thin sections, which are usually colored through the use of specific histological stains for the differential identification of particular structures. Before histological examination, samples must be fixed to preserve the biological material from deterioration and maintain the structure of both the cellular and molecular components. When the material under investigation is part of a 3D tissue or an organ, samples must be embedded in appropriate materials and then cut in thin slices before examination. To allow embedding in substances immiscible with H_2O, samples must first be dehydrated using increasing concentration of ethanol or other similar chemicals, and then cleared using hydrophobic agents (such as xylene) to remove the ethanol. Subsequent treatment with serial solution of different ratio of clearing agent and embedding material allows full removal of the clearing agent and complete infiltration of the embedding material inside the sample. Following infiltration, samples are placed in specific molds and submersed in liquid embedding materials, which are then hardened by temperature, light or chemical catalysts. Blocks are finally cut using specific knives, and sections stained and observed microscopically. In this thesis, both paraffin and plastic resin were used as embedding materials. Embedding in plastic resin is needed when investigating hard tissues and/or tissue-implant constructs, although sections thinner than 20 μm cannot be cut and immunohistochemical staining is not suitable. On the other hand,

paraffin allows cutting sections as thin as 4 μm and suitable for the majority of stainings. However, when working with bone, decalcification of the samples is required.

In study IV, after 5 weeks of culture in bioreactors, cell/coral constructs were rinsed in PBS and fixed in 4% paraformaldehyde at 4°C for 24 h. Samples were then decalcified in EDTA (pH 7) for 5 days, dehydrated through ethanol and isopropyl alcohol and embedded in paraffin. Four sections with a thickness of 4 μm were then cut from each sample, two at a depth of 20-25% and two at depth of 45-50% of the cell/coral constructs. For TOF-SIMS analysis instead, constructs were rinsed twice with PBS and fixed in 4% formaldehyde at 3-5°C. After fixation, samples were dehydrated in ethanol of increasing concentration, cleared with xylene, embedded in plastic resin (LR White) and allowed to harden on ice. Then, each block was cut at a level corresponding to a depth of about 50% inward the cell/coral construct using the Exakt cutting-grinding equipment as described elsewhere [361].

In study VI, after 6 weeks of culture under osteogenic conditions, cp-Ti and Ti6Al4V constructs were fixed, cleared and embedded in plastic resin (LR White) as described above. Samples were then sectioned and ground to a thickness of approximately 50-60 μm before staining.

6.29 Histochemical Staining

Staining of the sections facilitate the differential observation of specific microscopic structures. The staining reaction occurs due to the chemical union between the dye and the stained substance through salt linkages, hydrogen bonds, or others. In this thesis, different stainings were used in order to investigate mineralization and adipogenic differentiation of monolayer cultures, as well as tissue formation and collagen deposition within cell/scaffold constructs.

6.29.1 Von Kossa

Von Kossa staining allows the detection of calcium deposition within the ECM. It is a silver-based staining in which the silver cations replace calcium bound to phosphate within the mineral deposits, and turn to black after exposition to light.

In study I and III, cells were washed with PBS and then fixed in Histofix® for 30 min. After

washing with distilled H_2O, a solution of $AgNO_3$ (2% w/v) was added, and the plates kept in dark for 10 min. The plates were then rinsed 3 times with distilled H_2O before being exposed to bright light for 15 min. After washing with distilled H_2O, samples were quickly dehydrated adding ethanol (95%) and samples imaged using a light microscope equipped with a digital camera.

In study V, cells were rinsed with PBS and then fixed in glutaraldehyde (0.25%) for 15 min a 4°C. All the following steps were performed as described above.

6.29.2 Oil-red O

Oil-red O is a lysochrome that specifically binds lipids, triglycerides and lipoproteins, thus allowing detection and quantification of fat deposits within the sample.

In study III, hES-MPs and hMSCs cultured under osteogenic conditions at P5 were washed in PBS and fixed in Histofix® for 10 min. The cells were then stained with an oil-red O solution in 60% isopropanol for 1 h, followed by repeated washings with H_2O. Quantification of the lipid content was then obtained using the BioPix Software for histological quantification (www.biopix.se).

6.29.3 Haematoxylin-eosin-safranin

Haematoxylin-eosin-safranin (HES) staining is a combination of histological dyes that specifically stain the nuclei, the cytoplasm and the collagen fibers, respectively. Haematoxylin is recognized to bind the arginine-rich basic nucleoproteins such as histones, resulting in a typical blue-violet coloration. Eosin, which is usually used as counterstain to haematoxylin, is an acidic dye that colors the basic parts of the cell, resulting in a pale pink staining. Safranin is a nuclear stain with the ability to also confer a yellow color to collagen.

In study IV, paraffin-embedded sections were dewaxed in xylene (2 times for 5 min), followed by treatment with absolute ethanol (2 times for 5 min), 95% and 70% ethanol (5 min each). Sections were then washed in H_2O and then immersed in Harris' haematoxylin for 4 min. After washing, sections were immersed in a solution of eosin (1%) for 7 min, dehydrated in ethanol and

immersed in a solution of Spanish saffron (6% w/v) in pure ethanol. Sections were then treated with xylene and mounted with cover glasses.

6.29.4 Sirius Red

Sirius red is an elongated acidic molecule that specifically reacts with collagen molecules, which are rich in basic amino acids. The binding enhances the normal birefringence of collagen due to the parallel alignment of Sirius red molecules along the collagen fibers, thus allowing the specific detection of collagenous structures composed of aggregates of oriented molecules [362, 363]. When observed under a bright-field microscope, collagen appears red on a pale yellow background.

In study IV, sections were dewaxed as described above and then immersed in a solution of 0.1% Direct Red 80 in saturated picric acid for 1 h. Sections were then washed with H_2O and mounted with cover glasses.

6.29.5 Toluidine Blue

Toluidine blue is a basic dye widely used in histology. In alkaline solutions, the dye binds to nucleic acids, which appear blue under bright-field microscopy.

In study VI, plastic-embedded sections were rinsed in distilled H_2O, dried and rinsed again with a solution of H_2O_2 in H_2O (3:1) for 10 min. Sections were then immersed in a solution of toluidine blue for 10 min, rinsed with H_2O and dried overnight. Finally, the sections were mounted with cover glasses for microscopic investigation.

6.30 Immunohistochemistry

Immunohistochemistry (IHC) is a technique for antigen detection by means of specific antibodies, which was first introduced by Coons *et al.* in 1941 [364]. The binding of the antibody with the target antigen is visualized using reported molecules attached to the primary, secondary or tertiary antibodies, including fluorescent compounds, enzymes and metals [365]. In this thesis, fluorochrome-conjugated antibodies were used for antigen detection and visualization.

In study II, the expression of NANOG and OCT4 was verified by IHC. Briefly, cells were fixed in Histofix™ for 15 or 60 min, for OCT4 and NANOG staining, respectively. Subsequently, samples were washed with PBS and then blocked with a 5% solution of dry milk in PBS for 30 min. Primary antibodies for OCT4 and NANOG were added to the cells and incubated for 12 h at 4ºC. Negative controls, i.e. without primary antibody, were included for each cell type and marker. After washing with PBS, the cells were incubated with secondary antibodies (goat anti-mouse IgG-Alexa488 for OCT4 and donkey anti-goat IgG-Alexa488 for NANOG) in the dark for 2 h at room temperature. Finally, the cells were washed and mounted with DAKO mounting media containing 4´,6-diamidino-2-phenyldole (DAPI) for counterstaining of the nuclei.

6.31 Statistical Analyses

Different statistical tests were used in the present thesis for assessing significance of the results. Specific tests were selected in relation to the type of data and the number of groups investigated. Nonparametric tests were used when data could not be assumed to be sampled from a population following a Gaussian distribution, or when few data points were collected and a Gaussian distribution could not be assessed. Logarithmic transformation of the dataset was performed to meet the assumption of normality when using parametric tests.

In study I and III, the significance level of microarray data was determined using Welch's t-test on log2-transformed signal values.

The nonparametric Mann-Whitney U test was used to determine the significance level of RT-PCR data in study I, II, III, IV and VI, as well as for all the other analyses in study IV, V and VI when comparing two independent samples.

In study III, all data points were transformed to log10 scale in attempt to satisfy normality assumptions. A small value of 10^{-6} was added to all raw measurements to avoid infinity. Linear general least squares model for repeated measures was fit to all datasets where signals were detected for >1 week among at least one of the cell types. Autoregressive covariance structure with heterogeneous variances over time was chosen for the model. Contrasts were calculated to estimate the difference between the cell types for each week. Two-sided t-test was performed to test whether the contrasts differed significantly from zero. Where no repeated measurements were

performed, differences were determined by Student's independent t-test.

In study V, repeated measurements differences were determined using the nonparametric Wilcoxon signed-ranks test. When comparing data between more than two independent or related samples, the Kruskal-Wallis and Friedman tests were used, respectively.

In all analyses, results are expressed as means and standard deviations. All statistical analyses were performed using the SPSS Statistics 17.0 software. Open source statistical software package R was used for the model and contrast fitting in study III. Bonferroni was used for repeated measurements correction. For all the analyses, a value of $p \leq 0.05$ (*) was considered as significant difference.

6.32 Ethical Approval

Embryos were donated after informed consent and approval of the local ethics committees at University of Gothenburg.

Ethical approval to conduct hESCs studies was given by the Regional Ethics Committee in Gothenburg (Dnr 376-05).

The donation of bone marrow for isolation of hMSCs was approved by the ethical committee at the Medical Faculty at Gothenburg University (Dnr 532-04).

Animal experimentations were performed with prior received ethical approval by the Ethics Committee on Animal Research of Lariboisiere/Villemin in Paris, France and carried out in accordance with European Guidelines for Care and Use of Laboratory Animals (EEC Directives 86/609/CEE of 24.11.1986).

7. SUMMARY OF THE RESULTS

7.1 Study I

In this study, the osteogenic potential of MFG-hESCs and hMSCs was compared in monolayer cultures, and their ability to synthesize a mineralized matrix was investigated in relation to the expression of genes involved in ossification. Gene microarray data displayed a rather different profile of expression for genes involved in ossification in the undifferentiated state, as observed by hierarchical cluster analysis. Specifically, the results demonstrated that MFG-hESCs displayed higher expression of BMP4, OPN, BMP7 and ALP, whereas other genes involved in osteogenic specification, including TGFβ1, TGFβ2, ON, BMP1, COL1A1, FOXC1 and RUNX2 displayed higher expression in hMSCs. Among them, BMP4, ALP, TGFβ2, ON, COL1A1 and RUNX2 were found to be hub genes when performing PPI network analysis. Interestingly, the expression of the above genes was differentially affected following osteogenic stimulation of the cells and displayed a different profile along the investigation period, indicating that different molecular pathways take place during the differentiation of MFG-hESCs and hMSCs toward the osteogenic lineage. Interestingly, the osteogenic differentiation of MFG-hESCs was associated with the downregulation of genes involved in pluripotency and teratoma formation, including OCT4, NANOG, SOX2 and TDGF1. In addition to the differences observed in the expression of genes involved in ossification, both in the undifferentiated state and upon osteogenic stimulation, the results showed a difference also in the ability of MFG-hESCs and hMSCs to produce a mineralized matrix. Colorimetric assay of calcium and phosphate demonstrated that the matrix produced by MFG-hESCs displayed significantly higher content of mineral deposits than hMSCs after 3 and 4 weeks of culture under osteogenic conditions. Moreover, calcium was detectable after 2 weeks in the matrix produced by MFG-hESCs but not in that produced by hMSCs. Accordingly, after 4 weeks of culture under osteogenic conditions, MFG-hESCs displayed more extensive mineralized regions when stained with von Kossa compared to hMSCs. The above data were in line with the TOF-SIMS results, which revealed the presence of thicker and denser deposits of calcium and phosphate in cultures of MFG-hESCs compared to hMSCs after 6 weeks of culture under osteogenic conditions.

7.2 Study II

In study II, the gene expression profiles of hESCs, hES-MPs and hMSCs were investigated in order to explore the molecular changes occurring upon derivation of hES-MPs and assess any similarities and differences in gene expression profile between hES-MPs and hMSCs. Further, the proliferation potential and the immunological profile of hES-MPs and hMSCs were studied and compared. Scatter plot analysis of the microarray data per each pairwise comparison showed that hES-MPs and hMSCs displayed comparable gene expression profiles, with only 10 percent of the genes exhibiting a difference in FC ≥3. Hierarchical cluster analysis further demonstrated the high similarity between hES-MPs and hMSCs, resulting in three main groups, with hES-MPs and hMSCs clustering together. Microarray data showed that the derivation of hES-MPs was associated with downregulation of genes known to be specifically or highly expressed in hESCs, and upregulation of genes characteristic of mesodermal tissues. Interestingly, the majority of these genes were similarly expressed in hES-MPs and hMSCs. Among the downregulated genes were several factors involved in pluripotency and tumorigenicity, including OCT4, NANONG, SOX2, LIN28, TDGF1, EPHA1 and DNMT3B. On the other hand, hES-MPs derivation was associated with upregulation of genes encoding for proteins constituting the matrix of mesodermal tissues, factors involved in mesodermal differentiation and surface markers typical of the mesenchymal lineage, including RUNX2, COL1A1, ON, FN1, FBN1, TGFβR2, BMPR2, CD44 and many others. COL1A1, FN1 and CD44 were found to be hub genes when performing PPI network analysis. A summary of the aforementioned transcriptional changes occurring upon hES-MP derivation is shown in Figure 11.

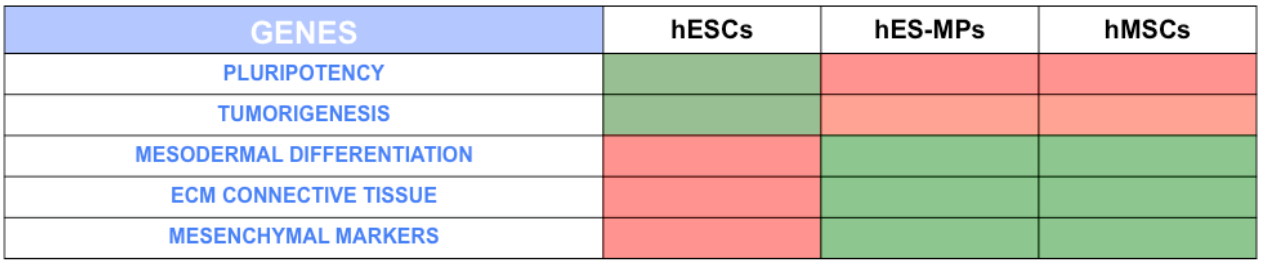

Figure 11: Expression level of key genes in hESCs, hES-MPs and hMSCs (green: high expression; red: low expression).

Besides the similarities in the gene expression profiles between hES-MPs and hMSCs, a panel of genes involved in cell proliferation and DNA replication displayed higher expression in hES-MPs

than in hMSCs, including HELLS, CDC25A, MCM5, FGF5 and ORC1L. In line with these findings, hES-MPs displayed a significantly higher proliferation capacity *in vitro* compared to hMSCs, exhibiting shorter PD time and retaining a stable proliferative potential up to passage 30, in addition to display longer telomeric sequences. Flow cytometry analysis for immunological markers demonstrated that hES-MPs did not express HLA-DR molecules, as opposite to hMSCs that displayed increased expression of HLA-DR after treatment with IFN-γ.

7.3 Study III

The objective of this study was to investigate and compare the osteogenic properties of hES-MPs and hMSCs, and assess the effects of prolonged expansion on matrix mineralization and osteogenic differentiation. Further, the immunological profile of both cell types after osteogenic stimulation was studied. The results demonstrated that at all passages investigated the ALP activity displayed a gradual increase along the experimental period. Slightly different profiles were observed for hES-MPs and hMSCs, with the hMSCs displaying significantly higher ALP activity. The ALP activity for both cell types was inversely proportional to the passage number. In a different fashion, colorimetric assay of calcium and phosphate demonstrated that the matrix produced by hES-MPs displayed significantly higher content of mineral deposits compared to hMSCs along the experimental period. Further, despite a general decrease in mineralization was observed after protracted expansion for both cell types, hES-MPs retained better mineralization properties than hMSCs. Accordingly, hES-MPs displayed more extensive mineralized regions at earlier time points when stained with von Kossa at P5 and P10 compared to hMSCs. TOF-SIMS analysis further demonstrated an earlier onset of mineralization in hES-MPs cultures at P5. In addition to the higher calcium and phosphate content observed, hES-MPs displayed specific differentiation toward the osteogenic lineage, with no signs of codifferentiation toward the adipogenic lineage as demonstrated by lack of oil-red O staining. RT-PCR results demonstrated that at P5 the expression profiles of RUNX2, COL1A1, OPN and OC were similar for both cell types, showing corresponding variations along the investigation period, although significant differences in the level of expression were observed. The expression level and profile of the same genes were different for both cell types after protracted expansion at P20. Flow cytometry analysis for immunological markers at P5 demonstrated that, unlike hMSCs, hES-MPs did not express HLA-DR molecules following osteogenic stimulation and IFN-γ treatment.

7.4 Study IV

In study IV, the effect of flow perfusion on the proliferation and osteogenic differentiation of hES-MPs and hMSCs interfaced with biocoral scaffolds was studied and compared. The results demonstrated that, when cultured under dynamic conditions, both constructs of hES-MPs and hMSCs displayed significant increase in DNA and protein content compared to the respective content at day 0, as well as the content observed when cultured under static conditions. Interestingly, constructs of hES-MPs displayed significantly higher content of DNA and proteins compared to hMSCs. Moreover, RT-PCR results demonstrated an effect of flow perfusion on the expression of genes involved in osteogenic differentiation or encoding for proteins constituting the matrix of bone tissue, although the effect was different between hES-MPs and hMSCs. For example, when cultured under dynamic conditions, hES-MPs displayed increased expression of COL1A1, ALP, ON and OPN whereas hMSCs displayed increased expression of RUNX2, COL1A1, ON and OPN. Overall, under dynamic conditions, the expression of the investigated genes was higher for constructs of hES-MPs than for constructs of hMSCs. In line with the proliferation and gene expression results, histological staining demonstrated that constructs of hES-MPs displayed a marked increase in tissue formation when cultured under dynamic conditions, and the newly formed tissue was associated with deposition of a dense network of collagen fibers. On the other hand, no substantial increase in tissue formation was observed for constructs of hMSCs when cultured under dynamic conditions compared to static conditions. TOF-SIMS analysis revealed that both constructs of hES-MPs and hMSCs displayed deposition of calcium phosphate minerals at the interface with the coral scaffolds in all conditions investigated, although flow perfusion stimulation appeared to promote matrix mineralization, and was associated with a higher content of calcium phosphate within the constructs.

7.5 Study V

In this study, constructs of hES-MPs interfaced to coral scaffolds were implanted subcutaneously in mice, and the *in vivo* survival rate was investigated in relation to a potential acute immune response to the transplanted cells. Bioluminescence imaging results demonstrated that, following implantation of the cell/coral constructs, the percentage decrease in signal was similar in all strains investigated, with nearly no signal detected 18 days after implantation of the constructs. The decrease in survival rate was similar irrespective of the immune conditions of the

testing animals employed, excluding the involvement of T, B and natural killer (NK) lymphocytes in determining the decrease in cell survival observed. In line with this finding, implantation of cell/coral scaffolds in immunocompetent Balb/c mice did not seem to provoke an increase in the number of white cells in the systemic circulation during the first 10 days after implantation. In addition, the serum concentration of specific cytokines involved in inflammation and cell-mediated immune response to non-syngeneic cells and tissues, including TNF-α, IFN-γ, IL-2 and IL-4 displayed no significant differences between sham mice and mice implanted with biocoral scaffolds alone or constructs of hES-MPs. Histological staining displayed patterns of fibro-inflammatory response, although no major differences were observed between constructs of hES-MPs and control samples.

7.6 Study VI

The objective of study VI was to investigate the potential of hES-MPs to be interfaced to FFF 3D cp-Ti and Ti6Al4V scaffolds, and study the possible effect of the biomaterial chemical composition on hES-MPs behavior, in terms of proliferation and osteogenic differentiation. SEM imaging and TOF-SIMS analysis demonstrated that both scaffolds displayed similar surface topography and composition, as well as comparable oxide layer thickness irrespective of the chemical composition of the building material. Proliferation studies demonstrated that the content of DNA within the scaffolds after 1 and 2 weeks of culture was similar for both cp-Ti and Ti6Al4V. In addition, flow cytometry data showed that the proportion of viable and dead cells was the same independently of the chemical composition of the employed scaffold after 10 days of culture. In accordance with the flow cytometry data, LDH activity results demonstrated similar trends when hES-MPs were interfaced to cp-Ti and Ti6Al4V along the entire experimental period. Moreover, RT-PCR studies showed that the expression of genes involved in osteogenic differentiation and encoding for proteins constituting the matrix of bone tissue, including RUNX2, COL1A1, OPN and OC was not significantly affected by the chemical composition of the investigated scaffolds. On the other hand, similar variations in the expression of the investigated genes were observed after 1 and 2 weeks of culture under osteogenic conditions for both cp-Ti and Ti6Al4V scaffolds. In a similar fashion, no significant differences in ALP activity were observed when the hES-MPs were interfaced to the different scaffolds, indicating no adverse effect exerted by the two materials on hES-MPs behavior.

8. GENERAL DISCUSSION

8.1 Clinical need for bone-engineered substitutes

To date, a large number of patients experience bone fractures or need reconstruction of the skeletal system following surgical excision and congenital defects [177-180]. This number is expected to steadily increase considering the population growth, extension of life expectancy, shift in demographics and changes in life style, characterized for example by a general increase in the number and severity of injuries [366]. The majority of patients in need for bone replacement procedures are the elderly, whose bones display poor mechanical properties and, most importantly, exhibit limited regeneration potential, which entails profound implications with respect to the type and strategy of treatment. Bone engineering holds the promise to alleviate the burden of bone deficiencies by constructing *bona fide* substitutes with the potential to secure an enduring and functional reconstruction of large skeletal defects, although no general consensus exist hitherto regarding the optimal combination of cells, scaffolding materials and cultivation conditions. In this view, it is of great importance to assess the potential of stem cells derived from different sources, i.e. adult or embryonic tissues, for bone engineering applications.

8.2 The stem cell dilemma

Basically, stem cells can be derived from two main sources such as embryonic and adult tissues. Both embryonic and adult stem cells display pros and cons in relation to their potential to be employed as source of cells for bone engineering applications. An optimal cell source for such application should display some key characteristics, including ready accessibility and homogeneity, high proliferation potential, proper functionality and clinical safety. hESCs are highly proliferative and have the ability to virtually differentiate in all specialized cells constituting the human body [367]. However, the major disadvantages with hESCs for the large-scale production of tissue-engineered substitutes is represented by the elaborate culture conditions required [31] and risk of tumor formation after implantation [34]. On the other hand, stem cells isolated from adult tissues, such as hMSCs are easy to handle, can differentiate toward specific lineage and their safety in clinical applications has been shown [219-223], although their clinical efficacy in tissue engineering applications is still contentious. Nonetheless, their heterogeneity, limited proliferative potential and loss of functionality associated with protracted

expansion and/or increased donor age [271-273, 277, 279, 368] represent today an important impediment for the bulk production of functional cells for tissue engineering applications. To overcome the limitations encountered with both embryonic and adult stem cells, many efforts have recently been made to establish alternative cell lines that combine the advantages of both sources and display high potential for tissue engineering applications, as illustrated in Figure 12.

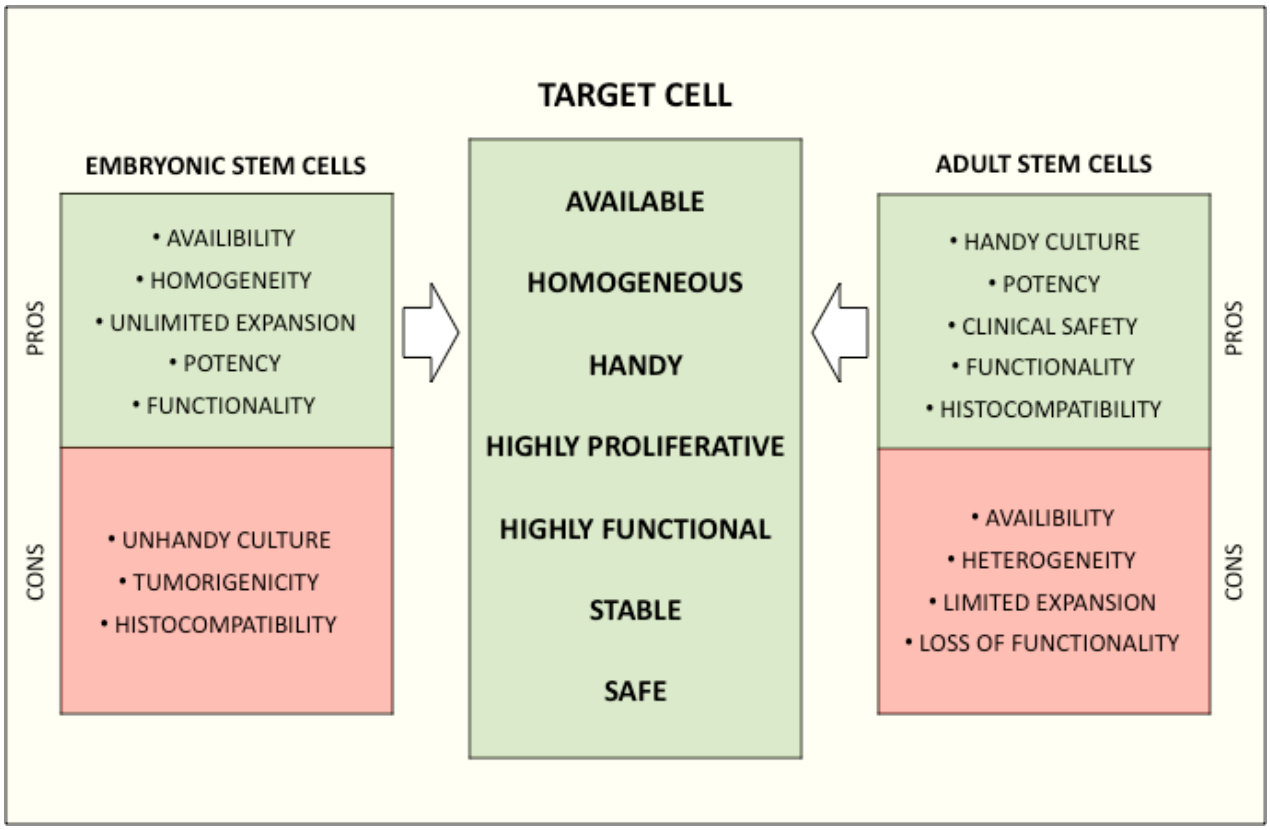

Fig 12: Illustration of the optimal cellular properties for tissue engineering application.

The MFG-hESCs and hES-MPs were previously shown to display interesting characteristics for a potential use in tissue engineering applications, especially considering the straightforward and reproducible derivation, homogeneity, high expandability and ability to be cultured under xeno-free conditions using standard protocols for adult stem cells [31, 35]. However, for a potential use of these cells in bone engineering, a thorough characterization and a comparative advantage over cells derived from adult tissue such as hMSCs must been demonstrated, which has been the main objective of this thesis.

8.3 Ossification genes display different profile of expression in MFG-hESCs and hMSCs

Numerous genes are recognized to play a role during bone histogenesis. Some of these genes displayed a different profile of expression in undifferentiated MFG-hESCs and hMSCs, as well as upon osteogenic stimulation of the cells, reflecting the different origin of the two cell types and highlighting that alternative differentiation pathways may take place during osteogenesis of MFG-hESCs and hMSCs. Variation in the expression level of genes involved in ossification were also reported by Guillot *et al*. when comparing hMSCs derived from fetal and adult tissues [369]. In particular, MFG-hESCs displayed significantly higher expression of BMP4 and OPN both in the undifferentiated state and after stimulation with osteogenic factors. BMP4 is known to be involved in skeletal development, remodeling and repair [106], and its overexpression has recently been reported to promote the osteogenic differentiation of rabbit adult stem cells *in vitro* and *in vivo* [370]. Further, the expression level of BMP4 was shown to correlate with the formation of large bone-like nodules in osteogenic cultures of hESCs [371]. OPN instead, which functions as a bridge between the organic and mineral component of bone tissues [93], is recognized to play a role in the early formation of bone matrix [372] and generally used as a marker of osteogenic differentiation. The finding that BMP4 and OPN were identified as hub genes in PPI networks suggest they may play a central role in the molecular pathways leading to osteogenic differentiation of MFG-hESCs. On the other hand, the transcriptional activator RUNX2 and the downstream gene COL1A1 [156, 157] displayed higher expression in hMSCs compared to MFG-hESCs, although the expression differences between the two cell types markedly diminished during differentiation, indicating a substantial upregulation of these genes in hMFG-hESCs following osteogenic stimulation. In a different fashion, ALP displayed higher expression in undifferentiated hMFG-hESCs compared to hMSCs but was significantly upregulated in hMSCs after osteogenic stimulation, indicating again a rather different responsiveness of the two cell types to the osteogenic factors. Similar results were observed by Shimko *et al.* when comparing murine embryonic and adult stem cells cultured under osteogenic conditions, corroborating the idea that embryonic stem cells undergo osteogenic differentiation using nontraditional osteoblastic pathways [373]. ALP is recognized to play a role during osteogenesis [99] and its upregulation during osteogenic differentiation is considered to favor the mineralization of the bone matrix [374]. Nonetheless, hMSCs displayed significantly higher transcriptional levels of

SRGN compared to MFG-hESCs both in the undifferentiated state and during osteogenic differentiation. SRGN is a proteoglycan found to influence the bone mineralization process through inhibition of HA crystal growth [375], and its high expression in hMSCs may counterbalance the effects of ALP in promoting the deposition of calcium phosphate crystals within the matrix.

8.4 MFG-hESCs display higher mineralization properties than hMSCs

The ECM of mature bone tissue is composed of 60-70 percent of calcium phosphate crystals in the form of HA [95], which provide mechanical strength and stiffness [110]. In this view, the content of calcium phosphate deposits within the matrix synthesized by the cells is of particular interest to assess their potential for bone engineering applications. Our study demonstrated a higher content of calcium phosphate deposits within the matrix synthesized by MFG-hESCs compared to hMSCs, in accordance with recently reported studies showing higher mineralization properties displayed by murine embryonic stem cells compared to adult stem cells [373]. An explanation for this may be the higher expression of SRGN observed in hMSCs as discussed in paragraph 8.3, as well as the higher expression of NCPs with inhibitory effects on HA crystallization and growth such as ON and OC [102, 376]. On the other hand, the observed difference in mineral content between MFG-hESCs and hMSCs may be associated with the specific macromolecular organization of the collagen fibers [377] and the overall charge distribution of the molecules within matrix [108]. In support of this idea there is the knowledge that collagen alteration in several pathological conditions influence HA crystallization and deposition [378]. In addition, the observed difference may result from the higher expression of TGFβ1 found in hMSCs, which was recently demonstrated to inhibit mineralization in culture of rat calvarial osteoblasts [379], although the biological mechanism responsible for this effect has not yet been elucidated. On the other hand, the difference in mineral content may be associated with a different osteogenic commitment of the investigated cells upon stimulation. In fact, after osteogenic stimulation, hMSCs displayed codifferentiation toward the adipogenic lineage, which likely influencd their capacity to produce a matrix with high content of mineral deposits. The ability of MFG-hESCs to synthesize a matrix with high content of calcium phosphate deposits underscore their potential for a future use in bone engineering applications. Nevertheless, additional studies are need to investigate the size and composition stoichiometry of the calcium phosphate crystals within the matrix, and how these affect the mechanical properties of the newly formed tissue in 3D systems.

Owing to their potential to synthesize a mineralized matrix, the MFG-hESCs certainly represent a suitable technology platform for the screening of novel agents with an effect on bone mineralization for the treatment of bone degenerative disorders.

8.5 Osteogenic differentiation of MFG-hESCs is associated with downregulation of hESC-specific genes

The use of ESCs in biomedical applications is today limited by their ability to form teratomas after *in vivo* implantation [285]. The tumorigenic capability of hESCs is associated with the expression of specific stemness genes, including genes involved in self-renewal and pluripotency such as OCT4, NANOG, SOX2 and TDGF1 [380-383]. The expression of these genes is recognized to be downregulated following *in vitro* differentiation during embryoid body formation [384], as well as in stem cells derived from adult tissues [385]. The expression of the above genes displayed a gradual decrease upon osteogenic differentiation of MFG-hESCs in monolayer cultures to a similar level as observed in hMSCs. This finding suggests that preliminary differentiation of MFG-hESCs may abolish their tumorigenic potential and enable their use for future applications in bone engineering. Supporting this idea is the finding reported by Bielby *et al*., showing that prestimulation of hESCs with osteogenic supplements was sufficient to avoid the formation of teratoma after subcutaneous implantation in SCID mice. Nonetheless, additional *in vivo* studies are needed to validate the above assumption in order to fully assess the safety of MFG-hESCs for clinical applications. In fact, additional genes may be responsible for the tumorigenic potential of undifferentiated MFG-hESCs and no sufficient data exist regarding the threshold expression of these genes to guarantee their safety after implantation. On the other hand, osteogenic stimulation may not result in the terminal differentiation of the entire cell population, raising the concern that some cells may still display tumorigenic potential following osteogenic stimulation and compromise the outcome of the intervention. However, hES-MPs and hMSCs displayed limited survival and proliferation following *in vivo* implantation, suggesting that the microenvironmental conditions at the implantation site may play an important role in further contrasting a possible uncontrolled proliferation of MFG-hESCs after application in clinical settings.

8.6 hES-MPs and hMSCs display comparable gene expression profiles

hES-MPs resemble cells of the mesenchymal lineage in terms of morphology, surface marker profile and mesodermal commitment [35], suggesting they may replace hMSCs for a large variety of applications, including development biology studies, drug screening, production of human biologics and stem-cell based therapies. The reported similarities likely result from the profound alterations observed in the global gene expression profile of hES-MPs following the derivation process. In fact, scatter plot analysis demonstrated that hES-MPs and hMSCs displayed similar transcriptomes, with 90 percent of the genes exhibiting a FC $\leq$3, while much larger variations were observed when comparing hES-MPs with the parental cell lines. Important alterations involved the downregulation of several signature genes of undifferentiated hESCs, including genes responsible for pluripotency and self-renewal such as the OCT family of genes (POU5F1**,** POU5F1P3 and POU5F1P4), NANOG, SOX2, TDGF1, LIN28, GDF3, ALP, GAL, DPPA4, GABRB3, and ZIC3 [344, 386-391]. The repression of these genes during hES-MPs derivation provides a molecular evidence for the lineage commitment restriction observed in hES-MPs [35]. In line with this observation, hES-MPs derivation did not result in increased expression of the keratin genes KRT18, KRT19, KRT7 and KRT8, and was associated with downregulation of several claudins, including CLDN3, CLDN6, CLDN8 and CLDN10 to a similar level as observed in hMSCs. Keratin genes encode for intermediate filaments typical of epithelial tissues [392], whereas claudin genes encode for the membrane proteins constituting the tight junctions in epithelial and endothelial cell sheets [393]. The low expression of these genes demonstrates lack of differentiation toward the ectodermal and endodermal lineage upon hES-MPs derivation, and is in accordance with previously reported findings showing that hES-MPs were negative for markers typical of the ectodermal and endodermal lineage [35]. On the other hand, hES-MPs derivation was associated with upregulation of a panel of genes characteristic of mesodermal tissues, including COL1A1, COL1A2, COL3A1, COL5A1, COL11A1, COL6A1, COL6A2, DDR2, BGN, FN1, FBN1, MFAP5, and genes encoding for proteins involved in cell-to-cell and cell-to-matrix interaction such as CD44, CD58, CD47 and CD166. Interestingly, the expression level of these genes was similar in hES-MPs and hMSCs, underlining functional similarities between the two cell types. Other signs of hES-MPs commitment toward the mesodermal lineage include the increased expression of genes encoding membrane receptors responsive to growth factors inducing mesodermal differentiation such as TGFβR2 and BMPR2 [394, 395], and overexpression of RUNX2 and TFAP2A, which are known to direct osteogenic differentiation

[157, 396]. The equivalent gene expression profiles observed support the idea that hES-MPs and hMSCs are functionally comparable cell types, and substantiate the potential of hES-MPs to be used as source of cells for engineering tissues of the mesodermal lineage. In addition to reflect a similar phenotype, the observed high similarities in gene expression suggest that hES-MPs may follow similar biological response to environmental stimuli and represent pertinent models for the screening of different substances and the development of new pharmaceuticals.

8.7 hES-MPs display higher proliferation potential than hMSCs

Engineering tissue substitutes requires employing highly proliferative cells showing high degree of stability upon expansion, especially in view of the reproducible and large-scale production of replacement tissues for future tissue engineering applications. hMSCs display limited proliferation capability and this ability tend to decrease with donor age [272-274, 397] raising concerns about their practical use for the large scale production of engineered tissues. On the other hand, in study II we demonstrated that hES-MPs display high proliferative capacity, characterized by retained proliferative potential over prolonged expansion (up to P30) and shorter PD time compared to hMSCs. In fact, the proliferative ability of hMSCs started decreasing after 8-10 passages and was completely abolished at P25. In addition, prolonged expansion of hMSCs was associated with important morphological aberrations as previously reported by other groups [272], reflecting a senescent phenotype characterized by profound cellular alterations. The decrease in proliferation potential of hMSCs during long-term *in vitro* culture has earlier been demonstrated to be associated with shortening of the telomeric sequences [274]. In contrast, hES-MPs were found to display longer telomeres compared to hMSCs both a PD5 and PD50, although no differences in telomerase activity was detected. Therefore, the different length of the telomeric sequences observed in hES-MPs and hMSCs plausibly reflects the intrinsic different origin of the two cell types. In fact, the isolation from adult tissues implies that hMSCs have undergone a higher number of cell divisions (which is also proportional to the donor age), resulting in the shortening of their telomeric sequences [398]. On the other hand, alternative telomere lengthening mechanisms [399] may be active in hES-MPs and responsible for the observed difference. The extended cellular lifespan observed for hES-MPs represents a significant advantage for their use in tissue engineering applications. Of additional interest for such applications is the shorter PD time observed for hES-MPs during expansion because it allows the fast production of a sufficient number of cells needed for treatment. The different proliferation potential of hES-MPs and

hMSCs is attributable to differences in the expression level of genes involved in cell proliferation. In regard to this, microarray data showed that hES-MPs displayed higher expression of HELLS, CDC25A, MCM5, MCM10, BUB1, ORC1L and FGF5 compared to hMSCs. For example, HELLS encodes for a helicase which is ubiquitously expressed in rapidly dividing cells [400, 401], and targeted disruption of HELLS was shown to result in increased replicative senescence and alteration of the gene expression pattern of the senescence-related genes CDKN2A and BMI1 [402]. On the other hand, MCM5, MCM10 and ORC1L are required for DNA replication [403-405], whereas the mitogens FGF5 and CDC25A are known to accelerate S-phase entry [406, 407]. The higher expression of these genes in hES-MPs may be responsible for the increased proliferation observed compared to hMSCs. The higher proliferation potential of hES-MPs may also be associated with the increased expression of EREG and the related receptor EGFR. EREG is a member of the EGF family and able to promote cell proliferation via the EGF signaling pathway [408]. In line with the results observed in monolayer cultures, hES-MPs displayed higher proliferation rate also when cells were cultured in 3D systems as demonstrated in study IV. Three days after seeding onto biocoral scaffolds, constructs of hES-MPs displayed a 2.8-fold higher content of DNA compared to constructs of hMSCs, indicating a shorter PD time displayed by hES-MPs compared to hMSCs. The difference in DNA content became even larger following flow perfusion stimulation of the cell/scaffold constructs, resulting in a stark increase in tissue formation both in terms of density and area of formed tissue. A possible explanation for this finding may be the higher expression of EGFR observed in hES-MPs, which was recently demonstrated to be activated following mechanical stimulation of the cells [409], although other unknown mechanisms may account for the observed differences. In fact, no data exist today regarding the expression level of the above genes in hES-MPs and hMSCs following osteogenic stimulation, and additional studies are required to better validate the above assumptions. Overall, the higher proliferative potential of the hES-MPs provides these cells with a great advantage over hMSCs for bulk production of cells for therapy and tissue engineering applications.

8.8 hES-MPs do not exhibit tumorigenic potential

Transplantation of hESCs into immunodeficient animal models leads to the formation of teratomas. On the other hand, hES-MPs were previously demonstrated not to form teratomas following implantation under the kidney capsule of SCID mice [35]. In line with this finding, constructs of hES-MPs did not show any sign of uncontrolled proliferation after subcutaneous

implantation in the immunodeficient Nude and Fox mice. The lack of tumorigenic potential in hES-MPs may be ascribed to the significant dowregulation of genes involved in pluripotency occurring during the derivation process. In fact, pluripotency is strongly associated with teratoma formation as discussed in paragraph 8.5, and one of the most well known genes to induce these processes is TDGF1 [383, 410]. Further, hES-MPs displayed decreased expression of EPHA1, known to be overexpressed in many tumors [411-413], and DNMT3B known to silence tumor suppressor genes in cancer cells [414]. Another important tumor suppressor gene is p53, whose inactivation is a common feature in many tumors [415] and whose transcription is induced upon binding of NR2F2 to the p53 promoter [416]. The significantly increased expression of NRF2F during hES-MP formation, as well as the downregulation of the p53-associated transcription factor TFAP2A [417], likely represent additional mechanisms for the hES-MP cells to decrease their tumorigenicity. Other tumor suppressor genes significantly upregulated upon hES-MPs derivation were CDKN2A (p16) and CAV1. In regard to this, Rubio *et al.* recently reported that the initial steps leading to hMSCs transformation *in vitro* were the activation of c-myc and repression of p16 [418]. On the other hand, CAV1 is a protein marker for caveolae organelles, which functions as negative regulator of cell transformation with a central role in the pathogenesis of tumors and metastasis [419-421]. Their identification as hub genes in PPI suggests that CDKN2A and CAV1 may play a central role in regulating cell proliferation and limiting cell transformation of hES-MPs. hESCs express high level of telomerase, which allows them to divide repeatedly by ensuring a constant extension of the telomeric sequences at the chromosome ends [422]. Similarly, high level of telomerase activity are seen in many human cancers [423], suggesting that the cell immortality conferred by telomerase plays a key role in tumor development. Interestingly, our data demonstrated that hES-MPs displayed decreased expression of genes encoding for the telomerase subunits compared to hESCs, and similar telomerase activity as seen in hMSCs both at low and high passage, providing additional support for a potential use of hES-MPs in clinical settings. Nonetheless, the higher proliferation ability of hES-MPs compared to hMSCs raises the concern for a potential accumulation of chromosomal aberrations, which may occur during cell division and eventually lead to neoplastic transformation of the cells. For example, during each cell division cycle, the newly duplicated chromosomes must be distributed evenly into the two daughter cells so that each cell receives exactly one copy of each chromosome. Errors in this process result in abnormal balance of chromosomes and, overcome a certain threshold of aneuploidy, may lead to the generation of cancer-specific phenotypes independent of gene

mutation [424]. Accurate sister chromatid segregation relies on the attachment and alignment of chromosomes to the mitotic spindle. This process is controlled by the spindle assembly checkpoint, which prevents anaphase onset until all replicated chromatids have formed proper attachments to a functional bipolar spindle [425]. Several genes encoding for proteins with a role in this process, such as CDC20, MAD2, BUB1B, NDC80, NUF2, CENPA, ERCC6L, SPC24, MLF1IP, AURKB, SPC25, CENPM, ZWINT and CDCA8 were identified as hub genes in PPI networks of genes showing significantly increased expression in hES-MPs compared to hMSCs, indicating a strong control function of mitosis important in order to reduce the risk of tumor formation. Taken together, the results presented in this thesis, in addition to the previously reported data [35], provide strong evidence for the lack of tumorigenic potential of hES-MPs, which is a prerequisite for possible future applications of these cells. However, additional studies are needed to investigate genome integrity and mutation rate of the investigated cells, especially in relation to the degree of *in vitro* expansion, in order to fully validate their stability and safety for clinical applications.

8.9 hES-MPs display optimal osteogenic potential and higher mineralization properties compared to hMSCs

Engineering bone substitutes requires using stem cells with the potential to differentiate toward the osteogenic lineage and synthesize a matrix with high content of calcium phosphate deposits. When cultured under osteogenic conditions in monolayer cultures, hES-MPs and hMSCs displayed similar levels and patterns of expression for genes involved in osteogenic differentiation and encoding for proteins constituting the matrix of bone tissue such as RUNX2, COL1A1, OC and OPN [77, 157, 164], indicating a similar responsiveness of the two cell types to the osteogenic factors. This assumption is in line with the expression results observed in monolayer cultures, showing similar level of RUNX2 and COL1A1 in undifferentiated hES-MPs and hMSCs. Interestingly, after protracted expansion, both cell types manifested a significant reduction in the expression of RUNX2 compared to the expression levels detected at low passage, in accordance with results reported by others in late-stage culture of hMSCs [426]. However, the observed decrease was lower for hES-MPs compared to hMSCs, denoting a rather higher sensitivity of hES-MPs to osteogenic stimulation after prolonged expansion. A different behavior was observed when cells were interfaced to the biocoral scaffolds and cultured in 3D

conditions. First of all, before osteogenic stimulation, the cells displayed significant differences in the expression of the investigated genes, including RUNX2 and COLA1A, in contrast with the results observed in monolayer cultures, indicating a possible role played by the properties of the biomaterial in affecting cell behavior. In support of this idea, Rochet *et al*. demonstrated that gene expression was affected when culturing osteoblastic cells on calcium phosphate substitutes compared to classic monolayer cultures [427]. On the other hand, the discrepancy observed in gene expression between monolayer and 3D cultures in biocoral scaffolds may result from the intrinsic differences in culture dimensionality. In fact, cell orientation and adhesion are important factors influencing cell functionality [428], and data have recently been published demonstrating the effects of culture dimensionality on cell behavior irrespective of the biomaterial used [429]. Secondly, the expression of the marker genes investigated was differently affected following the osteogenic stimulation of the cell/coral constructs both under static and dynamic conditions. Interestingly, when cultured under dynamic conditions, hES-MPs displayed significantly increased expression of COL1A1, ALP, ON and OPN compared to static conditions, whereas hMSCs displayed increased expression of RUNX2, COL1A1, ON and OPN, indicating a different responsiveness of the two cell types to mechanical stimulation. The finding may find explanation in the differential levels of key genes involved in the signaling pathways leading to osteogenic differentiation as discussed in paragraph 8.7, although no clear understanding exists today. Despite the general differences observed, hES-MPs displayed an overall higher expression of genes involved in bone histogenesis compared to hMSCs, demonstrating optimal differentiation ability and high potential for a successful use in bone engineering applications.

ALP is recognized to play a role during osteogenesis [99] and its upregulation during osteogenic differentiation is considered to favor the mineralization of the bone matrix [374]. Undifferentiated hES-MPs and hMSCs displayed low level of ALP expression both in monolayer and 3D cultures in biocoral scaffolds, indicating that ALP was not affected by the culture conditions in both cell types. However, following osteogenic stimulation, both cell types displayed a gradual increase in ALP expression and activity along the experimental period, although the ALP activity was generally higher for hMSCs than hES-MPs. Similar results were previously reported by Arpornmaeklong *et al*. when comparing the osteogenic potential of hMSCs and human embryonic-derived MSCs [430], underscoring a different responsiveness of the two cell types to the osteogenic factors used for stimulation. Noteworthy, this trend was inversed after flow perfusion of the cells, indicating that hES-MPs are more sensitive to mechanical

stimulation compared to hMSCs. The different sensitivity of hES-MPs and hMSCs likely result from the observed differences in the global gene expression profile, although no clues regarding the exact mechanisms underlying the different biological response to the used chemical and mechanical stimulation exist today. Despite the differences in the activity of ALP detected, hES-MPs displayed higher mineralization properties compared to hMSCs in monolayer cultures, suggesting that the composition and macromolecular properties of the matrix synthesized by hES-MPs may provide more optimal conditions for the deposition and growth of calcium phosphate crystals compared to hMSCs as discussed in paragraph 8.4. Nonetheless, our results demonstrate that the amount of calcium and phosphate deposits within the matrix produced by both cell types was inversely proportional to the number of passages, underlining an impaired mineralization potential owing to prolonged expansion. The decrease in mineral content may be in part due to alteration in the structural and chemical characteristics of the matrix associated with the protracted expansion and in part to the decline in ALP activity observed for both cell types. However, the decrease in mineralization observed after protracted expansion was higher for hMSCs compared to hES-MPs, and likely associated with the senescence-related alterations as discussed in paragraph 8.7. On the other hand, no similar changes were observed for hES-MPs, suggesting that an extended or more appropriate stimulation may still result in the synthesis of a sufficiently mineralized matrix, showing optimal characteristics for bone engineering applications. Differently, the decreased mineral content in late-passage hES-MPs may be attributable to the upregulation of OC observed, in relation to the results reported by Ducy *et al*., demonstrating increased bone mineralization in OC-deficient mice [102].

The ability of hES-MPs to synthesize a matrix with high content of calcium phosphate minerals was also observed when cells were interfaced to coral scaffolds and cultured in 3D conditions. In accordance with the results observed in monolayer cultures, mineralization appeared to take place preferably at the interface with the substrate. However, as opposite to hMSCs, under flow perfusion stimulation constructs of hES-MPs displayed calcium phosphate deposits further down inside the scaffold pores, which represent an essential requirement for the construction of functional substitutes for bone engineering applications. The more extensive mineralization observed for constructs of hES-MPs under dynamic conditions possibly reflects the denser network of collagen fibers seen under these conditions, which provide the natural substrate for the HA crystals to form.

In addition to the properties discussed above, optimal cells for bone engineering applications must display specific and stable commitment toward the osteogenic lineage. In regard to this, hES-MPs displayed full commitment toward the osteogenic lineage when properly stimulated, as opposed to hMSCs that displayed sign of codifferentiation toward the adipogenic lineage. The osteogenic and adipogenic differentiation pathways have recently been shown to be overlapped [431], and considerable evidence exists to support that unbalance in hMSCs differentiation toward the osteogenic and adipogenic lineages contributes to bone loss in aged patients [127, 432]. Based on this knowledge, it is important to note that hMSCs derived from aged patients may fail to provide a sufficient number of cells with optimal osteogenic potential for the construction of functional bone substitutes. In fact, the osteogenic properties of the hMSCs used in this thesis were inversely proportional to the donor age, and only the hMSCs with higher osteogenic potential were used for the above comparison, indicating that even larger differences could be observed if using hMSCs derived from older patients. Moreover, it is important to note that standard culture conditions for the osteogenic differentiation of cells of the mesenchymal lineage were used, and that more optimal conditions specifically established for hES-MPs may further increase their osteogenic potential and mineralization properties.

8.10 hES-MPs are hypoimmunogenic and do not elicit immune response *in vivo*

The derivation from adult tissues allows the use of hMSCs in autogeneic conditions and overcome possible complications associated with an immune reaction against the transplanted cells. However, as discussed in paragraph 8.9, hMSCs derived from aged patients may fail to provide a sufficient number of functional cells for the construction of bone substitutes, and allogeneic hMSCs may be required for treatment in similar situations. In fact, increasing evidence exists regarding the hypoimmunogenic and immunomodulatory properties of hMSCs [268, 269, 433], which support the idea the hMSCs may be exploited in allogenic settings, although conflicting results have been reported [269, 434]. Particularly, the hypoimmunogenicity of hMSCs has been linked to the low surface expression of HLA class I (HLA-ABC) and II (HLA-DR) molecules [435], and lack of the costimulatory molecules CD80 and CD86 [433, 436]. Interestingly, undifferentiated hES-MPs displayed similar surface profile for the above immunological markers as hMSC, which suggests they may equivalently find application for the construction of bone substitutes in

allogeneic settings. In support of this idea, the expression of HLA-DR in hES-MPs was not stimulated following treatment with IFN-γ as opposed to hMSCs. In fact, transplantation of an allograft triggers an inflammatory response with concomitant release of a panel of different cytokines including IFN-γ, which is know to stimulate the expression of HLA molecules, and in turn promotes the allorecognition of the transplanted cells. Based on this model, the stimulation of HLA-DR molecules may be responsible for the cell-mediated immune response against MSCs observed following transplantation in allogeneic conditions [269]. Cell-mediated immune rejection to non-syngeneic cells and tissues is principally driven via recognition of HLA class I and II molecules by CD8-positive T cytotoxic (Tc) and CD4-positive T helper (Th) lymphocytes, respectively [437]. Therefore, the lack of HLA-DR molecules observed in hES-MPs suggests that they exhibit an immunoprivileged phenotype and do not elicit the activation of T lymphocytes after implantation in non-syngeneic hosts. In line with this, knocking out the HLA class II molecules has been proposed as a possible strategy to prevent immune rejection in allogeneic tissue engineering applications [438]. Upon expansion and differentiation toward a specific lineage, cells may undertake profound alteration in the expression of several genes, and this may result in the modification of the expression profile of HLA molecules, therefore affecting the immunological properties of the cells. However, the immunological profile of hES-MPs was not affected following expansion and osteogenic differentiation, substantiating their possible use for bone engineering applications in allogeneic settings. In accordance with the above findings, hES-MPs did not seem to elicit an immune response following implantation in xenogeneic conditions. Immune rejection to non-syngeneic transplants results in massive cell death caused by the combined action of the innate and adaptive compartment of the host immune system [439], with an important role played by NK cells, as well as T and B lymphocytes [440-442]. However, after transplantation in immunocompetent and immunocompromised mice, the survival rate of hES-MPs showed similar trends irrespective of the presence of the above immune cells, thus providing evidence that no cell-mediated response occurred against the transplanted cells. Furthermore, episodes of acute rejection often result in a variation in the number of white cells in the peripheral blood, characterized by either a decline (leucopenia) or an increase (leucocytosis) in leukocyte count [443, 444]. The decline in peripheral leucocytes may be associated with a direct involvement of leucocytes locally at the implantation site, and has been reported to be associated in some cases with unfavorable clinical outcomes [444]. However, hES-MPs transplantation did not provoke any significant variation in the number of leucocytes, therefore excluding any possible

activation and clonal expansion of alloreactive lymphocytes and other inflammatory cells. Following recognition of HLA class II molecules, Th cells specialize in two different subsets such as Th1 and Th2 cells [445]. Th1 lymphocytes produce mainly IL-2, TNF-α and IFN-γ, which promote the cytotoxic activity of Tc lymphocytes [446, 447], whereas Th2 lymphocytes produce e.g. IL-4 among others [448]. On the other hand, NK cells have the ability to kill target cells lacking or expressing low level of HLA molecules [449], and release IFN-γ and TNF-α following activation in the acute phase [450]. Transplantation of hES-MPs did not result in an increase in the serum concentration of these cytokines, indicating no activation of Th lymphocytes associated with allorecognition, in accordance with the results observed in study II and III showing lack of expression of HLA-DR molecules, and excluding any activation of NK cells. Not least, gene expression data showed that hES-MPs and hMSCs display similar level of the non-classical HLA-G molecule. HLA-G, which is expressed by fetal tissues during pregnancy, is recognized to inhibit monocyte, dendritic, NK, B and T cells through interaction with inhibitory receptors expressed on these cells [451, 452]. Its expression in hES-MPs may play an additional role in determining the tolerogenic properties observed, although its expression at a protein level must be verified in order to confirm this assumption. Taken together, the data demonstrate that hES-MPs display favorable immune properties and do not elicit any major reaction after *in vivo* transplantation in non-syngeneic conditions. However, for a clinical use of hES-MPs in bone engineering applications additional studies are needed to fully assess their tolerogenic properties *in vivo*.

8.11 hES-MPs are not affected by the chemical composition of cp-Ti and Ti6Al4V scaffolds

Interfacing hES-MPs with EBM-fabricated cp-Ti and Ti6Al4V scaffolds represents an appealing strategy for the fabrication of customized third-generation biomaterials for orthopedic and dental applications, although leaching of vanadium from the Ti6Al4V alloy may exert an adverse effect as previously demonstrated [453]. However, despite the different chemical composition of the building materials, both the EBM-fabricated cp-Ti and Ti6Al4V scaffolds displayed similar surface properties with respect to topography, oxide thickness and composition, suggesting that fabrication using the EBM technology may circumvent any alleged disadvantages associated with the presence of vanadium within the scaffolds. In accordance with this

assumption, hES-MPs displayed similar behavior when interfaced to cp-Ti and Ti6Al4V scaffolds, in terms of attachment, proliferation and expression of genes involved in osteogenic differentiation. The main objective of interfacing stem cells with biomaterials is to cover the biomaterial surface with a layer of cells able to foster integration of the material into the natural tissue and stimulate the local tissue repair by providing specific functional cues. Frosch *et al*. recently reported improved joint resurfacing using MSC-coated titanium implants, suggesting a positive effect played by stem cells in promoting tissue regeneration [454], although no clear understanding about the underlying mechanisms exists today. Soon after seeding, hES-MPs formed a dense layer of cells in tight contact with the geometrical features of the scaffolds independently of the chemical composition of the material used, and displayed a similar profile of survival during the 6 weeks under investigation, thus excluding any short-term cytotoxic effect associated with the presence of vanadium within the Ti6Al4V alloy. At the implant site, circulating progenitor cells migrate, adhere and differentiate into functional osteoblasts, eventually favoring bone tissue formation and healing. In this view, it is important to investigate whether the materials used in this study influence the expression of genes involved in osteogenic differentiation and constituting the matrix of bone tissue. No significant differences in the expression of RUNX2, COL1A1, OC and OPN, as well as in the activity of ALP were observed when hES-MPs were interfaced to the cp-Ti and Ti6Al4V scaffolds, providing further evidence that, despite the different chemical composition of the building materials, both the EBM-fabricated scaffolds investigated in this thesis may be employed for the design of third-generation biomaterials for orthopedic and dental applications, especially in conditions characterized by poor bone quality.

9. SUMMARY AND CONCLUSIONS

In study I, the osteogenic potential of MFG-hESCs and hMSCs was compared in monolayer cultures, and their ability to synthesize a mineralized matrix was investigated in relation to the expression of genes involved in ossification. The results show that despite MFG-hESCs and hMSCs seem to undergo dissimilar signaling pathways leading to osteogenic differentiation, MFG-hESCs exhibit higher mineralization properties compared to hMSCs, thus showing high potential for bone engineering applications.

In study II, the gene expression profiles of hESCs, hES-MPs and hMSCs were investigated under expansion in order to explore the molecular changes occurring upon derivation of hES-MPs and assess any similarities and differences in gene expression profile between hES-MPs and hMSCs. Further, the proliferation potential and the immunological profile of hES-MPs and hMSCs were studied and compared. The results show that hES-MPs and hMSCs display comparable gene expression profiles, whereas hES-MPs exhibit higher proliferation ability and lower expression of immunological markers compared to hMSCs.

In study III, the objective was to investigate and compare the osteogenic properties of hES-MPs and hMSCs, as well as the surface expression of immunological markers following osteogenic stimulation. The results show that hES-MPs express key markers of osteogenic differentiation, exhibit specific osteogenic commitment and display higher mineralization properties compared to hMSCs, along with a more favorable immune profile.

In study IV, the effect of flow perfusion on the proliferation and osteogenic differentiation of hES-MPs and hMSCs interfaced with biocoral scaffolds was studied and compared. The results show that flow perfusion promotes proliferation and osteogenic differentiation of both cell types. Further, constructs of hES-MPs display significantly increased proliferation, osteogenic differentiation and tissue formation compared to hMSCs under dynamic conditions.

In study V, the objective was to investigate the immunological properties of hES-MPs *in vivo* after subcutaneous implantation in non-syngeneic conditions. The results show that hES-MPs do not elicit any major immune response during the acute phase following implantation.

In study VI, the main objective of the study was to investigate the potential of hES-MPs to be interfaced to EBM-fabricated cp-Ti and Ti6Al4V scaffolds, and study the possible effect of the material chemical composition on hES-MPs behavior. The results show that both scaffolds support cell attachment and growth, and do not seem to alter the expression of genes involved in osteogenesis.

In conclusion, this thesis demonstrates that cells of embryonic origin, under experimental *in vitro* conditions, display comparative advantages over stem cells derived from adult tissues. In particular, in comparison with hMSCs, hES-MPs reveal higher proliferation potential and biosynthetic activity, as well as a more favorable immune profile, which are essential features for the large-scale production of bone substitutes for replacement therapies. Nonetheless, further investigation is required to validate the functionality of MFG-hESCs and hES-MPs *in vivo* and assess their safety for possible future clinical applications.

10. FUTURE DIRECTIONS

MFG-hESCs and hES-MPs represent optimal technology platforms for the generation of experimental models to study bone histogenesis and explore tissue functionality in different conditions, and display comparative advantages over hMSCs from a bone engineering perspective. However, many scientific hypotheses remain and additional comparative studies are needed to fully determine the relative potential of the investigated cells for clinical applications.

First of all, it is of great importance to define more appropriate cultivation conditions, specifically established for MFG-hESCs and hES-MPs, with the objective to further improve their osteogenic commitment and biosynthetic activity. Following this, systematic studies are fundamental to assess the relative functionality *in vitro* using proper 3D models, as well as *in vivo* using different animal models with defects of critical size. The effect of protracted expansion on lineage commitment and biological functionality must also be addressed for a potential use of these cells for the large-scale production of functional bone substitutes. Cell survival, composition and properties of the synthesized matrix, as well as the role of substrate properties on cell differentiation, matrix synthesis and mineral deposition are important aspects to be addressed before MFG-hESCs and hES-MPs may be used for the construction of *bona fide* substitutes for bone engineering applications.

Not least, for an eventual clinical application of MFG-hESCs and hES-MPs, it is of crucial importance to verify their relative safety, with regards to their potential to undergo cellular transformation and/or elicit any inflammatory and immune adverse reaction. The relative mutation rate and related apoptotic sensitivity to DNA damage of the investigated cells must also be assessed, with special emphasis on the effect of prolonged expansion on genomic integrity and accumulation of biological alterations in general. In particular for MFG-hESCs, it is necessary to understand whether the commitment toward the osteogenic lineage is associated with a reduction in their ability to form teratoma after *in vivo* implantation and, mostly important, the time frame when this phenotypic switch occurs. Finally, it is paramount to investigate the ability of MFG-hESCs and hES-MPs to be tolerated in non-syngeneic conditions, both in the acute and chronic phase after transplantation. Alternatively, it is interesting to investigate the possibility to derive patient-specific MFG-hESCs and hES-MPs by means of nuclear reprogramming technologies with the objective to generate large amount of cells for personalized bone engineering

applications, thus bypassing the problem of a possible immune rejection and need for immune suppression.

11. AKNOWLEDGEMENTS

I show my deepest gratitude to Professor Peter Thomsen, my boss and friend, for his patience and trust, for supporting my ideas all the times, for permitting this important journey and steering me toward its end.

I gratefully thank my supervisor Dr. Camilla Karlsson for paving me the way through the maze of the scientific world, for her constant help, for her important instructions and valuable suggestions, for the time dedicated.

A special thanks also to Professor Anders Lindahl for the support, important suggestions and critical discussions.

I express a sincere appreciation to all my coauthors for sharing their time and expertise, for their fundamental contribution to the final realization of this thesis.

I thank all my colleagues and investigators within the Department of Biomaterials, Department of Clinical Chemistry and Transfusion Medicine, and the BIOMATCELL project for the genuine encouragement and constructive moments.

I thank Dr. Hossein Agheli for the interesting scientific discussions and clear explanations.

I express a profound gratitude to all people at the Laboratoire de Bioingéniérie et Biomécanique Ostéoarticulaires in Paris. I especially thank Dr. Herve Petite for giving me the opportunity to join his group, for the joyful moments and support. I also thank Dr. Delphine Logeart-Avramoglou and Dr. Morad Bensidhoum for the patience and understanding, for the important lessons and all fun we had together. I particularly thank Ms. Martina Sladkova for her important contribution and attention to details, for her kind personality.

I heartily thank my lovely family, Marcello, Tettina, Francy and Cry and Scimmietta, Nonnina and zi Mari' for the infinite love, constant support and outstanding nature.

I finally thank my friends who make my life extraordinary and beautiful.

On behalf of my coauthors and myself I sincerely acknowledge BIOMATCELL VINN Excellence Center of Biomaterials and Cell Therapy, Region Västra Götaland, Swedish Research Council (K2009-52X-09495-22-3 and 2005-7544), JOIN(ed)T Marie Curie Action and the Centre National de la Recherche Scientifique for the financial support of the studies presented in this thesis.

12. REFERENCES

1. Langer R, Vacanti JP. Tissue engineering. Science. 1993;260:920-926.
2. Abouna GM. Organ shortage crisis: problems and possible solutions. Transplant Proc. 2008;40:34-38.
3. Asgari E, Zhou W, Sacks S. Complement in organ transplantation. Curr Opin Organ Transplant. 2010;15:486-491.
4. Villard J. Immunity after organ transplantation. Swiss Med Wkly. 2006;136:71-77.
5. Lysaght MJ, O'Loughlin JA. Demographic scope and economic magnitude of contemporary organ replacement therapies. ASAIO J. 2000;46:515-521.
6. Birdsall N. Population growth. Its magnitude and implications for development. Finance Dev. 1984;21:10-15.
7. Greenbaum S. Longevity Rules: How to Age Well into the Future. Carmichael: ESKATON; 2010.
8. Alexander H. The clinical impact of tissue engineering. Tissue Eng. 1995;1:197-202.
9. Nerem RM. Tissue engineering: the hope, the hype, and the future. Tissue Eng. 2006;12:1143-1150.
10. Nerem RM, Sambanis A. Tissue engineering: from biology to biological substitutes. Tissue Eng. 1995;1:3-13.
11. Bernhard Palsson JAH, Robert Plonsey, Joseph D. Bronzino. Tissue Engineering. Boca Raton, Florida: CRC PRESS; 2003.
12. Goodbye, flat biology? Nature. 2003;424:861. Editorial.
13. Vandenburgh H. High-content drug screening with engineered musculoskeletal tissues. Tissue Eng Part B Rev. 2010;16:55-64.
14. Blitterswijk Cv. Tissue Engineering. London: Elsevier Academic Press; 2008.
15. Howard D, Buttery LD, Shakesheff KM, et al. Tissue engineering: strategies, stem cells and scaffolds. J Anat. 2008;213:66-72.
16. Muschler GF, Nakamoto C, Griffith LG. Engineering principles of clinical cell-based tissue engineering. J Bone Joint Surg Am. 2004;86-A:1541-1558.
17. Passier R, van Laake LW, Mummery CL. Stem-cell-based therapy and lessons from the heart. Nature. 2008;453:322-329.
18. Atala A. Tissue engineering and regenerative medicine: concepts for clinical application. Rejuvenation Res. 2004;7:15-31.
19. Robert Lanza RL, Joseph Vacanti. Principles of Tissue Engineering. London: Elsevier Academi Press; 2007.
20. Martin I, Wendt D, Heberer M. The role of bioreactors in tissue engineering. Trends Biotechnol. 2004;22:80-86.
21. Weissman IL. Translating stem and progenitor cell biology to the clinic: barriers and opportunities. Science. 2000;287:1442-1446.
22. Sell S. Stem Cells Handbook. Totowa, New Jersey: Humana Press; 2004.
23. Panno J. Stem Cell Research: Medical Applications and Ethical Controversy. New York, New York: Facts On File; 2005.
24. Polak JM, Bishop AE. Stem cells and tissue engineering: past, present, and future. Ann N Y Acad Sci. 2006;1068:352-366.
25. Takahashi K, Yamanaka S. Induction of pluripotent stem cells from mouse embryonic and adult fibroblast cultures by defined factors. Cell. 2006;126:663-676.

26. Stadtfeld M, Nagaya M, Utikal J, et al. Induced pluripotent stem cells generated without viral integration. Science. 2008;322:945-949.
27. Warren L, Manos PD, Ahfeldt T, et al. Highly efficient reprogramming to pluripotency and directed differentiation of human cells with synthetic modified mRNA. Cell Stem Cell. 2010;7:618-630.
28. Hipp J, Atala A. Sources of stem cells for regenerative medicine. Stem Cell Rev. 2008;4:3-11.
29. Lengner CJ. iPS cell technology in regenerative medicine. Ann N Y Acad Sci. 2010;1192:38-44.
30. Vats A, Tolley NS, Bishop AE, et al. Embryonic stem cells and tissue engineering: delivering stem cells to the clinic. J R Soc Med. 2005;98:346-350.
31. Bigdeli N, Andersson M, Strehl R, et al. Adaptation of human embryonic stem cells to feeder-free and matrix-free culture conditions directly on plastic surfaces. J Biotechnol. 2008;133:146-153.
32. Yamashita T, Kawai H, Tian F, et al. Tumorigenic Development of Induced Pluripotent Stem Cells in Ischemic Mouse Brain. Cell Transplant. 2010.
33. Gutierrez-Aranda I, Ramos-Mejia V, Bueno C, et al. Human induced pluripotent stem cells develop teratoma more efficiently and faster than human embryonic stem cells regardless the site of injection. Stem Cells. 2010;28:1568-1570.
34. Przyborski SA. Differentiation of human embryonic stem cells after transplantation in immune-deficient mice. Stem Cells. 2005;23:1242-1250.
35. Karlsson C, Emanuelsson K, Wessberg F, et al. Human embryonic stem cell-derived mesenchymal progenitors-Potential in regenerative medicine. Stem Cell Res. 2009.
36. Hillel AT, Elisseeff JH. Embryonic progenitor cells in adipose tissue engineering. Facial Plast Surg.26:405-412.
37. Barberi T, Willis LM, Socci ND, et al. Derivation of multipotent mesenchymal precursors from human embryonic stem cells. PLoS Med. 2005;2:e161.
38. Hwang NS, Varghese S, Lee HJ, et al. In vivo commitment and functional tissue regeneration using human embryonic stem cell-derived mesenchymal cells. Proc Natl Acad Sci U S A. 2008;105:20641-20646.
39. Hynes RO. The extracellular matrix: not just pretty fibrils. Science. 2009;326:1216-1219.
40. Park JB, Bronzino JD. Biomaterials: Principles and Applications. Boca Raton: CRC Press LLC; 2003.
41. El-Ghannam A. Bone reconstruction: from bioceramics to tissue engineering. Expert Rev Med Devices. 2005;2:87-101.
42. Liu X, Ma PX. Polymeric scaffolds for bone tissue engineering. Ann Biomed Eng. 2004;32:477-486.
43. Boccaccini AR, Blaker JJ. Bioactive composite materials for tissue engineering scaffolds. Expert Rev Med Devices. 2005;2:303-317.
44. JOON B. PARK JDB. Biomaterials. Boca Raton: CRC Press LLC; 2003.
45. Freeman M, Gurdon JB. Regulatory principles of developmental signaling. Annu Rev Cell Dev Biol. 2002;18:515-539.
46. Vunjak-Novakovic G, Meinel L, Altman G, et al. Bioreactor cultivation of osteochondral grafts. Orthod Craniofac Res. 2005;8:209-218.
47. Ingber DE, Mow VC, Butler D, et al. Tissue engineering and developmental biology: going biomimetic. Tissue Eng. 2006;12:3265-3283.

48. Mendes SC, Tibbe JM, Veenhof M, et al. Bone tissue-engineered implants using human bone marrow stromal cells: effect of culture conditions and donor age. Tissue Eng. 2002;8:911-920.
49. Yaeger PC, Masi TL, de Ortiz JL, et al. Synergistic action of transforming growth factor-beta and insulin-like growth factor-I induces expression of type II collagen and aggrecan genes in adult human articular chondrocytes. Exp Cell Res. 1997;237:318-325.
50. Qi J, Chi L, Maloney M, et al. Interleukin-1beta increases elasticity of human bioartificial tendons. Tissue Eng. 2006;12:2913-2925.
51. Song HM, Nacamuli RP, Xia W, et al. High-dose retinoic acid modulates rat calvarial osteoblast biology. J Cell Physiol. 2005;202:255-262.
52. Kao CL, Tai LK, Chiou SH, et al. Resveratrol promotes osteogenic differentiation and protects against dexamethasone damage in murine induced pluripotent stem cells. Stem Cells Dev. 2010;19:247-258.
53. Bilodeau K, Mantovani D. Bioreactors for tissue engineering: focus on mechanical constraints. A comparative review. Tissue Eng. 2006;12:2367-2383.
54. Williams DF. The Williams Dictionary of Biomaterials. Liverpool, UK: Liverpool University Press; 1999.
55. Wang TW, Wu HC, Wang HY, et al. Regulation of adult human mesenchymal stem cells into osteogenic and chondrogenic lineages by different bioreactor systems. J Biomed Mater Res A. 2009;88:935-946.
56. Schop D, van Dijkhuizen-Radersma R, Borgart E, et al. Expansion of human mesenchymal stromal cells on microcarriers: growth and metabolism. J Tissue Eng Regen Med. 2010;4:131-140.
57. Bjerre L, Bunger CE, Kassem M, et al. Flow perfusion culture of human mesenchymal stem cells on silicate-substituted tricalcium phosphate scaffolds. Biomaterials. 2008;29:2616-2627.
58. Li D, Tang T, Lu J, et al. Effects of flow shear stress and mass transport on the construction of a large-scale tissue-engineered bone in a perfusion bioreactor. Tissue Eng Part A. 2009;15:2773-2783.
59. Grayson WL, Frohlich M, Yeager K, et al. Engineering anatomically shaped human bone grafts. Proc Natl Acad Sci U S A. 2010;107:3299-3304.
60. Freed LE, Vunjak-Novakovic G. Cultivation of cell-polymer tissue constructs in simulated microgravity. Biotechnol Bioeng. 1995;46:306-313.
61. Dutt K, Harris-Hooker S, Ellerson D, et al. Generation of 3D retina-like structures from a human retinal cell line in a NASA bioreactor. Cell Transplant. 2003;12:717-731.
62. Hoerstrup SP, Zund G, Sodian R, et al. Tissue engineering of small caliber vascular grafts. Eur J Cardiothorac Surg. 2001;20:164-169.
63. Hildebrand DK, Wu ZJ, Mayer JE, Jr., et al. Design and hydrodynamic evaluation of a novel pulsatile bioreactor for biologically active heart valves. Ann Biomed Eng. 2004;32:1039-1049.
64. Chen HC, Hu YC. Bioreactors for tissue engineering. Biotechnol Lett. 2006;28:1415-1423.
65. Tissue engineering. Nat Biotechnol. 2000;18 Suppl:IT56-58.
66. Shevchenko RV, James SL, James SE. A review of tissue-engineered skin bioconstructs available for skin reconstruction. J R Soc Interface. 2009;7:229-258.
67. Vinatier C, Mrugala D, Jorgensen C, et al. Cartilage engineering: a crucial combination of cells, biomaterials and biofactors. Trends Biotechnol. 2009;27:307-314.

68. Service RF. Tissue engineering. Coming soon to a knee near you: cartilage like your very own. Science. 2008;322:1460-1461.
69. Rossi CA, Pozzobon M, De Coppi P. Advances in musculoskeletal tissue engineering: Moving towards therapy. Organogenesis. 2010;6:167-172.
70. Vara DS, Salacinski HJ, Kannan RY, et al. Cardiovascular tissue engineering: state of the art. Pathol Biol (Paris). 2005;53:599-612.
71. Hecker L, Birla RK. Engineering the heart piece by piece: state of the art in cardiac tissue engineering. Regen Med. 2007;2:125-144.
72. Fiegel HC, Kaufmann PM, Bruns H, et al. Hepatic tissue engineering: from transplantation to customized cell-based liver directed therapies from the laboratory. J Cell Mol Med. 2008;12:56-66.
73. Asnaghi A, Macchiarini P, Mantero S. Tissue engineering toward organ replacement: a promising approach in airway transplant. Int J Artif Organs. 2009;32:763-768.
74. Atala A. Tissue engineering for the replacement of organ function in the genitourinary system. Am J Transplant. 2004;4 Suppl 6:58-73.
75. Schmidt CE, Leach JB. Neural tissue engineering: strategies for repair and regeneration. Annu Rev Biomed Eng. 2003;5:293-347.
76. Taichman RS. Blood and bone: two tissues whose fates are intertwined to create the hematopoietic stem-cell niche. Blood. 2005;105:2631-2639.
77. Rod R. Seeley TDS, Philip Tate. Anatomy & Physiology. New York, NY: McGraw-Hill; 2006.
78. Nather A. Bone Grafts Aand Bone Substitutes: Basic Science and Clinical Applications. Singapore: World Scientific Publishing Company; 2005.
79. Pittenger MF, Mackay AM, Beck SC, et al. Multilineage potential of adult human mesenchymal stem cells. Science. 1999;284:143-147.
80. Prockop DJ. Marrow stromal cells as stem cells for nonhematopoietic tissues. Science. 1997;276:71-74.
81. Aubin JE. Advances in the osteoblast lineage. Biochem Cell Biol. 1998;76:899-910.
82. Lian JB, Stein GS. Development of the osteoblast phenotype: molecular mechanisms mediating osteoblast growth and differentiation. Iowa Orthop J. 1995;15:118-140.
83. Dallas SL, Bonewald LF. Dynamics of the transition from osteoblast to osteocyte. Ann N Y Acad Sci. 2010;1192:437-443.
84. Vaananen HK, Zhao H, Mulari M, et al. The cell biology of osteoclast function. J Cell Sci. 2000;113 (Pt 3):377-381.
85. Bar-Shavit Z. The osteoclast: a multinucleated, hematopoietic-origin, bone-resorbing osteoimmune cell. J Cell Biochem. 2007;102:1130-1139.
86. Rodan GA. Bone homeostasis. Proc Natl Acad Sci U S A. 1998;95:13361-13362.
87. Robey PG, Young MF, Fisher LW, et al. Thrombospondin is an osteoblast-derived component of mineralized extracellular matrix. J Cell Biol. 1989;108:719-727.
88. Ganss B, Kim RH, Sodek J. Bone sialoprotein. Crit Rev Oral Biol Med. 1999;10:79-98.
89. Bonucci E, Silvestrini G, Bianco P. Extracellular alkaline phosphatase activity in mineralizing matrices of cartilage and bone: ultrastructural localization using a cerium-based method. Histochemistry. 1992;97:323-327.
90. Termine JD, Kleinman HK, Whitson SW, et al. Osteonectin, a bone-specific protein linking mineral to collagen. Cell. 1981;26:99-105.
91. Hauschka PV, Lian JB, Cole DE, et al. Osteocalcin and matrix Gla protein: vitamin K-dependent proteins in bone. Physiol Rev. 1989;69:990-1047.

92. Butler WT. The nature and significance of osteopontin. Connect Tissue Res. 1989;23:123-136.
93. Sodek J, Ganss B, McKee MD. Osteopontin. Crit Rev Oral Biol Med. 2000;11:279-303.
94. Oldberg A, Franzen A, Heinegard D. The primary structure of a cell-binding bone sialoprotein. J Biol Chem. 1988;263:19430-19432.
95. Rey C, Combes C, Drouet C, et al. Bone mineral: update on chemical composition and structure. Osteoporos Int. 2009;20:1013-1021.
96. Luiz Carlos Junqueira JC. Basic Histology: Text & Atlas. Columbus, OH: McGraw-Hill Companies, Inc; 2003.
97. Hankenson K. Contextual regulation of bone development, remodeling and regeneration by thrombospondin matricellular proteins. J Musculoskelet Neuronal Interact. 2006;6:368-369.
98. Salgado AJ, Oliveira JT, Pedro AJ, et al. Adult stem cells in bone and cartilage tissue engineering. Curr Stem Cell Res Ther. 2006;1:345-364.
99. Siffert RS. The role of alkaline phosphatase in osteogenesis. J Exp Med. 1951;93:415-426.
100. Bellows CG, Aubin JE, Heersche JN. Initiation and progression of mineralization of bone nodules formed in vitro: the role of alkaline phosphatase and organic phosphate. Bone Miner. 1991;14:27-40.
101. Hauschka PV, Wians FH, Jr. Osteocalcin-hydroxyapatite interaction in the extracellular organic matrix of bone. Anat Rec. 1989;224:180-188.
102. Ducy P, Desbois C, Boyce B, et al. Increased bone formation in osteocalcin-deficient mice. Nature. 1996;382:448-452.
103. Jundt G, Berghauser KH, Termine JD, et al. Osteonectin--a differentiation marker of bone cells. Cell Tissue Res. 1987;248:409-415.
104. Nakase T, Sugimoto M, Sato M, et al. Switch of osteonectin and osteopontin mRNA expression in the process of cartilage-to-bone transition during fracture repair. Acta Histochem. 1998;100:287-295.
105. Hernandez CJ, Majeska RJ, Schaffler MB. Osteocyte density in woven bone. Bone. 2004;35:1095-1099.
106. Shore EM, Xu M, Shah PB, et al. The human bone morphogenetic protein 4 (BMP-4) gene: molecular structure and transcriptional regulation. Calcif Tissue Int. 1998;63:221-229.
107. Weiner S, Traub W. Bone structure: from angstroms to microns. FASEB J. 1992;6:879-885.
108. Nudelman F, Pieterse K, George A, et al. The role of collagen in bone apatite formation in the presence of hydroxyapatite nucleation inhibitors. Nat Mater. 2010;9:1004-1009.
109. Glimcher MJ, Hodge AJ, Schmitt FO. Macromolecular Aggregation States in Relation to Mineralization: The Collagen-Hydroxyapatite System as Studied in Vitro. Proc Natl Acad Sci U S A. 1957;43:860-867.
110. Turner CH. Bone strength: current concepts. Ann N Y Acad Sci. 2006;1068:429-446.
111. Wang X, Shen X, Li X, et al. Age-related changes in the collagen network and toughness of bone. Bone. 2002;31:1-7.
112. Schaffler MB, Burr DB. Stiffness of compact bone: effects of porosity and density. J Biomech. 1988;21:13-16.
113. Currey J. Comparative Mechanical Properties and Histology of Bone. American Zoologist. 1984;24:5-12.

114. Boskey AL. Variations in bone mineral properties with age and disease. J Musculoskelet Neuronal Interact. 2002;2:532-534.
115. Dickenson RP, Hutton WC, Stott JR. The mechanical properties of bone in osteoporosis. J Bone Joint Surg Br. 1981;63-B:233-238.
116. Ferretti JL, Cointry GR, Capozza RF, et al. Bone mass, bone strength, muscle-bone interactions, osteopenias and osteoporoses. Mech Ageing Dev. 2003;124:269-279.
117. Reilly DT, Burstein AH. Review article. The mechanical properties of cortical bone. J Bone Joint Surg Am. 1974;56:1001-1022.
118. Rho JY, Kuhn-Spearing L, Zioupos P. Mechanical properties and the hierarchical structure of bone. Med Eng Phys. 1998;20:92-102.
119. Reilly DT, Burstein AH, Frankel VH. The elastic modulus for bone. J Biomech. 1974;7:271-275.
120. Ford CM, Keaveny TM. The dependence of shear failure properties of trabecular bone on apparent density and trabecular orientation. J Biomech. 1996;29:1309-1317.
121. Hall BK, Miyake T. All for one and one for all: condensations and the initiation of skeletal development. Bioessays. 2000;22:138-147.
122. John P. Bilezikian LGR, Gideon A. Rodan. Principles of bone biology. San Diego: Academic Press; 1996.
123. Bush PG, Hall AC, Macnicol MF. New insights into function of the growth plate: clinical observations, chondrocyte enlargement and a possible role for membrane transporters. J Bone Joint Surg Br. 2008;90:1541-1547.
124. Fernandez-Tresguerres-Hernandez-Gil I, Alobera-Gracia MA, del-Canto-Pingarron M, et al. Physiological bases of bone regeneration II. The remodeling process. Med Oral Patol Oral Cir Bucal. 2006;11:E151-157.
125. Cowin SC. Mechanical modeling of the stress adaptation process in bone. Calcif Tissue Int. 1984;36 Suppl 1:S98-103.
126. Seeman E. Bone quality: the material and structural basis of bone strength. J Bone Miner Metab. 2008;26:1-8.
127. Duque G. Bone and fat connection in aging bone. Curr Opin Rheumatol. 2008;20:429-434.
128. Dimitriou R, Tsiridis E, Giannoudis PV. Current concepts of molecular aspects of bone healing. Injury. 2005;36:1392-1404.
129. Einhorn TA. The cell and molecular biology of fracture healing. Clin Orthop Relat Res. 1998:S7-21.
130. Ulrich M, Wiesamnn HP. Bone and Cartilage Engineering. Berlin: Springer; 2006.
131. Deng ZL, Sharff KA, Tang N, et al. Regulation of osteogenic differentiation during skeletal development. Front Biosci. 2008;13:2001-2021.
132. Huang W, Yang S, Shao J, et al. Signaling and transcriptional regulation in osteoblast commitment and differentiation. Front Biosci. 2007;12:3068-3092.
133. Gong Y, Slee RB, Fukai N, et al. LDL receptor-related protein 5 (LRP5) affects bone accrual and eye development. Cell. 2001;107:513-523.
134. Boyden LM, Mao J, Belsky J, et al. High bone density due to a mutation in LDL-receptor-related protein 5. NEJM. 2002;346:1513-1521.
135. Li X, Liu P, Liu W, et al. Dkk2 has a role in terminal osteoblast differentiation and mineralized matrix formation. Nat Genet. 2005;37:945-952.
136. Bennett CN, Longo KA, Wright WS, et al. Regulation of osteoblastogenesis and bone mass by Wnt10b. Proc Natl Acad Sci U S A. 2005;102:3324-3329.

137. Kang Q, Sun MH, Cheng H, et al. Characterization of the distinct orthotopic bone-forming activity of 14 BMPs using recombinant adenovirus-mediated gene delivery. Gene Ther. 2004;11:1312-1320.
138. Tsuji K, Bandyopadhyay A, Harfe BD, et al. BMP2 activity, although dispensable for bone formation, is required for the initiation of fracture healing. Nat Genet. 2006;38:1424-1429.
139. Sanford LP, Ormsby I, Gittenberger-de Groot AC, et al. TGFbeta2 knockout mice have multiple developmental defects that are non-overlapping with other TGFbeta knockout phenotypes. Development. 1997;124:2659-2670.
140. Tezuka K, Yasuda M, Watanabe N, et al. Stimulation of osteoblastic cell differentiation by Notch. J Bone Miner Res. 2002;17:231-239.
141. Sciaudone M, Gazzerro E, Priest L, et al. Notch 1 impairs osteoblastic cell differentiation. Endocrinology. 2003;144:5631-5639.
142. Deregowski V, Gazzerro E, Priest L, et al. Notch 1 overexpression inhibits osteoblastogenesis by suppressing Wnt/beta-catenin but not bone morphogenetic protein signaling. J Biol Chem. 2006;281:6203-6210.
143. Moon YS, Smas CM, Lee K, et al. Mice lacking paternally expressed Pref-1/Dlk1 display growth retardation and accelerated adiposity. Mol Cell Biol. 2002;22:5585-5592.
144. Chiang C, Litingtung Y, Lee E, et al. Cyclopia and defective axial patterning in mice lacking Sonic hedgehog gene function. Nature. 1996;383:407-413.
145. St-Jacques B, Hammerschmidt M, McMahon AP. Indian hedgehog signaling regulates proliferation and differentiation of chondrocytes and is essential for bone formation. Genes Dev. 1999;13:2072-2086.
146. Kirkpatrick TJ, Au KS, Mastrobattista JM, et al. Identification of a mutation in the Indian Hedgehog (IHH) gene causing brachydactyly type A1 and evidence for a third locus. J Med Genet. 2003;40:42-44.
147. Hellemans J, Coucke PJ, Giedion A, et al. Homozygous mutations in IHH cause acrocapitofemoral dysplasia, an autosomal recessive disorder with cone-shaped epiphyses in hands and hips. Am J Hum Genet. 2003;72:1040-1046.
148. Maeda Y, Nakamura E, Nguyen MT, et al. Indian Hedgehog produced by postnatal chondrocytes is essential for maintaining a growth plate and trabecular bone. Proc Natl Acad Sci U S A. 2007;104:6382-6387.
149. Woei Ng K, Speicher T, Dombrowski C, et al. Osteogenic differentiation of murine embryonic stem cells is mediated by fibroblast growth factor receptors. Stem Cells Dev. 2007;16:305-318.
150. Sobue T, Naganawa T, Xiao L, et al. Over-expression of fibroblast growth factor-2 causes defective bone mineralization and osteopenia in transgenic mice. J Cell Biochem. 2005;95:83-94.
151. Valverde-Franco G, Liu H, Davidson D, et al. Defective bone mineralization and osteopenia in young adult FGFR3-/- mice. Hum Mol Genet. 2004;13:271-284.
152. Carlton MB, Colledge WH, Evans MJ. Crouzon-like craniofacial dysmorphology in the mouse is caused by an insertional mutation at the Fgf3/Fgf4 locus. Dev Dyn. 1998;212:242-249.
153. Webster MK, Donoghue DJ. FGFR activation in skeletal disorders: too much of a good thing. Trends Genet. 1997;13:178-182.
154. Komori T. Regulation of osteoblast differentiation by transcription factors. J Cell Biochem. 2006;99:1233-1239.
155. Nusse R. Wnt signaling in disease and in development. Cell Res. 2005;15:28-32.

156. Komori T, Yagi H, Nomura S, et al. Targeted disruption of Cbfa1 results in a complete lack of bone formation owing to maturational arrest of osteoblasts. Cell. 1997;89:755-764.
157. Ducy P, Zhang R, Geoffroy V, et al. Osf2/Cbfa1: a transcriptional activator of osteoblast differentiation. Cell. 1997;89:747-754.
158. Nakashima K, Zhou X, Kunkel G, et al. The novel zinc finger-containing transcription factor osterix is required for osteoblast differentiation and bone formation. Cell. 2002;108:17-29.
159. Brault V, Moore R, Kutsch S, et al. Inactivation of the beta-catenin gene by Wnt1-Cre-mediated deletion results in dramatic brain malformation and failure of craniofacial development. Development. 2001;128:1253-1264.
160. Hu H, Hilton MJ, Tu X, et al. Sequential roles of Hedgehog and Wnt signaling in osteoblast development. Development. 2005;132:49-60.
161. Hill TP, Spater D, Taketo MM, et al. Canonical Wnt/beta-catenin signaling prevents osteoblasts from differentiating into chondrocytes. Dev Cell. 2005;8:727-738.
162. Gaur T, Lengner CJ, Hovhannisyan H, et al. Canonical WNT signaling promotes osteogenesis by directly stimulating Runx2 gene expression. J Biol Chem. 2005;280:33132-33140.
163. Yoshida CA, Furuichi T, Fujita T, et al. Core-binding factor beta interacts with Runx2 and is required for skeletal development. Nat Genet. 2002;32:633-638.
164. Kern B, Shen J, Starbuck M, et al. Cbfa1 contributes to the osteoblast-specific expression of type I collagen genes. J Biol Chem. 2001;276:7101-7107.
165. Lian JB, Stein GS, Stein JL, et al. Osteocalcin gene promoter: unlocking the secrets for regulation of osteoblast growth and differentiation. J Cell Biochem Suppl. 1998;30-31:62-72.
166. Komori T. Runx2, a multifunctional transcription factor in skeletal development. J Cell Biochem. 2002;87:1-8.
167. Ducy P. Cbfa1: a molecular switch in osteoblast biology. Dev Dyn. 2000;219:461-471.
168. Han J, Ishii M, Bringas P, Jr., et al. Concerted action of Msx1 and Msx2 in regulating cranial neural crest cell differentiation during frontal bone development. Mech Dev. 2007;124:729-745.
169. Hassan MQ, Javed A, Morasso MI, et al. Dlx3 transcriptional regulation of osteoblast differentiation: temporal recruitment of Msx2, Dlx3, and Dlx5 homeodomain proteins to chromatin of the osteocalcin gene. Mol Cell Biol. 2004;24:9248-9261.
170. Lee MH, Kim YJ, Yoon WJ, et al. Dlx5 specifically regulates Runx2 type II expression by binding to homeodomain-response elements in the Runx2 distal promoter. J Biol Chem. 2005;280:35579-35587.
171. Bialek P, Kern B, Yang X, et al. A twist code determines the onset of osteoblast differentiation. Dev Cell. 2004;6:423-435.
172. D'Alonzo RC, Selvamurugan N, Karsenty G, et al. Physical interaction of the activator protein-1 factors c-Fos and c-Jun with Cbfa1 for collagenase-3 promoter activation. J Biol Chem. 2002;277:816-822.
173. Hess J, Porte D, Munz C, et al. AP-1 and Cbfa/runt physically interact and regulate parathyroid hormone-dependent MMP13 expression in osteoblasts through a new osteoblast-specific element 2/AP-1 composite element. J Biol Chem. 2001;276:20029-20038.

174. Xiao G, Jiang D, Ge C, et al. Cooperative interactions between activating transcription factor 4 and Runx2/Cbfa1 stimulate osteoblast-specific osteocalcin gene expression. J Biol Chem. 2005;280:30689-30696.
175. Jensen LJ, Kuhn M, Stark M, et al. STRING 8--a global view on proteins and their functional interactions in 630 organisms. Nucleic Acids Res. 2009;37:D412-416.
176. Braddock M, Houston P, Campbell C, et al. Born again bone: tissue engineering for bone repair. News Physiol Sci. 2001;16:208-213.
177. Biswas G, Khandelwal NK, Venkatramu NK, et al. Congenital sternal cleft. Br J Plast Surg. 2001;54:259-261.
178. Jaffe KA, Morris SG, Sorrell RG, et al. Massive bone allografts for traumatic skeletal defects. South Med J. 1991;84:975-982.
179. Mehrara BJ, Disa JJ, Pusic A. Scalp reconstruction. J Surg Oncol. 2006;94:504-508.
180. Jia WT, Zhang CQ, Sheng JG, et al. Free vascularized fibular grafting in combination with a locking plate for the reconstruction of a large tibial defect secondary to osteomyelitis in a child: a case report and literature review. J Pediatr Orthop B.19:66-70.
181. Hüsing B, Bührlen B, Gaisser S. Human Tissue Engineered Products: Today's Markets and Future Prospects. 2003.
182. Laurencin C, Khan Y, El-Amin SF. Bone graft substitutes. Expert Rev Med Devices. 2006;3:49-57.
183. Hollinger JO, Winn S, Bonadio J. Options for tissue engineering to address challenges of the aging skeleton. Tissue Eng. 2000;6:341-350.
184. Kannus P, Niemi S, Parkkari J, et al. Why is the age-standardized incidence of low-trauma fractures rising in many elderly populations? J Bone Miner Res. 2002;17:1363-1367.
185. Randell A, Sambrook PN, Nguyen TV, et al. Direct clinical and welfare costs of osteoporotic fractures in elderly men and women. Osteoporos Int. 1995;5:427-432.
186. Pasco JA, Sanders KM, Hoekstra FM, et al. The human cost of fracture. Osteoporos Int. 2005;16:2046-2052.
187. Commercial Opportunities from an Aging Population. Business Insights. 2004.
188. Bieniek J, Swiecki Z. Porous and porous-compact ceramics in orthopedics. Clin Orthop Relat Res. 1991:88-94.
189. Moore WR, Graves SE, Bain GI. Synthetic bone graft substitutes. ANZ J Surg. 2001;71:354-361.
190. Arcuri MR. Titanium implants in maxillofacial reconstruction. Otolaryngol Clin North Am. 1995;28:351-363.
191. Albert A, Leemrijse T, Druez V, et al. Are bone autografts still necessary in 2006? A three-year retrospective study of bone grafting. Acta Orthop Belg. 2006;72:734-740.
192. Banwart JC, Asher MA, Hassanein RS. Iliac crest bone graft harvest donor site morbidity. A statistical evaluation. Spine (Phila Pa 1976). 1995;20:1055-1060.
193. Finkemeier CG. Bone-grafting and bone-graft substitutes. J Bone Joint Surg Am. 2002;84-A:454-464.
194. Delloye C. Tissue allografts and health risks. Acta Orthop Belg. 1994;60 Suppl 1:62-67.
195. Hing KA. Bone repair in the twenty-first century: biology, chemistry or engineering? Philos Transact A Math Phys Eng Sci. 2004;362:2821-2850.
196. Mellado-Valero A, Ferrer-Garcia JC, Calvo-Catala J, et al. Implant treatment in patients with osteoporosis. Med Oral Patol Oral Cir Bucal.15:e52-57.
197. Yaturu S. Diabetes and skeletal health. J Diabetes. 2009;1:246-254.

198. Frohlich M, Grayson WL, Wan LQ, et al. Tissue engineered bone grafts: biological requirements, tissue culture and clinical relevance. Curr Stem Cell Res Ther. 2008;3:254-264.
199. Cowan CM, Soo C, Ting K, et al. Evolving concepts in bone tissue engineering. Curr Top Dev Biol. 2005;66:239-285.
200. Logeart-Avramoglou D, Anagnostou F, Bizios R, et al. Engineering bone: challenges and obstacles. J Cell Mol Med. 2005;9:72-84.
201. Olivier V, Faucheux N, Hardouin P. Biomaterial challenges and approaches to stem cell use in bone reconstructive surgery. Drug Discov Today. 2004;9:803-811.
202. De Bruyn PP, Kabisch WT. Bone formation by fresh and frozen, autogenous and homogenous transplants of bone, bone marrow and periosteum. Am J Anat. 1955;96:375-417.
203. Mieszawska AJ, Fourligas N, Georgakoudi I, et al. Osteoinductive silk-silica composite biomaterials for bone regeneration. Biomaterials. 2010;31:8902-8910.
204. Asti A, Gastaldi G, Dorati R, et al. Stem Cells Grown in Osteogenic Medium on PLGA, PLGA/HA, and Titanium Scaffolds for Surgical Applications. Bioinorg Chem Appl. 2010:831031.
205. Hu J, Smith LA, Feng K, et al. Response of human embryonic stem cell-derived mesenchymal stem cells to osteogenic factors and architectures of materials during in vitro osteogenesis. Tissue Eng Part A. 2010;16:3507-3514.
206. Weinand C, Nabili A, Khumar M, et al. Factors of Osteogenesis Influencing Various Human Stem Cells on Third-Generation Gelatin/beta-Tricalcium Phosphate Scaffold Material. Rejuvenation Res. 2011;14(2).
207. Park SH, Gil ES, Kim HJ, et al. Relationships between degradability of silk scaffolds and osteogenesis. Biomaterials. 2010;31:6162-6172.
208. Leong DT, Nah WK, Gupta A, et al. The osteogenic differentiation of adipose tissue-derived precursor cells in a 3D scaffold/matrix environment. Curr Drug Discov Technol. 2008;5:319-327.
209. Zhang ZY, Teoh SH, Chong MS, et al. Superior osteogenic capacity for bone tissue engineering of fetal compared with perinatal and adult mesenchymal stem cells. Stem Cells. 2009;27:126-137.
210. Kahle M, Wiesmann HP, Berr K, et al. Embryonic stem cells induce ectopic bone formation in rats. Biomed Mater Eng. 2010;20:371-380.
211. Zong C, Xue D, Yuan W, et al. Reconstruction of rat calvarial defects with human mesenchymal stem cells and osteoblast-like cells in poly-lactic-co-glycolic acid scaffolds. Eur Cell Mater. 2010;20:109-120.
212. Binderman I, Yaffe A, Zohar R, et al. Tissue engineering of bone: an ectopic rat model. Front Biosci (Schol Ed). 2011;3:61-68.
213. Supronowicz P, Gill E, Trujillo A, et al. Human Adipose-Derived Side Population Stem Cells Cultured on Demineralized Bone Matrix for Bone Tissue Engineering. Tissue Eng Part A. 2011;17:789-798.
214. Chen Q, Yang Z, Sun S, et al. Adipose-derived stem cells modified genetically in vivo promote reconstruction of bone defects. Cytotherapy. 2010;12:831-840.
215. Klein JD, Turner CG, Ahmed A, et al. Chest wall repair with engineered fetal bone grafts: an efficacy analysis in an autologous leporine model. J Pediatr Surg. 2010;45:1354-1360.
216. Oliveira JM, Kotobuki N, Tadokoro M, et al. Ex vivo culturing of stromal cells with dexamethasone-loade carboxymethylchitosan/poly(amidoamine) dendrimer nanoparticles promotes ectopic bone formation. Bone. 2010;46:1424-1435.

217. Petite H, Viateau V, Bensaid W, et al. Tissue-engineered bone regeneration. Nat Biotechnol. 2000;18:959-963.
218. Vehof JW, Spauwen PH, Jansen JA. Bone formation in calcium-phosphate-coated titanium mesh. Biomaterials. 2000;21:2003-2009.
219. Quarto R, Mastrogiacomo M, Cancedda R, et al. Repair of large bone defects with the use of autologous bone marrow stromal cells. NEJM. 2001;344:385-386.
220. Vacanti CA, Bonassar LJ, Vacanti MP, et al. Replacement of an avulsed phalanx with tissue-engineered bone. NEJM. 2001;344:1511-1514.
221. Morishita T, Honoki K, Ohgushi H, et al. Tissue engineering approach to the treatment of bone tumors: three cases of cultured bone grafts derived from patients' mesenchymal stem cells. Artif Organs. 2006;30:115-118.
222. Kitoh H, Kitakoji T, Tsuchiya H, et al. Transplantation of marrow-derived mesenchymal stem cells and platelet-rich plasma during distraction osteogenesis--a preliminary result of three cases. Bone. 2004;35:892-898.
223. Takafumi Yoshikawa YU, Munehisa Koizumi, Yasuhito Tanaka. Spinal fusion using tissue engineered bone-A prospective, randomized clinical pilot trial. Stem Cell Studies. 2011;1.
224. Gawlitta D, Farrell E, Malda J, et al. Modulating endochondral ossification of multipotent stromal cells for bone regeneration. Tissue Eng Part B Rev. 2010;16:385-395.
225. Scotti C, Tonnarelli B, Papadimitropoulos A, et al. Recapitulation of endochondral bone formation using human adult mesenchymal stem cells as a paradigm for developmental engineering. Proc Natl Acad Sci U S A. 2010;107:7251-7256.
226. Williams DF. On the mechanisms of biocompatibility. Biomaterials. 2008;29:2941-2953.
227. Albrektsson T, Johansson C. Osteoinduction, osteoconduction and osseointegration. Eur Spine J. 2001;10 Suppl 2:S96-101.
228. Karageorgiou V, Kaplan D. Porosity of 3D biomaterial scaffolds and osteogenesis. Biomaterials. 2005;26:5474-5491.
229. Stevens MM, George JH. Exploring and engineering the cell surface interface. Science. 2005;310:1135-1138.
230. Kieswetter K, Schwartz Z, Dean DD, et al. The role of implant surface characteristics in the healing of bone. Crit Rev Oral Biol Med. 1996;7:329-345.
231. Dalby MJ, McCloy D, Robertson M, et al. Osteoprogenitor response to semi-ordered and random nanotopographies. Biomaterials. 2006;27:2980-2987.
232. Kroeze RJ, Helder MN, Govaert LE, et al. Biodegradable polymers in bone tissue engineering. Materials. 2009;2:833-856.
233. Park JB. The use of hydrogels in bone-tissue engineering. Med Oral Patol Oral Cir Bucal. 2011;16:e115-118.
234. Shors EC. Coralline bone graft substitutes. Orthop Clin North Am. 1999;30:599-613.
235. Alvarez K, Nakajima H. Metallic scaffolds for bone regeneration. Materials. 2009;2:790-832.
236. Tanner KE. Bioactive composites for bone tissue engineering. Proc Inst Mech Eng H. 2010;224:1359-1372.
237. Sopyana I, Melb M, Rameshc S, et al. Porous hydroxyapatite for artificial bone applications. Science and Technology of Advanced Materials. 2007;8:116-123.
238. Sachlos E, Czernuszka JT. Making tissue engineering scaffolds work. Review: the application of solid freeform fabrication technology to the production of tissue engineering scaffolds. Eur Cell Mater. 2003;5:29-39; discussion 39-40.

239. Hutmacher DW, Cool S. Concepts of scaffold-based tissue engineering--the rationale to use solid free-form fabrication techniques. J Cell Mol Med. 2007;11:654-669.
240. Hu Y, Winn SR, Krajbich I, et al. Porous polymer scaffolds surface-modified with arginine-glycine-aspartic acid enhance bone cell attachment and differentiation in vitro. J Biomed Mater Res A. 2003;64:583-590.
241. Amiji M, Park K. Surface modification of polymeric biomaterials with poly(ethylene oxide), albumin, and heparin for reduced thrombogenicity. J Biomater Sci Polym Ed. 1993;4:217-234.
242. Saito N, Okada T, Horiuchi H, et al. A biodegradable polymer as a cytokine delivery system for inducing bone formation. Nat Biotechnol. 2001;19:332-335.
243. Moioli EK, Hong L, Guardado J, et al. Sustained release of TGFbeta3 from PLGA microspheres and its effect on early osteogenic differentiation of human mesenchymal stem cells. Tissue Eng. 2006;12:537-546.
244. Kim H, Kim HW, Suh H. Sustained release of ascorbate-2-phosphate and dexamethasone from porous PLGA scaffolds for bone tissue engineering using mesenchymal stem cells. Biomaterials. 2003;24:4671-4679.
245. Hasenbein ME, Andersen TT, Bizios R. Micropatterned surfaces modified with select peptides promote exclusive interactions with osteoblasts. Biomaterials. 2002;23:3937-3942.
246. Mendes VC, Moineddin R, Davies JE. Discrete calcium phosphate nanocrystalline deposition enhances osteoconduction on titanium-based implant surfaces. J Biomed Mater Res A. 2009;90:577-585.
247. Chiu LL, Radisic M. Scaffolds with covalently immobilized VEGF and Angiopoietin-1 for vascularization of engineered tissues. Biomaterials.31:226-241.
248. Marot D, Knezevic M, Novakovic GV. Bone tissue engineering with human stem cells. Stem Cell Res Ther.1:10.
249. Ashton BA, Allen TD, Howlett CR, et al. Formation of bone and cartilage by marrow stromal cells in diffusion chambers in vivo. Clin Orthop Relat Res. 1980:294-307.
250. Bab I, Passi-Even L, Gazit D, et al. Osteogenesis in in vivo diffusion chamber cultures of human marrow cells. Bone Miner. 1988;4:373-386.
251. Friedenstein AJ, Chailakhyan RK, Gerasimov UV. Bone marrow osteogenic stem cells: in vitro cultivation and transplantation in diffusion chambers. Cell Tissue Kinet. 1987;20:263-272.
252. Lee OK, Kuo TK, Chen WM, et al. Isolation of multipotent mesenchymal stem cells from umbilical cord blood. Blood. 2004;103:1669-1675.
253. Secco M, Zucconi E, Vieira NM, et al. Multipotent stem cells from umbilical cord: cord is richer than blood! Stem Cells. 2008;26:146-150.
254. Fukuchi Y, Nakajima H, Sugiyama D, et al. Human placenta-derived cells have mesenchymal stem/progenitor cell potential. Stem Cells. 2004;22:649-658.
255. De Bari C, Dell'Accio F, Tylzanowski P, et al. Multipotent mesenchymal stem cells from adult human synovial membrane. Arthritis Rheum. 2001;44:1928-1942.
256. Nakahara H, Goldberg VM, Caplan AI. Culture-expanded human periosteal-derived cells exhibit osteochondral potential in vivo. J Orthop Res. 1991;9:465-476.
257. Zuk PA, Zhu M, Ashjian P, et al. Human adipose tissue is a source of multipotent stem cells. Mol Biol Cell. 2002;13:4279-4295.
258. Williams JT, Southerland SS, Souza J, et al. Cells isolated from adult human skeletal muscle capable of differentiating into multiple mesodermal phenotypes. Am Surg. 1999;65:22-26.

259. Wagner W, Wein F, Seckinger A, et al. Comparative characteristics of mesenchymal stem cells from human bone marrow, adipose tissue, and umbilical cord blood. Exp Hematol. 2005;33:1402-1416.
260. Noel D, Caton D, Roche S, et al. Cell specific differences between human adipose-derived and mesenchymal-stromal cells despite similar differentiation potentials. Exp Cell Res. 2008;314:1575-1584.
261. Bruder SP, Kurth AA, Shea M, et al. Bone regeneration by implantation of purified, culture-expanded human mesenchymal stem cells. J Orthop Res. 1998;16:155-162.
262. Ciapetti G, Ambrosio L, Marletta G, et al. Human bone marrow stromal cells: In vitro expansion and differentiation for bone engineering. Biomaterials. 2006;27:6150-6160.
263. Song IH, Caplan AI, Dennis JE. In vitro dexamethasone pretreatment enhances bone formation of human mesenchymal stem cells in vivo. J Orthop Res. 2009;27:916-921.
264. Scaglione S, Wendt D, Miggino S, et al. Effects of fluid flow and calcium phosphate coating on human bone marrow stromal cells cultured in a defined 2D model system. J Biomed Mater Res A. 2008;86:411-419.
265. Gastaldi G, Asti A, Scaffino MF, et al. Human adipose-derived stem cells (hASCs) proliferate and differentiate in osteoblast-like cells on trabecular titanium scaffolds. J Biomed Mater Res A. 2010;94:790-799.
266. Mason C, Dunnill P. Assessing the value of autologous and allogeneic cells for regenerative medicine. Regen Med. 2009;4:835-853.
267. Ryan JM, Barry FP, Murphy JM, et al. Mesenchymal stem cells avoid allogeneic rejection. J Inflamm (Lond). 2005;2:8.
268. Nauta AJ, Fibbe WE. Immunomodulatory properties of mesenchymal stromal cells. Blood. 2007;110:3499-3506.
269. Nauta AJ, Westerhuis G, Kruisselbrink AB, et al. Donor-derived mesenchymal stem cells are immunogenic in an allogeneic host and stimulate donor graft rejection in a nonmyeloablative setting. Blood. 2006;108:2114-2120.
270. Ho AD, Wagner W, Franke W. Heterogeneity of mesenchymal stromal cell preparations. Cytotherapy. 2008;10:320-330.
271. Wagner W, Ho AD. Mesenchymal stem cell preparations--comparing apples and oranges. Stem Cell Rev. 2007;3:239-248.
272. Wagner W, Horn P, Castoldi M, et al. Replicative senescence of mesenchymal stem cells: a continuous and organized process. PLoS ONE. 2008;3:e2213.
273. Baxter MA, Wynn RF, Jowitt SN, et al. Study of telomere length reveals rapid aging of human marrow stromal cells following in vitro expansion. Stem Cells. 2004;22:675-682.
274. Kim J, Kang JW, Park JH, et al. Biological characterization of long-term cultured human mesenchymal stem cells. Arch Pharm Res. 2009;32:117-126.
275. Van Zant G, Liang Y. The role of stem cells in aging. Exp Hematol. 2003;31:659-672.
276. Chambers SM, Shaw CA, Gatza C, et al. Aging hematopoietic stem cells decline in function and exhibit epigenetic dysregulation. PLoS Biol. 2007;5:e201.
277. Fan M, Chen W, Liu W, et al. The effect of age on the efficacy of human mesenchymal stem cell transplantation after a myocardial infarction. Rejuvenation Res. 2010;13:429-438.
278. Stolzing A, Jones E, McGonagle D, et al. Age-related changes in human bone marrow-derived mesenchymal stem cells: consequences for cell therapies. Mech Ageing Dev. 2008;129:163-173.

279. Zhou S, Greenberger JS, Epperly MW, et al. Age-related intrinsic changes in human bone-marrow-derived mesenchymal stem cells and their differentiation to osteoblasts. Aging Cell. 2008;7:335-343.
280. Sottile V, Thomson A, McWhir J. In vitro osteogenic differentiation of human ES cells. Cloning Stem Cells. 2003;5:149-155.
281. Cao T, Heng BC, Ye CP, et al. Osteogenic differentiation within intact human embryoid bodies result in a marked increase in osteocalcin secretion after 12 days of in vitro culture, and formation of morphologically distinct nodule-like structures. Tissue Cell. 2005;37:325-334.
282. Karp JM, Ferreira LS, Khademhosseini A, et al. Cultivation of human embryonic stem cells without the embryoid body step enhances osteogenesis in vitro. Stem Cells. 2006;24:835-843.
283. Tian XF, Heng BC, Ge Z, et al. Comparison of osteogenesis of human embryonic stem cells within 2D and 3D culture systems. Scand J Clin Lab Invest. 2008;68:58-67.
284. Ahn SE, Kim S, Park KH, et al. Primary bone-derived cells induce osteogenic differentiation without exogenous factors in human embryonic stem cells. Biochem Biophys Res Commun. 2006;340:403-408.
285. Blum B, Benvenisty N. The tumorigenicity of human embryonic stem cells. Adv Cancer Res. 2008;100:133-158.
286. Lian Q, Lye E, Suan Yeo K, et al. Derivation of clinically compliant MSCs from CD105+, CD24- differentiated human ESCs. Stem Cells. 2007;25:425-436.
287. Lee EJ, Lee HN, Kang HJ, et al. Novel embryoid body-based method to derive mesenchymal stem cells from human embryonic stem cells. Tissue Eng Part A.16:705-715.
288. Olivier EN, Rybicki AC, Bouhassira EE. Differentiation of human embryonic stem cells into bipotent mesenchymal stem cells. Stem Cells. 2006;24:1914-1922.
289. Houglum KP, Brenner DA, Chojkier M. Ascorbic acid stimulation of collagen biosynthesis independent of hydroxylation. Am J Clin Nutr. 1991;54:1141S-1143S.
290. Tajima S, Pinnell SR. Regulation of collagen synthesis by ascorbic acid. Ascorbic acid increases type I procollagen mRNA. Biochem Biophys Res Commun. 1982;106:632-637.
291. Murad S, Grove D, Lindberg KA, et al. Regulation of collagen synthesis by ascorbic acid. Proc Natl Acad Sci U S A. 1981;78:2879-2882.
292. Chung CH, Golub EE, Forbes E, et al. Mechanism of action of beta-glycerophosphate on bone cell mineralization. Calcif Tissue Int. 1992;51:305-311.
293. McCulloch CA, Tenenbaum HC. Dexamethasone induces proliferation and terminal differentiation of osteogenic cells in tissue culture. Anat Rec. 1986;215:397-402.
294. Mikami Y, Lee M, Irie S, et al. Dexamethasone modulates osteogenesis and adipogenesis with regulation of osterix expression in rat calvaria-derived cells. J Cell Physiol.226:739-748.
295. Agata H, Asahina I, Yamazaki Y, et al. Effective bone engineering with periosteum-derived cells. J Dent Res. 2007;86:79-83.
296. Mizuno M, Kuboki Y. TGF-beta accelerated the osteogenic differentiation of bone marrow cells induced by collagen matrix. Biochem Biophys Res Commun. 1995;211:1091-1098.
297. Huang Z, Ren PG, Ma T, et al. Modulating osteogenesis of mesenchymal stem cells by modifying growth factor availability. Cytokine. 2010;51:305-310.

298. Ito T, Sawada R, Fujiwara Y, et al. FGF-2 increases osteogenic and chondrogenic differentiation potentials of human mesenchymal stem cells by inactivation of TGF-beta signaling. Cytotechnology. 2008;56:1-7.
299. Zheng YH, Su K, Jian YT, et al. Basic fibroblast growth factor enhances osteogenic and chondrogenic differentiation of human bone marrow mesenchymal stem cells in coral scaffold constructs. J Tissue Eng Regen Med.
300. Levi B, James AW, Wan DC, et al. Regulation of human adipose-derived stromal cell osteogenic differentiation by insulin-like growth factor-1 and platelet-derived growth factor-alpha. Plast Reconstr Surg.126:41-52.
301. Han CY, Wang Y, Yu L, et al. Small molecules with potent osteogenic-inducing activity in osteoblast cells. Bioorg Med Chem Lett. 2009;19:1442-1445.
302. Lee SJ, Lee HK, Cho SY, et al. Identification of osteogenic purmorphamine derivatives. Mol Cells. 2008;26:380-386.
303. Beloti MM, Bellesini LS, Rosa AL. Purmorphamine enhances osteogenic activity of human osteoblasts derived from bone marrow mesenchymal cells. Cell Biol Int. 2005;29:537-541.
304. Kao CL, Tai LK, Chiou SH, et al. Resveratrol promotes osteogenic differentiation and protects against dexamethasone damage in murine induced pluripotent stem cells. Stem Cells Dev.19:247-258.
305. Sistino JJ. Bioreactors for tissue engineering--a new role for perfusionists? J Extra Corpor Technol. 2003;35:200-202.
306. Martin RB. The importance of mechanical loading in bone biology and medicine. J Musculoskelet Neuronal Interact. 2007;7:48-53.
307. Qi MC, Hu J, Zou SJ, et al. Mechanical strain induces osteogenic differentiation: Cbfa1 and Ets-1 expression in stretched rat mesenchymal stem cells. Int J Oral Maxillofac Surg. 2008;37:453-458.
308. Sittichokechaiwut A, Edwards JH, Scutt AM, et al. Short bouts of mechanical loading are as effective as dexamethasone at inducing matrix production by human bone marrow mesenchymal stem cell. Eur Cell Mater.20:45-57.
309. Zayzafoon M, Gathings WE, McDonald JM. Modeled microgravity inhibits osteogenic differentiation of human mesenchymal stem cells and increases adipogenesis. Endocrinology. 2004;145:2421-2432.
310. Martin I, Smith T, Wendt D. Bioreactor-based roadmap for the translation of tissue engineering strategies into clinical products. Trends Biotechnol. 2009;27:495-502.
311. Le Nihouannen D, Guehennec LL, Rouillon T, et al. Micro-architecture of calcium phosphate granules and fibrin glue composites for bone tissue engineering. Biomaterials. 2006;27:2716-2722.
312. Sikavitsas VI, van den Dolder J, Bancroft GN, et al. Influence of the in vitro culture period on the in vivo performance of cell/titanium bone tissue-engineered constructs using a rat cranial critical size defect model. J Biomed Mater Res A. 2003;67:944-951.
313. Scheraga HA. The thrombin-fibrinogen interaction. Biophys Chem. 2004;112:117-130.
314. Hjort K, Theslöf M. Characterisation of Ti Scaffolds Made by FFF for Osteogenic Induction. Department of Materials and Manufacturing Technology. Vol Master. Göteborg: Chalmers University of Technology; 2008.
315. Webb PA. A review of rapid prototyping (RP) techniques in the medical and biomedical sector. J Med Eng Technol. 2000;24:149-153.

316. Thomsen P, Malmstrom J, Emanuelsson L, et al. Electron beam-melted, free-form-fabricated titanium alloy implants: Material surface characterization and early bone response in rabbits. J Biomed Mater Res B Appl Biomater. 2009;90:35-44.
317. Sodhi RN. Time-of-flight secondary ion mass spectrometry (TOF-SIMS):--versatility in chemical and imaging surface analysis. Analyst. 2004;129:483-487.
318. Malmberg P, Nygren H. Methods for the analysis of the composition of bone tissue, with a focus on imaging mass spectrometry (TOF-SIMS). Proteomics. 2008;8:3755-3762.
319. Nygren H, Malmberg P. High resolution imaging by organic secondary ion mass spectrometry. Trends Biotechnol. 2007;25:499-504.
320. Hugo WB. A brief history of heat and chemical preservation and disinfection. J Appl Bacteriol. 1991;71:9-18.
321. Irigaray JL, Oudadesse H, Fadl H, et al. Effet de la temperature sur la structure cristalline d'un biocorail. Journal of Thermal Analysis and Calorimetry. 1993;39:3-14.
322. Hartung T, Balls M, Bardouille C, et al. Good Cell Culture Practice. ECVAM Good Cell Culture Practice Task Force Report 1. Altern Lab Anim. 2002;30:407-414.
323. Heins N, Englund MC, Sjoblom C, et al. Derivation, characterization, and differentiation of human embryonic stem cells. Stem Cells. 2004;22:367-376.
324. Heins N, Lindahl A, Karlsson U, et al. Clonal derivation and characterization of human embryonic stem cell lines. J Biotechnol. 2006;122:511-520.
325. Sjoblom C, Wikland M, Robertson SA. Granulocyte-macrophage colony-stimulating factor promotes human blastocyst development in vitro. Hum Reprod. 1999;14:3069-3076.
326. Dokras A, Sargent IL, Barlow DH. Human blastocyst grading: an indicator of developmental potential? Hum Reprod. 1993;8:2119-2127.
327. Zhang X, Godbey WT. Viral vectors for gene delivery in tissue engineering. Adv Drug Deliv Rev. 2006;58:515-534.
328. Ibrahimi A, Vande Velde G, Reumers V, et al. Highly efficient multicistronic lentiviral vectors with peptide 2A sequences. Hum Gene Ther. 2009;20:845-860.
329. Deroose CM, Reumers V, Gijsbers R, et al. Noninvasive monitoring of long-term lentiviral vector-mediated gene expression in rodent brain with bioluminescence imaging. Mol Ther. 2006;14:423-431.
330. van den Dolder J, Spauwen PH, Jansen JA. Evaluation of various seeding techniques for culturing osteogenic cells on titanium fiber mesh. Tissue Eng. 2003;9:315-325.
331. Mendes SC, Van Den Brink I, De Bruijn JD, et al. In vivo bone formation by human bone marrow cells: effect of osteogenic culture supplements and cell densities. J Mater Sci Mater Med. 1998;9:855-858.
332. Jaiswal N, Haynesworth SE, Caplan AI, et al. Osteogenic differentiation of purified, culture-expanded human mesenchymal stem cells in vitro. J Cell Biochem. 1997;64:295-312.
333. Roh JD, Nelson GN, Udelsman BV, et al. Centrifugal seeding increases seeding efficiency and cellular distribution of bone marrow stromal cells in porous biodegradable scaffolds. Tissue Eng. 2007;13:2743-2749.
334. Vunjak-Novakovic G, Obradovic B, Martin I, et al. Dynamic cell seeding of polymer scaffolds for cartilage tissue engineering. Biotechnol Prog. 1998;14:193-202.
335. David B, Bonnefont-Rousselot D, Oudina K, et al. A perfusion bioreactor for engineering bone constructs: An in vitro and in vivo study. Tissue Eng Part C Methods. 2010;17:505-516.

336. Mikhailov MV, Zasedatelev AS, Krylov AS, et al. [Mechanism of AT base pairs recognition by molecules of dye "Hoechst 33258"]. Mol Biol (Mosk). 1981;15:690-705.
337. Labarca C, Paigen K. A simple, rapid, and sensitive DNA assay procedure. Anal Biochem. 1980;102:344-352.
338. Baldi P, Hatfield GW. DNA Microarrays and Gene Expression: From Experiments to Data Analysis and Modelling. Cambridge: Cambridge Univesrity Press; 2002.
339. Walker JM, Rapley R. Medical Biomethods Book. Totowa, NJ: Humana Press, Inc.; 2005.
340. Higuchi R, Fockler C, Dollinger G, et al. Kinetic PCR analysis: real-time monitoring of DNA amplification reactions. Biotechnology (N Y). 1993;11:1026-1030.
341. Rozen S, Skaletsky H. Primer3 on the WWW for general users and for biologist programmers. Methods Mol Biol. 2000;132:365-386.
342. Luscombe NM, Greenbaum D, Gerstein M. What is bioinformatics? A proposed definition and overview of the field. Methods Inf Med. 2001;40:346-358.
343. Camon E, Magrane M, Barrell D, et al. The Gene Ontology Annotation (GOA) Database: sharing knowledge in Uniprot with Gene Ontology. Nucleic Acids Res. 2004;32:D262-266.
344. Assou S, Le Carrour T, Tondeur S, et al. A meta-analysis of human embryonic stem cells transcriptome integrated into a web-based expression atlas. Stem Cells. 2007;25:961-973.
345. Sturn A, Quackenbush J, Trajanoski Z. Genesis: cluster analysis of microarray data. Bioinformatics. 2002;18:207-208.
346. Gilbert DR, Schroeder M, van Helden J. Interactive visualization and exploration of relationships between biological objects. Trends Biotechnol. 2000;18:487-494.
347. Do JH, Choi DK. Clustering approaches to identifying gene expression patterns from DNA microarray data. Mol Cells. 2008;25:279-288.
348. Costanzo M, Baryshnikova A, Bellay J, et al. The genetic landscape of a cell. Science.327:425-431.
349. Han JD, Bertin N, Hao T, et al. Evidence for dynamically organized modularity in the yeast protein-protein interaction network. Nature. 2004;430:88-93.
350. Martin SJ, Reutelingsperger CP, McGahon AJ, et al. Early redistribution of plasma membrane phosphatidylserine is a general feature of apoptosis regardless of the initiating stimulus: inhibition by overexpression of Bcl-2 and Abl. J Exp Med. 1995;182:1545-1556.
351. Engvall E, Perlmann P. Enzyme-linked immunosorbent assay (ELISA). Quantitative assay of immunoglobulin G. Immunochemistry. 1971;8:871-874.
352. Blackburn EH. Structure and function of telomeres. Nature. 1991;350:569-573.
353. Connerty HV, Briggs AR. Determination of serum calcium by means of orthocresolphthalein complexone. Am J Clin Pathol. 1966;45:290-296.
354. Ripoll JP. [Colorimetric determination of calcium in serum using methylthymol blue]. Clin Chim Acta. 1976;72:133-139.
355. Fiske CH, Subbarow Y. The Colorimetric Determination of Phosphorus. J. Biol. Chem. 1925;66:375-400.
356. Axelrod B. The free energy of hydrolysis of p-nitrophenyl phosphate. Science. 1951;114:525-526.
357. Smith PK, Krohn RI, Hermanson GT, et al. Measurement of protein using bicinchoninic acid. Anal Biochem. 1985;150:76-85.
358. Clark AT, Bodnar MS, Fox M, et al. Spontaneous differentiation of germ cells from human embryonic stem cells in vitro. Hum Mol Genet. 2004;13:727-739.

359. Logeart-Avramoglou D, Oudina K, Bourguignon M, et al. In vitro and in vivo bioluminescent quantification of viable stem cells in engineered constructs. Tissue Eng Part C Methods.16:447-458.
360. Hoof J. Methods of Blood Collection in the Mouse. Lab Animal. 2000;29:47-53.
361. Donath K, Breuner G. A method for the study of undecalcified bones and teeth with attached soft tissues. The Sage-Schliff (sawing and grinding) technique. J Oral Pathol. 1982;11:318-326.
362. Puchtler H, Waldrop FS, Valentine LS. Polarization microscopic studies of connective tissue stained with picro-sirius red FBA. Beitr Pathol. 1973;150:174-187.
363. Junqueira LC, Bignolas G, Brentani RR. Picrosirius staining plus polarization microscopy, a specific method for collagen detection in tissue sections. Histochem J. 1979;11:447-455.
364. Coons AH, Creech HJ, Jones RN. Immunological properties of an antibody containing a fluorescent group. Proc Soc Exp Biol Med. 1941;47:200-202.
365. Ramos-Vara JA. Technical aspects of immunohistochemistry. Vet Pathol. 2005;42:405-426.
366. Kalache A, Fu D, Yoshida S. A Global Report on Falls Prevention in Older Age. World Health Organization. 2007.
367. Thomson JA, Itskovitz-Eldor J, Shapiro SS, et al. Embryonic stem cell lines derived from human blastocysts. Science. 1998;282:1145-1147.
368. Izadpanah R, Kaushal D, Kriedt C, et al. Long-term in vitro expansion alters the biology of adult mesenchymal stem cells. Cancer Res. 2008;68:4229-4238.
369. Guillot PV, De Bari C, Dell'Accio F, et al. Comparative osteogenic transcription profiling of various fetal and adult mesenchymal stem cell sources. Differentiation. 2008;76:946-957.
370. Lin L, Shen Q, Wei X, et al. Comparison of osteogenic potentials of BMP4 transduced stem cells from autologous bone marrow and fat tissue in a rabbit model of calvarial defects. Calcif Tissue Int. 2009;85:55-65.
371. Karner E, Unger C, Sloan AJ, et al. Bone matrix formation in osteogenic cultures derived from human embryonic stem cells in vitro. Stem Cells Dev. 2007;16:39-52.
372. Chen J, Singh K, Mukherjee BB, et al. Developmental expression of osteopontin (OPN) mRNA in rat tissues: evidence for a role for OPN in bone formation and resorption. Matrix. 1993;13:113-123.
373. Shimko DA, Burks CA, Dee KC, et al. Comparison of in vitro mineralization by murine embryonic and adult stem cells cultured in an osteogenic medium. Tissue Eng. 2004;10:1386-1398.
374. Sugawara Y, Suzuki K, Koshikawa M, et al. Necessity of enzymatic activity of alkaline phosphatase for mineralization of osteoblastic cells. Jpn J Pharmacol. 2002;88:262-269.
375. Theocharis AD, Seidel C, Borset M, et al. Serglycin constitutively secreted by myeloma plasma cells is a potent inhibitor of bone mineralization in vitro. J Biol Chem. 2006;281:35116-35128.
376. Romberg RW, Werness PG, Riggs BL, et al. Inhibition of hydroxyapatite crystal growth by bone-specific and other calcium-binding proteins. Biochemistry. 1986;25:1176-1180.
377. Yamauchi M, Katz EP, Otsubo K, et al. Cross-linking and stereospecific structure of collagen in mineralized and nonmineralized skeletal tissues. Connect Tissue Res. 1989;21:159-167; discussion 168-159.
378. Xu P, Huang J, Cebe P, et al. Osteogenesis imperfecta collagen-like peptides: self-assembly and mineralization on surfaces. Biomacromolecules. 2008;9:1551-1557.

379. Talley-Ronsholdt DJ, Lajiness E, Nagodawithana K. Transforming growth factor-beta inhibition of mineralization by neonatal rat osteoblasts in monolayer and collagen gel culture. In Vitro Cell Dev Biol Anim. 1995;31:274-282.
380. Li Y, Zhang Q, Yin X, et al. Generation of iPSCs from mouse fibroblasts with a single gene, Oct4, and small molecules. Cell Res. 2010;21:196-204.
381. Moretto-Zita M, Jin H, Shen Z, et al. Phosphorylation stabilizes Nanog by promoting its interaction with Pin1. Proc Natl Acad Sci U S A. 2010;107:13312-13317.
382. Chen Y, Shi L, Zhang L, et al. The molecular mechanism governing the oncogenic potential of SOX2 in breast cancer. J Biol Chem. 2008;283:17969-17978.
383. Strizzi L, Bianco C, Normanno N, et al. Cripto-1: a multifunctional modulator during embryogenesis and oncogenesis. Oncogene. 2005;24:5731-5741.
384. Bhattacharya B, Cai J, Luo Y, et al. Comparison of the gene expression profile of undifferentiated human embryonic stem cell lines and differentiating embryoid bodies. BMC Dev Biol. 2005;5:22.
385. Kim CG, Lee JJ, Jung DY, et al. Profiling of differentially expressed genes in human stem cells by cDNA microarray. Mol Cells. 2006;21:343-355.
386. Bhattacharya B, Miura T, Brandenberger R, et al. Gene expression in human embryonic stem cell lines: unique molecular signature. Blood. 2004;103:2956-2964.
387. Pan G, Thomson JA. Nanog and transcriptional networks in embryonic stem cell pluripotency. Cell Res. 2007;17:42-49.
388. Adewumi O, Aflatoonian B, Ahrlund-Richter L, et al. Characterization of human embryonic stem cell lines by the International Stem Cell Initiative. Nat Biotechnol. 2007;25:803-816.
389. Lim LS, Loh YH, Zhang W, et al. Zic3 is required for maintenance of pluripotency in embryonic stem cells. Mol Biol Cell. 2007;18:1348-1358.
390. Boyer LA, Lee TI, Cole MF, et al. Core transcriptional regulatory circuitry in human embryonic stem cells. Cell. 2005;122:947-956.
391. Maldonado-Saldivia J, van den Bergen J, Krouskos M, et al. Dppa2 and Dppa4 are closely linked SAP motif genes restricted to pluripotent cells and the germ line. Stem Cells. 2007;25:19-28.
392. Moll R, Divo M, Langbein L. The human keratins: biology and pathology. Histochem Cell Biol. 2008;129:705-733.
393. Lal-Nag M, Morin PJ. The claudins. Genome Biol. 2009;10:235.
394. Schuldiner M, Yanuka O, Itskovitz-Eldor J, et al. Effects of eight growth factors on the differentiation of cells derived from human embryonic stem cells. Proc Natl Acad Sci U S A. 2000;97:11307-11312.
395. Kramer J, Hegert C, Guan K, et al. Embryonic stem cell-derived chondrogenic differentiation in vitro: activation by BMP-2 and BMP-4. Mech Dev. 2000;92:193-205.
396. Fan Z, Yamaza T, Lee JS, et al. BCOR regulates mesenchymal stem cell function by epigenetic mechanisms. Nat Cell Biol. 2009;11:1002-1009.
397. Wagner W, Bork S, Horn P, et al. Aging and replicative senescence have related effects on human stem and progenitor cells. PLoS ONE. 2009;4:e5846.
398. Allsopp RC, Chang E, Kashefi-Aazam M, et al. Telomere shortening is associated with cell division in vitro and in vivo. Exp Cell Res. 1995;220:194-200.
399. Henson JD, Neumann AA, Yeager TR, et al. Alternative lengthening of telomeres in mammalian cells. Oncogene. 2002;21:598-610.
400. Geiman TM, Muegge K. Lsh, an SNF2/helicase family member, is required for proliferation of mature T lymphocytes. Proc Natl Acad Sci U S A. 2000;97:4772-4777.

401. Raabe EH, Abdurrahman L, Behbehani G, et al. An SNF2 factor involved in mammalian development and cellular proliferation. Dev Dyn. 2001;221:92-105.
402. Sun LQ, Lee DW, Zhang Q, et al. Growth retardation and premature aging phenotypes in mice with disruption of the SNF2-like gene, PASG. Genes Dev. 2004;18:1035-1046.
403. Ryu S, Holzschuh J, Erhardt S, et al. Depletion of minichromosome maintenance protein 5 in the zebrafish retina causes cell-cycle defect and apoptosis. Proc Natl Acad Sci U S A. 2005;102:18467-18472.
404. Izumi M, Yatagai F, Hanaoka F. Cell cycle-dependent proteolysis and phosphorylation of human Mcm10. J Biol Chem. 2001;276:48526-48531.
405. Takeda DY, Dutta A. DNA replication and progression through S phase. Oncogene. 2005;24:2827-2843.
406. Clase KL, Mitchell PJ, Ward PJ, et al. FGF5 stimulates expansion of connective tissue fibroblasts and inhibits skeletal muscle development in the limb. Dev Dyn. 2000;219:368-380.
407. Zhang X, Neganova I, Przyborski S, et al. A role for NANOG in G1 to S transition in human embryonic stem cells through direct binding of CDK6 and CDC25A. J Cell Biol. 2009;184:67-82.
408. Komurasaki T, Toyoda H, Uchida D, et al. Epiregulin binds to epidermal growth factor receptor and ErbB-4 and induces tyrosine phosphorylation of epidermal growth factor receptor, ErbB-2, ErbB-3 and ErbB-4. Oncogene. 1997;15:2841-2848.
409. Yano S, Komine M, Fujimoto M, et al. Mechanical stretching in vitro regulates signal transduction pathways and cellular proliferation in human epidermal keratinocytes. J Invest Dermatol. 2004;122:783-790.
410. Ciccodicola A, Dono R, Obici S, et al. Molecular characterization of a gene of the 'EGF family' expressed in undifferentiated human NTERA2 teratocarcinoma cells. EMBO J. 1989;8:1987-1991.
411. Zelinski DP, Zantek ND, Stewart JC, et al. EphA2 overexpression causes tumorigenesis of mammary epithelial cells. Cancer Res. 2001;61:2301-2306.
412. Shao Z, Zhang WF, Chen XM, et al. Expression of EphA2 and VEGF in squamous cell carcinoma of the tongue: correlation with the angiogenesis and clinical outcome. Oral Oncol. 2008;44:1110-1117.
413. Walker-Daniels J, Coffman K, Azimi M, et al. Overexpression of the EphA2 tyrosine kinase in prostate cancer. Prostate. 1999;41:275-280.
414. Rhee I, Bachman KE, Park BH, et al. DNMT1 and DNMT3b cooperate to silence genes in human cancer cells. Nature. 2002;416:552-556.
415. Lane DP. p53 and human cancers. Br Med Bull. 1994;50:582-599.
416. Huang Q, Raya A, DeJesus P, et al. Identification of p53 regulators by genome-wide functional analysis. Proc Natl Acad Sci U S A. 2004;101:3456-3461.
417. McPherson LA, Loktev AV, Weigel RJ. Tumor suppressor activity of AP2alpha mediated through a direct interaction with p53. J Biol Chem. 2002;277:45028-45033.
418. Rubio D, Garcia S, Paz MF, et al. Molecular characterization of spontaneous mesenchymal stem cell transformation. PLoS ONE. 2008;3:e1398.
419. Elsheikh SE, Green AR, Rakha EA, et al. Caveolin 1 and Caveolin 2 are associated with breast cancer basal-like and triple-negative immunophenotype. Br J Cancer. 2008;99:327-334.
420. Li J, Hassan GS, Williams TM, et al. Loss of caveolin-1 causes the hyper-proliferation of intestinal crypt stem cells, with increased sensitivity to whole body gamma-radiation. Cell Cycle. 2005;4:1817-1825.

421. Williams TM, Lisanti MP. Caveolin-1 in oncogenic transformation, cancer, and metastasis. Am J Physiol Cell Physiol. 2005;288:C494-506.
422. Hiyama E, Hiyama K. Telomere and telomerase in stem cells. Br J Cancer. 2007;96:1020-1024.
423. Shay JW, Bacchetti S. A survey of telomerase activity in human cancer. Eur J Cancer. 1997;33:787-791.
424. Duesberg P, Rasnick D, Li R, et al. How aneuploidy may cause cancer and genetic instability. Anticancer Res. 1999;19:4887-4906.
425. Bharadwaj R, Yu H. The spindle checkpoint, aneuploidy, and cancer. Oncogene. 2004;23:2016-2027.
426. Tanabe S, Sato Y, Suzuki T, et al. Gene expression profiling of human mesenchymal stem cells for identification of novel markers in early- and late-stage cell culture. J Biochem. 2008;144:399-408.
427. Rochet N, Loubat A, Laugier JP, et al. Modification of gene expression induced in human osteogenic and osteosarcoma cells by culture on a biphasic calcium phosphate bone substitute. Bone. 2003;32:602-610.
428. Gumbiner BM. Cell adhesion: the molecular basis of tissue architecture and morphogenesis. Cell. 1996;84:345-357.
429. Baharvand H, Hashemi SM, Kazemi Ashtiani S, et al. Differentiation of human embryonic stem cells into hepatocytes in 2D and 3D culture systems in vitro. Int J Dev Biol. 2006;50:645-652.
430. Arpornmaeklong P, Brown SE, Wang Z, et al. Phenotypic characterization, osteoblastic differentiation, and bone regeneration capacity of human embryonic stem cell-derived mesenchymal stem cells. Stem Cells Dev. 2009;18:955-968.
431. Muruganandan S, Roman AA, Sinal CJ. Adipocyte differentiation of bone marrow-derived mesenchymal stem cells: cross talk with the osteoblastogenic program. Cell Mol Life Sci. 2009;66:236-253.
432. Laschober GT, Brunauer R, Jamnig A, et al. Age-Specific Changes of Mesenchymal Stem Cells Are Paralleled by Upregulation of CD106 Expression As a Response to an Inflammatory Environment. Rejuvenation Res. 2011;14:1-13.
433. Tse WT, Pendleton JD, Beyer WM, et al. Suppression of allogeneic T-cell proliferation by human marrow stromal cells: implications in transplantation. Transplantation. 2003;75:389-397.
434. Grinnemo KH, Mansson A, Dellgren G, et al. Xenoreactivity and engraftment of human mesenchymal stem cells transplanted into infarcted rat myocardium. J Thorac Cardiovasc Surg. 2004;127:1293-1300.
435. Le Blanc K, Tammik C, Rosendahl K, et al. HLA expression and immunologic properties of differentiated and undifferentiated mesenchymal stem cells. Exp Hematol. 2003;31:890-896.
436. Weiss ML, Anderson C, Medicetty S, et al. Immune properties of human umbilical cord Wharton's jelly-derived cells. Stem Cells. 2008;26:2865-2874.
437. Ingulli E. Mechanism of cellular rejection in transplantation. Pediatr Nephrol. 2008;25:61-74.
438. Yang M, Liu L. MHC II gene knockout in tissue engineering may prevent immune rejection of transplants. Med Hypotheses. 2008;70:798-801.
439. Kim IK, Bedi DS, Denecke C, et al. Impact of innate and adaptive immunity on rejection and tolerance. Transplantation. 2008;86:889-894.

440. Benichou G, Yamada Y, Aoyama A, et al. Natural killer cells in rejection and tolerance of solid organ allografts. Curr Opin Organ Transplant. 2010.
441. Dilillo DJ, Griffiths R, Seshan SV, et al. B lymphocytes differentially influence acute and chronic allograft rejection in mice. J Immunol. 2011;186:2643-2654.
442. Game DS, Lechler RI. Pathways of allorecognition: implications for transplantation tolerance. Transpl Immunol. 2002;10:101-108.
443. Bastl CP, Hendler ED, Finkelstein FO. Leukocyte responses to acute renal transplant rejection. Clin Nephrol. 1975;4:228-233.
444. Daar AS, Morris PJ, Oliver DO. Leucocytosis is not a manifestation of rejection. Br Med J. 1977;2:1570-1571.
445. Mosmann TR, Cherwinski H, Bond MW, et al. Two types of murine helper T cell clone. I. Definition according to profiles of lymphokine activities and secreted proteins. J Immunol. 2005;175:5-14.
446. Bevan MJ. Helping the CD8(+) T-cell response. Nat Rev Immunol. 2004;4:595-602.
447. Mosmann TR. T lymphocyte subsets, cytokines, and effector functions. Ann N Y Acad Sci. 1992;664:89-92.
448. Cherwinski HM, Schumacher JH, Brown KD, et al. Two types of mouse helper T cell clone. III. Further differences in lymphokine synthesis between Th1 and Th2 clones revealed by RNA hybridization, functionally monospecific bioassays, and monoclonal antibodies. J Exp Med. 1987;166:1229-1244.
449. Ljunggren HG, Karre K. In search of the 'missing self': MHC molecules and NK cell recognition. Immunol Today. 1990;11:237-244.
450. Fauriat C, Long EO, Ljunggren HG, et al. Regulation of human NK-cell cytokine and chemokine production by target cell recognition. Blood. 2010;115:2167-2176.
451. Colonna M, Samaridis J, Cella M, et al. Human myelomonocytic cells express an inhibitory receptor for classical and nonclassical MHC class I molecules. J Immunol. 1998;160:3096-3100.
452. Carosella ED, Moreau P, Le Maoult J, et al. HLA-G molecules: from maternal-fetal tolerance to tissue acceptance. Adv Immunol. 2003;81:199-252.
453. Imai K, Nakamura M. In vitro embryotoxicity testing of metals for dental use by differentiation of embryonic stem cell test. Congenit Anom (Kyoto). 2006;46:34-38.
454. Frosch KH, Drengk A, Krause P, et al. Stem cell-coated titanium implants for the partial joint resurfacing of the knee. Biomaterials. 2006;27:2542-2549.